

University of Alberta

Methane combustion over Pt and Pt-Pd catalysts

by

Reza Abbasi

A thesis submitted to the Faculty of Graduate Studies and Research

in partial fulfillment of the requirements for the degree of

Master of Science

in

Chemical Engineering

Department of Chemical and Materials Engineering

©Reza Abbasi

Fall 2011

Edmonton, Alberta

Permission is hereby granted to the University of Alberta Libraries to reproduce single copies of this thesis and to lend or sell such copies for private, scholarly or scientific research purposes only. Where the thesis is converted to, or otherwise made available in digital form, the University of Alberta will advise potential users of the thesis of these terms.

The author reserves all other publication and other rights in association with the copyright in the thesis and, except as herein before provided, neither the thesis nor any substantial portion thereof may be printed or otherwise reproduced in any material form whatsoever without the author's prior written permission.

Abstract

A major challenge faced by the transportation sector is vehicle emissions of green house gases (GHG). This issue has led to extensive research on alternative fuels with a lower carbon footprint such as natural gas. Increased use of natural gas as a fuel shall increase methane emissions. Catalytic combustion provides an efficient approach to tackle the problem of fugitive methane emissions. This thesis reports on an investigation of lean methane oxidation over two different catalysts namely Pt and Pt/Pd catalysts. Catalytic activities and the influences of different pretreatments on the catalyst performance were studied through ignition-extinction experiments. It was found that catalysts had stable and high activity for methane combustion. However, these abilities were strongly compromised by the presence of additional water in the feed.

Acknowledgment

First and foremost, I would like to give my sincerest appreciate to my supervisor Dr Robert. E. Hayes for all help, patience and guidance over the past two years. His optimism, enthusiasm, insight and professionalism provided me a wonderful opportunity to study and experiment in an excellent research environment.

I am also entirely grateful of my co-supervisor Dr. Sieghard E. Wanke because of his priceless and indisputable advice on this project. The most important is his elaborate explanations and constant guidance in introducing me in to the field of catalytic combustion. Besides, I want to thank his help on this thesis.

I want to thank Dr Long Wu for his help in the building of the reaction system, on the use of lab equipment, and on his advice on experimental procedures. I would also like to give my gratitude to Dr. Joseph Mmbaga for his help, critics, discussions, and conversations from time to time. Finally, I deeply appreciate Umicore AG of Germany for the generous supply of catalysts which were used in this project.

Table of Contents

1. Introduction.....	1
1.1 Background.....	1
1.1.1 Global warming and the green house gases.....	2
1.1.2 Risk control in coal mines.....	5
1.3 Scope of project.....	6
1.4 Thesis organization.....	8
2. Methane catalytic combustion review.....	9
2.1 Characteristics and drawbacks of traditional combustion reaction, motivations for catalytic combustion.....	9
2.2 General catalytic combustion.....	14
2.3 Combustion Catalyst.....	18
2.3.1 Rare earth materials and other oxides.....	19
2.3.2 Noble metals.....	20
2.3.3 Characteristics of supported Pt and Pd catalysts and effect of different parameters on their performance and activity.....	22
2.3.4 Pt-Pd bimetallic catalyst.....	30
3. Experiments and procedures.....	32
3.1 Experimental apparatus and materials.....	33
3.2 Experimental procedures.....	37
3.2.1 Reactant compositions.....	37
3.2.2 Ignition and extinction curves of methane catalytic combustion.....	38
3.3 Catalyst characterization.....	39
3.3.1 Instrumental neutron activation analysis (INAA).....	39
3.3.2 X-Ray diffraction (XRD).....	40
3.3.3 X-ray photo electron spectroscopy (XPS).....	42
4. Results and Analysis.....	44
4.1 Preliminary tests.....	44
4.1.1. Pt-Pd bimetallic catalyst.....	44
4.1.2. Pt catalyst.....	49
4.2 Ignition and extinction experiments.....	53
4.2.1 Methane concentration effects.....	53

4.2.1.1 Pt-Pd bimetallic catalyst.....	53
4.2.1.2 Pt catalyst.....	61
4.2.2 The effect of added water.....	68
4.2.2.1 The effect of added water on Pt-Pd bimetallic catalyst.....	68
4.2.2.2 The effect of added water on Pt catalyst.....	86
4.3 Characterization of catalysts and analysis.....	103
4.3.1 Instrumental Neutron Activation Analysis (INAA).....	103
4.3.2 X-Ray diffraction (XRD).....	103
4.3.3 X-ray photo electron spectroscopy (XPS).....	112
5. Summary and future work.....	114
5.1 Summary.....	114
5.1.1 General behavior of the catalysts.....	114
5.2 Future work.....	115
5.2.1 Gas constitutes.....	115
5.2.2 Various pretreatments.....	116
5.2.3 Catalyst characterization.....	117
5.2.4 Further study on catalyst formulation.....	118
References.....	119
Appendix A: List of runs.....	135

List of Tables

Table 4.1 Instrumental Neutron Activation Analysis results.....103

Table 4.2 X-ray photo electron spectroscopy results.....113

List of Figures

2.1 Catalytic combustion of methane as a function of temperature, adapted from Lee and Trimm (1995).....	17
3.1 Sketch of the reactor system.....	33
3.2 Photograph of the reactor system.....	34
3.3 Photo of micro-reactor.....	34
3.4 Catalyst samples; Pt-Pd and Pt catalyst(left to right).....	36
4.1 Ignition and extinction curves of methane combustion: Run # Pt-Pd-01-12.....	46
4.2 Ignition and extinction curves of methane combustion: Run # Pt-Pd-01-13.....	47
4.3 Ignition and extinction curves of methane combustion: Run # Pt-Pd-01-14.....	48
4.4 Ignition and extinction curves of methane combustion: Run # Pt-01-12.....	50
4.5 Ignition and extinction curves of methane combustion: Run # Pt-01-13.....	51
4.6 Ignition and extinction curves of methane combustion: Run # Pt-01-14.....	52
4.7 Ignition and extinction curves of methane combustion: Run # Pt-Pd-01-15.....	55
4.8 Ignition and extinction curves of methane combustion: Run # Pt-Pd-01-16.....	56
4.9 Ignition and extinction curves of methane combustion: Run # Pt-Pd-01-18.....	57
4.10 Ignition and extinction curves of methane combustion: Run # Pt-Pd-01-17.....	58
4.11 Comparison of ignition curves with different methane concentrations: Run # Pt-Pd-01-15, Pt-Pd-01-16, Pt-Pd-01-17, Pt-Pd-01-18.....	59

4.12 Comparison of extinction curves with different methane Concentrations: Run # Pt-Pd-01-15,Pt-Pd-01-16,Pt-Pd-01-17, Pt-Pd-01-18.....	60
4.13 Ignition and extinction curves of methane combustion: Run # Pt-01-23.....	62
4.14 Ignition and extinction curves of methane combustion: Run # Pt-01-24.....	63
4.15 Ignition and extinction curves of methane combustion: Run # Pt-01-25.....	64
4.16 Ignition and extinction curves of methane combustion: Run # Pt-01-26.....	65
4.17 Comparison of ignition curves with different methane concentrations: Run # Pt-01-23, Pt-01-24, Pt-01-25, Pt-01-26.....	66
4.18 Comparison of extinction curves with different methane Concentrations: Run # Pt-01-23,Pt-01-24,Pt-01-25, Pt-01-26.....	67
4.19 Influence of 5 mol% water addition on conversion of methane over Pt-Pd bimetallic catalyst versus time on stream.....	70
4.20. Time dependence of methane conversion over Pt-Pd catalyst at 492 °C in the presence of 5 mol% water vapor.....	71
4.21 Ignition and extinction curves of methane combustion: Run # Pt-Pd-01-22-26.....	74
4.22 Ignition and extinction curves of methane combustion: Run # Pt-Pd-01-23-28.....	75
4.23 Ignition and extinction curves of methane combustion: Run # Pt-Pd-01-25-29.....	76
4.24 Ignition and extinction curves of methane combustion: Run # Pt-Pd-01-24-27.....	77
4.25 Comparison of ignition curves with different methane concentrations: Run # Pt-Pd-01-22-26, Pt-Pd-01-23-28, Pt-Pd-01-25-29, Pt-Pd-01-24-27.....	78
4.26 Comparison of extinction curves with different methane concentrations: Run # Pt-Pd-01-22-26, Pt-Pd-01-23-28, Pt-Pd-01-25-29, Pt-Pd-01-24-27.....	79
4.27 Ignition and extinction curves of methane combustion: Run # Pt-Pd-01-33.....	80

4.28 Ignition and extinction curves of methane combustion: Run # Pt-Pd-01-35.....	81
4.29 Ignition and extinction curves of methane combustion: Run # Pt-Pd-01-34.....	82
4.30 Ignition and extinction curves of methane combustion: Run # Pt-Pd-01-36.....	83
4.31 Comparison of ignition curves with different methane Concentrations: Run # Pt-Pd-01-33, Pt-Pd-01-35, Pt-Pd-01-34, Pt-Pd-01-36.....	84
4.32 Comparison of extinction curves with different methane concentrations: Run # Pt-Pd-01-33, Pt-Pd-01-35, Pt-Pd-01-34, Pt-Pd-01-36.....	85
4.33 Influence of 5 mol% water addition on conversion of methane over Pt catalyst versus time on stream.....	88
4.34. Time dependence of methane conversion over Pt catalyst at 547 °C in the presence of 5 mol% water vapor.....	89
4.35 Ignition and Extinction curves of methane combustion: Run # Pt-01-27.....	91
4.36 Ignition and Extinction curves of methane combustion: Run # Pt-01-28.....	92
4.37 Ignition and Extinction curves of methane combustion: Run # Pt-01-29.....	93
4.38 Ignition and Extinction curves of methane combustion: Run # Pt-01-30.....	94
4.39 Comparison of ignition curves with different methane concentrations: Run # Pt-01-27, Pt-01-28, Pt-01-29, Pt-01-30.....	95
4.40 Comparison of extinction curves with different methane concentrations: Run # Pt-01-27, Pt-01-28, Pt-01-29, Pt-01-30.....	96
4.41 Ignition and Extinction curves of methane combustion: Run # Pt-01-32.....	97
4.42 Ignition and Extinction curves of methane combustion: Run # Pt-01-33.....	98
4.43 Ignition and Extinction curves of methane combustion: Run # Pt-01-34.....	99

4.44 Ignition and Extinction curves of methane combustion: Run # Pt-01-31.....	100
4.45 Comparison of ignition curves with different methane concentrations: Run # Pt-01-32, Pt-01-33, Pt-01-34, Pt-01-31.....	101
4.46 Comparison of extinction curves with different methane concentrations: Run # Pt-01-32, Pt-01-33, Pt-01-34, Pt-01-31.....	102
4.47 XRD patterns for reduced and unreduced fresh Pt-Pd samples.....	106
4.48 XRD patterns for reduced and unreduced fresh Pt samples.....	107
4.49 XRD patterns for reduced and unreduced steam-aged Pt-Pd samples...	108
4.50 XRD patterns for reduced and unreduced steam-aged Pt samples.....	109
4.51 XRD patterns for unreduced fresh and steam-aged Pt samples.....	110
4.52 XRD patterns for unreduced fresh and steam-aged Pt-Pd samples.....	111

Symbol	Description	Unit
d_{avg}	the average metal crystal size	nm
λ	the wave length of the CuK- α radiation	nm
FWHH	the width at half height of the diffracted peak	radian
θ	half of the diffraction angle	radian

List of acronyms

CFRR	Catalytic Flow Reversal Reactor
EDX	Energy dispersive X-ray analysis
FWHH	Full width at half height
GC	Gas chromatograph
GHG	Greenhouse Gas
GWP	Global warming potential
HSA	High surface area
I-E	Ignition and extinction experiment
INAA	Instrumental neutron activation analysis
IPCC	Intergovernmental Panel on Climate Change
LSA	Low surface area
ppm	Parts per million (molar basis)
SS	Stainless steel
TC	Thermocouple
TEM	Transmission electron microscopy
UHP	Ultrahigh purity
USA	United States of America
VOC	Volatile organic compound
XPS	X-ray photoelectron spectroscopy
XRD	X-ray diffraction

Chapter 1: Introduction

1.1 Background

Fossil fuels have a profound effect on our life. On the one hand, they are the most important source of energy, and on the other hand, they are considered to be one of the most significant sources of pollution. To fulfill the growing demand of the energy and to reduce the vast environmental problems caused by the use of fossil fuels, two partial solutions have been proposed. The first is the use of alternative cleaner energy sources such as solar and wind energy. The second solution is to use and improve the appropriate technologies resulting in cleaner and more efficient use of fossil fuels. Because of higher release of thermal energy per unit of produced CO₂ and lower production of nitrogen oxides (NO_x) and sulphur dioxide (SO₂), the combustion of natural gas is considered to be the cleanest and the most efficient source of the energy among all traditional fuels, therefore natural gas is widely used as a source of energy in applications such as power generation, and potentially for automobile fuel.

The complete combustion of the methane, the primary component of natural gas, is represented by the following overall reaction:



Conventional burning of natural gas has some major draw backs. First, the only products of methane combustion should be carbon dioxide and water based on the overall combustion reaction; however, because traditional natural gas burners usually operate at temperatures as high as 2000 K, nitrogen oxides including NO₂ and NO will be produced. These oxides are precursors of acid rain that can cause severe environmental damage. In addition, in common combustion applications, methane is not converted completely, so the unconverted methane will be released in to the atmosphere

through the exhaust stream. The homogenous combustion of methane can only happen in a certain range of the flammability limits (5 to 16 % by volume of methane in the air). This means that lean mixtures of methane cannot be combusted with the traditional technologies. The above drawbacks have led to a series of serious constraints on the application of natural gas combustors. For example, both air and natural gas flow rates should be adjusted carefully to make a mixture capable of combustion; the combustion should be initiated by use of a spark resulting in ignition; the reactor should be constructed from special materials being able to tolerate the inherent high operational temperatures of the combustion process, and the last but not the least, because of the demands of the environmental protection, the effluent gas stream going out of the reactor should undergo appropriate treatments to eliminate the oxides of nitrogen.

1.1.1 Global warming and the green house gases

Global warming is one of the most serious challenges for mankind now. The resulting temperature rise because of the global warming could have devastating results such as, producing huge storms, changing the hydrologic cycle, and precipitation patterns. These changes can result in an increase in the risk of flooding, ocean warming, raising sea levels, and coastal flooding.

A major cause of global warming is thought by many to be the buildup of green house gases (GHG) in the atmosphere. GHG comprise less than one percent of the atmosphere and their levels are determined by a balance between the processes generating and destroying them. Human activities, such as the extensive use of fossil fuels, have been identified as the major cause of the increase in GHG concentration in the atmosphere, resulting in global warming, so the stabilization/ or reduction of GHG emission might reduce the harmful impact of global warming and help to stabilize the earth's ecosystem.

Major green house gases

Most of the sources of the GHG are natural; however, industrial activities have resulted in the appearance of new sources of GHG, and emission of some entirely new GHG. The most important GHG are discussed below:

A) Water vapor (H₂O)

Water vapor is a natural GHG with an atmosphere concentration of about 1%. Water vapor is considered to be the most common GHG. The effect of human activities on global concentration of water is almost negligible (EPA, 1998). As a result, water vapor's role as a green house gas is usually neglected in environmental studies.

B) Carbon dioxide (CO₂)

Carbon dioxide natural sources are the respiration of animals, and the decay of the organic materials. Deforestation and combustion of fossil fuels are considered to be the major human induced sources of CO₂. CO₂ is removed from the atmosphere mainly by photosynthesis and ocean absorption. Having the atmospheric concentration of less than 0.04%, carbon dioxide is mainly produced by human activities in the energy sector. The atmospheric concentration of CO₂ is 379 ppm, and the annual CO₂ atmospheric concentration growth rate is about 1.4 ppm (IPCC, 2007).

C) Methane (CH₄)

Although the atmospheric concentration level of methane has been affected by human activities, methane is another GHG which is produced naturally. Although having less atmospheric concentration than does CO₂, methane is a stronger GHG than is CO₂. Natural methane sources include decaying of garbage, termites, wetlands, and oceans. Human induces methane sources include landfills, domestic sewage, agriculture activities, and fossil fuel production and utilization.

D) Nitrous Oxide (N₂O)

The other naturally occurring GHG is nitrous oxide (N₂O). The atmospheric concentration of N₂O has increased because of human activities such as cultivation and use of nitrogen containing fertilizers, burning of fossil fuels and organic material, and nylon production. Soils and oceans are considered as the main natural sources of N₂O. The growth rate of N₂O has remained nearly constant since 1980 (IPCC, 2007).

E) Artificial GHG

There are some GHG produced only because of human activities, these GHG are called artificial GHG. These gases include chlorofluorocarbons (CFC), hydrochlorofluorocarbons (HCFC), perfluorocarbons (PFC), and hydrofluorocarbons (HFC). They were extensively used as coolant gases in refrigerators and air conditioners. CFC are the strongest GHG, as an illustration, HFC134a has a global warming potential (GWP) of 3400 times of that of CO₂ in a span of 20 years. For this reason, although having small volume fraction in the atmosphere, these artificial GHG account for about 10% of the overall contribution to the global warming caused by all GHG.

Carbon dioxide comprises 9-26% of all GHG, while methane is considered the second most important GHG, contributing 4-9 % to the GHG (Kiehl, J. T.; Kevin E. Trenberth, February 1997. "Earth's Annual Global Mean Energy Budget". *Bulletin of the American Meteorological Society* **78** (2): 197–208). If water, the most common GHG is excluded, CO₂ will be the top in the list and methane will be the second. Although having less global molar release than CO₂, methane has a global warming potential per kg (GWP) which is 23 times than that of CO₂. According to Equation (1.1), when converted, one mole of methane will produce one mole of CO₂. In other words, burning 16 tones of methane gives 44 tones of CO₂, however, because of the fact that methane has 23 times the GWP, the complete combustion of methane will result in an overall GWP decrease of 88%; therefore the conversion of fugitive emissions of methane to CO₂ will result in a very large decrease in

GHG. As stated before, homogenous combustion of methane requires relatively high methane concentration in air; however, exhaust streams from most of gas, oil, and petrochemical processes, and gas vented from coal mines have relatively low concentrations of methane, making them difficult to combust through common combustion technologies. In Canada, about 50 % of the GHG from oil and gas industries is in the form of methane emissions. Most of the emissions from oil and gas sectors result from extraction, processing, storage, and distribution of natural gas in terms of venting, leakage, or incomplete combustion. As stated in Canada's 2007 gas inventory, about 747,000 (kt CO₂ equivalent) GHG were emitted in Canada in 2007, from which 64,800 (kt CO₂ equivalent) were from fugitive gases, including about 21,300 (kt CO₂ equivalent) from natural gas, and 31,700 (kt CO₂ equivalent) from venting. As can be seen, fugitive emission contributes slightly less than 10% of the total greenhouse emissions in Canada, so reducing fugitive emissions can be a stepping stone towards reducing total GHG emissions.

1.1.2 Risk control in coal mines

Methane emissions in coal mines can cause serious problems. These methane emissions represent a hazard, especially when the coal is mined in an underground mine, and these emissions must be removed to ensure workers' safety. When accumulating up to the lower explosive limit of 5% by volume, lean methane emissions in mine atmosphere might become very dangerous, especially if mixed with coal dust ([Hayes, and Kolaczowski, 1997](#)).

Especially in the developing countries like India and China these emissions cause hundreds of deaths every year. As an example, a fatal methane explosion at one kilometer below the ground level took 101 lives at Zasyadko coal mine in Ukraine in 2007. Although less frequent in North America and Europe, gas explosions still occur, unfortunately. For example, a methane explosion took the lives of 26 miners at Westray mine in Nova Scotia, Canada, in 1992. Twelve miners were also killed by a gas explosion at the

Sago mine in West Virginia, USA in 2006. The most recent example of fatal coal mine explosion happened at the Big Branch mine 30 miles south of Charleston, in West Virginia, USA at April 5, 2010. At least twelve miners were killed and 10 were unaccounted for after the explosion.

(<http://www.nytime.com/2010/04/06/us/06westvirginia.html>, last visited July 18, 2010).

Ensuring that mine shaft methane concentration levels are at safe levels is crucial to workers' safety. As methane is present in the ground and it is released because of mining activities, the methane must be vented and the mine atmosphere must be cleaned and refreshed.

The technologies based on catalytic combustion, such as catalytic flow reversal reactor (CFRR) can present an efficient approach to tackle the problem of fugitive methane emissions (such as methane emissions in coal mines) (Salomons et al., 2003).

1.3 Scope of project

Catalytic combustion (defined mainly as an oxidation reaction happening on the surface of catalyst) has many unique features distinguishing it from the traditional homogenous combustion (Hayes, and Kolaczowski, 1997). The interest in catalytic combustion arises for two important reasons, for power generation and for mitigation of fugitive methane emissions.

Power can be generated by using the energy from combustion of natural gas in gas turbines (Choudhary et al., 2002). Natural gas has a clear advantage over other fuels because it burns most cleanly of all of the fossil fuels, with near-zero particulate matter. Burning natural gas results in production of smaller quantities of GHG (carbon dioxide and other pollutants) per unit of power generated because of high hydrogen to carbon ratio of natural gas. Nowadays, many power plants employ flame combustion (homogenous/thermal combustion) of natural gas to produce energy. It is worth mentioning that, the operating temperature of

flame combustion is in the range of 1773 to 2273 K. This high operation temperature range thermodynamically favors the formation of nitrogen oxides (NO_x), resulting from nitrogen and oxygen which are present in the air. NO_x emissions result in formation of photochemical smog. Moreover, NO_x emissions do have adverse effects on human health and aquatic and terrestrial ecosystems. According to the clean air act amendments (CAAA) which were introduced in the US in 1990, NO_x emissions must not exceed 25 ppm and the "best available control technology" must be implemented in new power plants. In addition, certain states of US enforce even more severe NO_x control regulations, for instance, Massachusetts and Texas are moving toward NO_x emission requirements of less than 9 ppm, while some areas in California require very low NO_x emission of 2.5 ppm (Smith et al., 2005).

All in all, allowable NO_x emission limits have been decreased over the last 10 years, this trend is expected to continue in the future (Smith et al., 2005). Catalytic combustion has the potential to be used as a replacement for homogenous combustion to meet the needs in reduction in NO_x emissions down to low single digit levels. Catalytic combustion is a flameless combustion usually proceeding at much lower operational temperatures than does the homogenous combustion. This lower operational temperature results in generating less nitrogen oxides, so the use of a catalytic reactor within the combustion system helps to maintain combustion flame temperature (and thus NO_x emission) at much lower levels than today's traditional flame combustors.

Fugitive methane emissions are dilute methane emissions in which methane concentration lies below the lower methane flammability limits (about 5 volume percent of methane in air), so these emissions cannot be destroyed by conventional homogenous combustion.

The mitigation of fugitive methane emissions is beneficial for both climate change reasons and safety. Moreover, these emissions are considered to be a source of wasted energy (Hayes, 2004). By converting these emissions to carbon dioxide through combustion, useful energy can be produced.

Catalytic combustion is a viable option to mitigate fugitive methane emissions and, as stated before, catalytic combustion happens at lower temperatures than homogenous combustion, so it produces less environmentally harmful by-products, moreover it can be used successfully to mitigate emissions which cannot maintain a conventional flame. In addition, the catalytic combustion unit is usually smaller than is a conventional firebox, so it can be located physically in or near areas where conventional units would not be allowed (Hayes and Kolaczowski, 1997).

The latter application of catalytic combustion is the focal point of this project. In this project, the effects of using different commercial catalysts (Pt-based and bimetallic Pt-Pd based catalysts) for the catalytic combustion of lean methane mixtures will be investigated. The catalytic combustion of methane was done under various experimental conditions such as different feed composition and different temperatures. In addition, to simulate the composition of exhausted gases resulting from natural gas engines, extra water was added to the feed.

1.4 Thesis organization

There are five chapters in this thesis. Chapter 1 introduces the problems caused by methane emissions and catalytic combustion is introduced as a viable solution to tackle the problem of fugitive methane emissions. Chapter 2 is a detailed review of methane catalytic combustion. Chapter 3 describes the experimental set up, experimental procedures, and analytical equipment. In Chapter 4, the results of ignition-extinction experiments on Pt and Pt-Pd bimetallic catalysts in the presence and absence of water are presented and discussed in detail. Results of catalyst characterization by instrumental neutron activation analysis, x-ray diffraction and x-ray photoelectron spectroscopy are also presented in Chapter 4. Finally, in Chapter 5, a summary of current research and recommendations for future work on this topic is presented.

Chapter 2: Methane catalytic combustion review

2.1 Characteristics and drawbacks of traditional combustion reaction, motivations for catalytic combustion

From prehistoric times, fossil fuel combustion has been the major source of the energy. In the modern era, with increasing energy demand, the use of combustion process in the energy sector has increased. On the other hand, combustion of the fossil fuels is one of the most important sources of the environmental pollution, so the environmental impacts of the combustion have become a major challenge in energy sector development and planning. To fulfill tightening environmental pollution regulations, the pollution from the combustion should be reduced by maximizing the efficiency of the combustion processes.

Among the fossil fuels, natural gas will be increasingly used as a source of energy in the future. Since the methane molecule contains four C-H bonds and only one carbon atom, combustion of methane yields the lowest amount of CO₂ (gas leading to the greenhouse effect) per unit of produced energy. With stricter regulations on CO₂ emissions to the atmosphere, this makes natural gas even more attractive as a fuel for the purposes of energy production. In addition, oil is considered to be a dwindling resource for energy; however the supply of natural gas and coal-derived methane is expected to last through the foreseeable future (Ciuparu, et.al, 2002). In a complete combustion reaction, a compound reacts with an oxidizing element, such as oxygen, and the products are compounds of each element in the fuel with the oxidizing element. In principle, carbon dioxide and water should be the only products of hydrocarbon combustion; however, most of the time, the combustion reaction is incomplete, which results in production of some pollutant components. To get a clear understanding of the combustion process, the combustion pattern in complete and incomplete combustion are described as follows: (“Automobile Emissions: An overview”, (August 1994)).

Complete combustion reaction

Fuel + air → carbon dioxide + water + unreacted nitrogen

Incomplete combustion reaction

Fuel + air → carbon dioxide + carbon monoxide + water +
unburned hydrocarbons + nitrogen oxides

A) Carbon monoxide (CO):

In the case of the incomplete combustion, CO will be produced; CO is one of the most harmful air pollutants. Internal combustion engines are one of the most important production sources of CO. CO is an odorless gas with a density similar to the density of the air. When CO is inhaled, it will react with the blood's hemoglobin to produce carboxyhemoglobin (COHb) which is a very stable complex of carbon monoxide and hemoglobin (in fact it is 310 times more stable than the complex of the oxygen and hemoglobin) which forms in red blood cells, and hinders delivery of oxygen to the body (López-Herce, et.al, 2005). The maximum concentration of CO in the streets of big cities might be more than 100 ppm; however, its concentration in the tunnels with automobile traffic can be about 300 ppm (Ebtakar T, 2004). Stopping in places with the CO concentration of 9 ppm for more than 8 hours or stopping in the places with the CO concentration of 35 ppm for more than 1 hour can damage the health of the people seriously (Ebtakar T, 2004).

B) Hydrocarbons (HC)

Other important pollutants resulting from the incomplete combustion is the hydrocarbons (with the general formula of C_xH_y). Based on the current statistics, about 50 percent of the

hydrocarbons in the air of the cities are a direct result of the performance of the vehicles. In addition to green house effects, hydrocarbons can produce health dangers as well.

C) Nitrogen oxides (NO_x)

Nitrogen oxides, which can be generated during combustion in air, are described by the generic formula NO_x . NO_x are considered to be important air pollutants. These oxides will result in acid rain, fog mist, destruction of the ozone layer and harm to the breathing system. High temperature and the presence of the oxygen and nitrogen are the most important causes of the NO_x production. Nitric oxide NO is the species that is usually generated initially in homogeneous combustion. Also quantities of nitrogen dioxide, NO_2 may be generated as a result of possible reactions between NO and O_2 . It is worth mentioning that, there is also possibility of the formation of significant amounts of nitrous oxide N_2O by catalytic reactions such as catalytic convertors, fluidized bed combustors (FBC), and selective catalytic reduction units (Hayes and Kolaczowski, 1997). N_2O is considered as an important green house gas because it is persistent in the atmosphere and it forms the main source of NO in the stratosphere. Hence, when the use of NO_x is considered in the context of catalytic or homogeneous combustion, the possibility of all species should be considered (Hayes and Kolaczowski, 1997). As NO is the species initially produced during homogeneous combustion, the different mechanisms through which NO is formed in combustion processes are described below (Ciuparu, et.al, 2002, Hayes and Kolaczowski, 1997):

1. Thermal NO is formed by coupling of oxygen and nitrogen in the air through the Zeldovich mechanism. The quantity of thermal NO is significant at temperatures higher than $1500\text{ }^\circ\text{C}$. The rate of thermal NO production increases nearly linearly with residence time and strongly depends on the flame temperature not only because of the exponential increase in the reaction rate but also due

to a shift in the N_2 , O_2 , NO equilibrium towards NO at higher temperatures.

2. Prompt NO will be formed as a result of fast coupling of nitrogen in the air with radicals that are formed at the flame front. Prompt NO is usually formed in combustion chambers operating with fuel-rich flames. Moderate temperatures and fuel-rich conditions favor a high level of prompt NO .

3. Fuel bound NO is formed by oxidation of nitrogen compounds present in the fuel. This oxidation process happens via the formation of intermediates. HCN is the most common intermediate formed during fuel NO production. Fuel NO levels depend only slightly on the flame temperature. Conversion of fuel nitrogen to NO is high in lean flames.

Natural gas, which consists mostly of methane, is a very clean fuel, with low contents of nitrogen and sulfur. This makes thermal NO the dominant path of NO_x production in most conventional natural gas-burning devices. Reduction of thermal NO is usually achieved by reducing the flame temperature and the residence time and/or by dilution or ultra-lean operation. However, in homogeneous combustion, this will promote the formation of CO and HC as well as producing an unstable combustion regime (Ciuparu, et.al, 2002).

D) Nitrogen (N_2)

The inlet air to the combustion chamber includes 79 percent of nitrogen, only a negligible portion of the nitrogen will transform to NO_x in the combustion process.

E) Carbon dioxide (CO_2)

As a result of the complete combustion, CO_2 is produced; CO_2 will stay as a stable gas in the air for a long time. Increasing the low concentration of CO_2 in the atmosphere does not have any harmful

effects on the animals; however, its increase is believed to be responsible for increase in temperature of the atmosphere.

F) Water vapor (H₂O)

Water vapor is one of the main products of the combustion; it is resulted from the bond formation between the hydrogen in the fuel and the oxygen of the air.

The most important concern of using natural gas as a fuel is the fact that, methane is a potent greenhouse gas (GHG).

Different GHG have different effects on the energy balance of the earth, so to compute and compare various GHG impact on global warming IPCC in its 1990 report introduced the concept of global warming potential (GWP) . GWP reflects the relative strength of individual GHG with respect to carbon dioxide impact on global warming over a defined period of time. GWP is defined as the cumulative radiative forcing between the present and some specified future time which is caused by a unit mass of GHG emitted now, expressed with respect to carbon dioxide.

For the reference purpose, the GWPs of methane as developed by IPCC are 62, 23 and 7 based on 20, 100 and 500 year time period. (the mean atmospheric lifetimes of carbon dioxide and methane are 50-100 and 12 years respectively). As it can be seen from the GWP values of methane for different time periods, GWP not only takes in to consideration the abilities of different GHG to absorb radiation, but also it takes in to consideration different atmospheric lifetimes of GHGs. The most commonly used value of GWP is based on 100 year time period. Based on 100 year lifecycle analysis, methane has a global warming potential 23 times that of CO₂, that is, one tonne of methane is equivalent to 23 tonnes of carbon dioxide; so, the removal of methane by conversion to carbon dioxide can offer the possibility of a substantial reduction in GHG potential. The combustion of one tonne of methane yields 2.75 tonnes of carbon dioxide, for a net reduction in GHG potential of 88%. Methane makes the second largest contribution to global

warming of all the GHG (about 19%), neglecting water, after carbon dioxide (about 64%) (Hayes, 2004).

A technology being able to achieve a complete combustion of the methane at relatively low operational temperatures (to avoid production of thermal NO_x) is highly desirable. Catalytic combustion is such a technology.

Catalytic combustion of methane has the following two important advantages over homogenous combustion of methane:

1. - Catalytic combustion of the methane can occur at lower temperatures in comparison with the homogenous combustion of the methane. This lower operational temperature will result in lower heat loss, easier control of the combustion system and most importantly less NO_x production.

2. -Catalytic combustion has no flammability limits, the flammability limit means the required range within which the homogenous combustion is feasible, this limit for methane is 5 to 16 volume percent of methane in the air. Homogenous combustion does not occur outside these limits.

Due to these advantages, catalytic combustion is an appropriate solution for the complete combustion of methane at lower temperatures with lower pollution emission without sacrificing the performance of the system (Hayes and Kolaczowski, 1997). In addition, selectivity of the catalytic combustion is excellent as carbon dioxide and water are usually the only products of the combustion (Lee and Trimm, 1995).

2.2 General catalytic combustion

Catalysis and combustion have a long time partnership that originated in 1818 when Sir Humphrey Davy, who was asked to study the safety lamps in coal mines, discovered that methane and oxygen on hot platinum wires can produce a considerable amount of heat in a flameless combustion. In 1836, Berzelius summarized the observations of the earlier chemists by stating that, small

amount of the foreign substances can greatly change the rate and the course of the chemical reactions, the effect of these foreign substances were called catalytic effects; In 1894, Ostwald, expanded the Berzelius's definition of catalyst and stated that, a catalyst is a substance increasing the rate of the chemical reaction without being consumed. In over 150 years since Berzelius's work, catalysts have played a major role in the chemical production, engineering research and innovation.

The interest in the catalytic combustion process and its corresponding reaction systems has been increasing recently because of the wide potential applications of this technology in different industries such as: using the catalytic combustion in the power generation systems (Lee and Trimm, 1995; Deutschmann et al., 2000; Lyubovsky et al., 2003), the extensive use of the catalytic combustion to reduce fugitive methane levels (Salomons et al., 2003), the wide use of catalytic convertors in the vehicles to reduce the emission levels of harmful gases (Lampert et al., 1997; Fujimoto et al., 1998), and the catalytic partial oxidation resulting in production of intermediate raw materials which are crucial to synthesize high value products.

The overall reaction of complete oxidation of methane is given by the equation:



The overall catalytic combustion process can be broken down in to the following sequence of individual steps:

- 1- Mass transfer of the reactants from the bulk fluid to the external surface of the catalyst and then diffusion of reactants in the catalyst pores.
- 2- Adsorption of the reactants on the surface of the catalyst.
- 3- Chemical reaction on the surface of the catalyst.

4-Desorption of the products from the catalyst surface.

5- Diffusion of the products in the catalyst pores and then mass transfer of the products from the external catalyst surface to the bulk fluid.

These steps occur simultaneously and the overall rate of the reaction is the rate of the determining step (i.e. the step with highest resistance). In other words, the overall rate of the reaction is governed by the rate limiting step (i.e. rate determining step) which is the step that is intrinsically the slowest step. Catalytic combustion is a highly exothermic reaction which produces a considerable amount of thermal energy when the reaction goes on, this large amount of released heat shall result in fast increase in the temperature of the reaction mixture. Knowing the relationship between parameters such as catalyst activity, and the mechanism and relative importance of heat and mass transfer process from the catalyst to the fluid flow, is necessary to get a clear understanding of the catalytic combustion.

The general pattern of the catalytic combustion is widely studied and it is well established. As it can be seen from [Figure 2.1 \(Lee and Trimm, 1995\)](#) increasing the temperature of a reaction mixture to a value indicated by point A in [Figure 2.1](#) will result in the start of combustion (initiation).

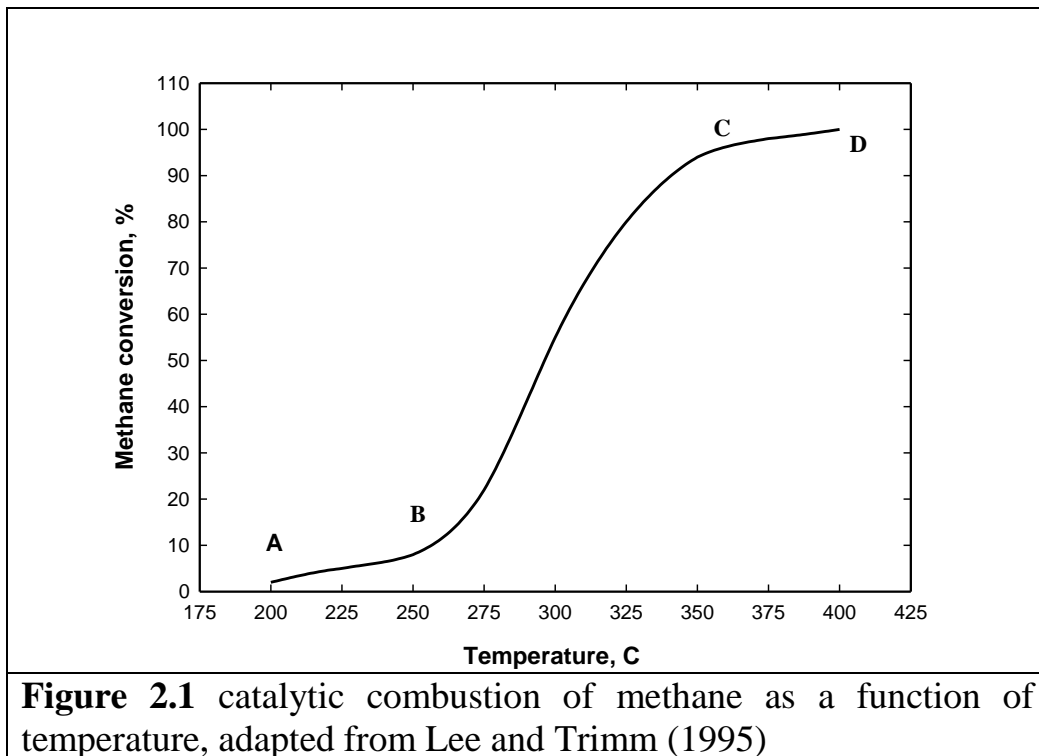


Figure 2.1 catalytic combustion of methane as a function of temperature, adapted from Lee and Trimm (1995)

(The initiation temperature depends on the catalyst and type of the hydrocarbon feed). By increasing the temperature to higher values a point will be reached where temperature increase will result in exponential increase in the rate of the chemical reaction (this is in the region around point B in Figure 2.1). When the temperature is increased more, a temperature will be reached where the mass transfer may become the controlling step (region around point C in Figure 2.1). Finally by increasing the temperature to the higher values, a point will be reached where all of the reactant is consumed (at temperatures above Point D in Figure 2.1). Based on the general pattern of the catalytic combustion, an important term called the "light off" temperature (aka "ignition" temperature) is defined, The light off temperature is defined as the inlet gas temperature where conversion is 50% (Hayes, and Kolaczkowski, 1997). It is worth mentioning that the kinetics of the catalytic combustion is only relevant to the regions where the intrinsic surface reaction is the controlling step (probably regions around Points A and B in the Figure 2.1). Once heat and mass transfer steps become the controlling steps; (probably region around Point C), geometry of the catalytic combustor and porosity of the catalyst and support are decisive parameters in determining the behavior of

the catalytic system. As mentioned above, the reaction will finally reach a point where at least one of the reactants is completely consumed, a large amount of thermal energy will be released as a result of complete consumption of the reactant(s), this huge amount of thermal energy can result in significant temperature increase, so the stability of the catalyst at such high operating temperatures is another important factor affecting the performance of the catalytic system (Lee and Trimm, 1995).

All in all, important factors such as reactivity of the catalyst (Region around Points A and B), heat and mass transfer effects (Region around Point C) and the maximum operational temperature reached (Region around Point D) should be considered simultaneously in designing and choosing the appropriate catalyst formulation for the application purpose.

2.3 Combustion Catalyst

Metal oxides and noble metals such as Pt, Rh, and Pd are used extensively as combustion catalysts. In general the activity of the noble metals is higher than metal oxide catalysts (Anderson, et. al, 1961). The catalytic combustion catalyst can be either supported or unsupported. Supported catalysts are usually preferred to bulk metal catalysts because of much better utilization of the metal which is present as small particles on the support surface (a large fraction of catalytic metal is at the surface) and the supported catalysts have much higher thermal stability than powdered metal catalysts. The support may also play a role in the oxidation reactions providing oxygen storage capability. In general an ideal catalyst for the catalytic combustion should have the following characteristics:

1- High activity

2-Relatively low ignition temperature, having low ignition temperature will greatly reduce the production of the NO_x, help to control emissions especially during start-up, and at the same time it

will reduce the construction cost of the reactor by decreasing the operational limits.

3- High thermal stability

4- Stable activity and high resistance to the poisons.

5-Low price

6-Nontoxicity

Unfortunately, no catalyst fulfills all of the above mentioned specifications, however the above specifications can be used to judge the performance of the catalysts and choose the appropriate catalyst for specific application(s).

2.3.1 Rare earth materials and other oxides:

Rare earth materials and metal oxides can be used as catalyst for the catalytic combustion without any modifications. Several rare earth oxides were tested by [Choudhary et al \(1992\)](#) using a pulse micro reactor; The results of the experiments in the presence of oxygen showed that the activities of these oxides are as follows: $\text{Sm}_2\text{O}_3 > \text{La}_2\text{O}_3 > \text{Yb}_2\text{O}_3 > \text{Eu}_2\text{O}_3 > \text{CeO}_2$. In all cases the conversion of the methane were lower than 30 percent indicating that none of these oxides is appropriate for the methane catalytic conversion at the tested conditions. Rare earth metals can also be used as additives to promote the catalytic activity of the metal oxides.

[Choudhary et al \(1997\)](#) tested the activity of MgO catalysts doped with rare earth material for different rare earth to magnesium ratios at 650-850 °C ; The results of the experiments showed that the presence of the rare earth material can greatly increase the activity of the catalyst mainly because of the important fact that the number of the basic sites will significantly increase and the number of acid sites will significantly decrease owing to the presence of the rare earth material. The general formula for this kind of the catalyst is A-BO_x , where A is the rare earth metal promoter component and BO_x is the metal oxide. It is worth mentioning that in the case of a catalyst doped with metal chloride, the promoter is likely to

evaporate at high temperatures which results in unrecoverable catalyst deactivation.

Perovskite-type catalysts are another group of the catalysts which have been suggested for the catalytic combustion of the methane. Perovskites are mixed metal oxides with FCC (face centre cubic structure) with large applications in the fields such as transistors, fuel cells and superconductive materials. The general structure formula for the perovskites is ABO_3 , in this formula A is the rare earth element (or the lanthanide cation) and B is a transition metal which is mostly responsible for the catalytic activity of the catalyst while A is mostly responsible for the structural stability of the perovskite catalyst. As shown by [Choudhary et al \(1992\)](#) $LaBO_3$ perovskite catalyst where (B= Mn, Co, Fe, Ni) shows comparatively high catalytic activity for the complete combustion of hydrocarbons. Perovskite based catalysts are relatively cheap and active, and they are more thermally stable for the methane catalytic combustion applications than noble metals catalysts, so they are potentially viable alternatives for the noble metals catalysts.

2.3.2 Noble metals

Noble metals such as Pt, Rh and Pd are used for the catalytic combustion of methane. The activity of the noble metals is generally higher than metal oxide catalysts. The noble metal catalysts can be used with or without support for the catalytic applications; however the supported ones are preferred for the oxidation reactions. The application of the noble metals other than Pd and Pt are limited for the purpose of the catalytic combustion because of the facts that the other noble metals have lower supplies, and they oxidize easier in comparison with Pd and Pt. Pt and Pd are thus the most widely used catalysts for the catalytic combustion of methane because of their excellent activity at relatively low temperatures and their better stability in comparison with other noble metals.

Pd easily transforms to PdO at temperatures lower than 1100 K, however PtO₂ can hardly be generated below 825 K and it is a very unstable compound. Because of the greater stability of PdO in comparison with PtO₂, in the case of Pd based catalyst the active phase is the PdO while in the case of Pt based catalyst the active phase is metallic Pt. The activity of the PdO is greater than that of Pt which will result in higher conversions for the PdO catalyst (especially on the methane lean side). As various parameters, such as loading of the metal, presence of the support and the pretreatments, can greatly affect the performance of the catalyst, a wide range of results have been reported in the literature for the performance and activity of the noble metal combustion catalysts. For example, in the case of the Pd/silica catalyst with a loading of 2.55% wt for a feed gas mixture of CH₄, CO, NO, and trace of H₂ and CO₂, the reaction started at 250°C, the mixture ignited at 325°C, and the complete conversion of methane is reached at around 400°C. These temperature values were relatively independent of the methane concentration. These corresponding values for the Pt catalyst were 450°C, 675°C and 900 °C respectively (Salaun, et. al, 2009). However, Pt catalysts show more resistance to the poisons such as sulphur (Meeyoo, et. al., 1998), water (Gelin, et. al., 2003) and Pt catalysts hardly sinter at low temperatures (Hurtado, et al., 2004). All in all, the performance of Pt based catalysts is more stable and it is a relatively "simple" catalyst mainly because of the fact that its phase behavior is much simpler than Pd based catalyst which undergoes complex phase transformations during the reaction with changing the temperature. Topics such as whether Pd or PdO is more active are still a matter of debate.

Although Pd catalysts are known as the most active catalyst for the catalytic combustion of methane, under certain circumstances Pt catalysts are proved to be more efficient methane combustion catalysts. Kinetic studies have showed that for the deep oxidation of lower alkanes (methane, ethane, propane and normal butane) over Pd, Ni and Pt catalysts supported on fibers, Pt catalyst supported on fiber is the superior catalyst for combustion of all alkanes but methane (Aryafar, et. al., 1997).

Burch, et.al (1994) showed that Pt/ alumina catalyst is a more efficient catalyst than is Pd/ alumina catalyst for high conversions of methane in the cases of stoichiometric or rich mixtures (with respect to methane). It is thought that Pt is a more important component than Pd in the multi metallic catalysts for the emission control of automobiles with natural fuels. Due to the great importance of the Pd, Pt and the bimetallic Pd/Pt catalyst for the catalytic combustion of methane, a detailed literature review for these catalysts will be presented in the next parts of this chapter.

2.3.3 Characteristics of supported Pt and Pd catalysts and effect of different parameters on their performance and activity

a) The effect of feed composition:

The oxygen/methane ratio in the feed has strong effects on the oxidation of methane to CO₂. Under O₂ rich conditions, the combustion of methane on Pt/alumina and Pd/alumina produces carbon dioxide (Trimm, et. al, 1980, Mouaddib, et. al, 1992). Under oxygen deficient conditions, carbon monoxide is also a product of the catalytic combustion (Trimm, et. al, 1980, Mouaddib, et. al, 1992). Selectivity to the carbon monoxide is also a strong function of temperature. Under oxygen lean conditions, the conversion of methane to carbon dioxide and water increases by increasing the temperature until the complete consumption of oxygen. At this point the formation of carbon monoxide is observed (Mouaddib, et. al, 1992). From this point, with increasing temperature the selectivity of carbon monoxide increases, until the point where carbon monoxide becomes the main product of the catalytic combustion for low O₂/CH₄ ratios (Trimm, et.al, 1980).

Since carbon monoxide is a product of methane catalytic combustion for lean oxygen mixtures, methane combustion over Pt/alumina and Pd/alumina was studied in the presence or absence of carbon monoxide in the feed (Oh, et. al, 1992). Under O₂/lean

and O₂/ rich conditions, the characteristics of methane catalytic combustion with feed containing carbon monoxide were exactly the same as those characteristics observed for the feed which was completely free of carbon monoxide. In both cases with increasing the temperature, the conversion of methane increased, after the light-off temperatures are passed, the similar asymptotic methane conversion levels were observed for temperatures above 550°C. Therefore it is believed that methane conversion is almost independent of the carbon monoxide content in the feed.

b) The effect of precious metal loading

The effect of the loading of the precious metal on the activity of the catalyst has been investigated widely in the literature. As an illustration, for methane conversions less than 10 percent (kinetic controlled regime), increasing the Pt loading in the range of (0.1 to- 2 wt %) caused the increase in the overall oxidation rate of methane (Niwa, M., et.al, 1983). Similarly, an increase in the Pt or Pd loading in the range (2.7 to-10 % wt) on γ -Al₂O₃ support increased the overall rate of the methane oxidation. Although, the overall rate of the methane oxidation increased as a result of the increase in the loading of Pt or Pd, the calculated activity per unit surface area of the metal decreased by increasing the loading (Cullis, et. al, 1983). As another example, the effect of increasing the Pt loading was investigated (0.027 to-100 wt %); these experiments showed that, when the loading was less than 1.4 wt %, the activity was almost independent of the Pt loading; however, for loadings above than 1.4 wt %, the activity of the catalyst increased until a maximum of activity reached at about 5 wt %; Further experiments showed that increasing Pt loading above 10 wt% caused the rate of reaction to decrease significantly (Otto, 1989).

c) Structure sensitivity

The search for a relation between catalytic activity and the properties of the supported material includes the study of the

influence of mean particle dimensions of metal crystals (metal dispersion) on the activity of catalyst. Structure sensitive reactions are defined as reactions which are affected by surface structure of the catalyst (i.e. crystallographic orientation). Boudart proposed a classification of catalytic reactions, depending on the behavior of catalyst activity with the metal dispersion in to two classes; 1) facile or structure in-sensitive reactions 2) demanding or structure-sensitive reactions. One criterion to decide whether a reaction is structure sensitive or not is to plot the catalytic activity or reaction rate (mol/s/g of catalyst) versus metal surface area (m^2/gr) as suggested by [Boudart et.al \(1966\)](#). If a reaction is structure insensitive, then rate of reaction per gram of metal increases linearly when the metal surface area per gram of metal increases. However, for a structure sensitive reaction, the rate of reaction per gram of metal is a nonlinear function of metal surface area per gram of metal catalyst. Another criterion to decide whether a reaction is structure sensitive is that, should the TOF (turn over frequency) calculated per number of surface atoms changes with catalyst particle shape or size, then the reaction is structure sensitive ([Page, 1987](#)).

Catalytic combustion of methane on precious metals was reported as a structure sensitive reaction in many cases ([Otto, 1989](#), [Hicks, et. al, 1990](#)). Structure sensitivity of the catalytic combustion of methane might be due to different reactivity of adsorbed oxygen on Pd and Pt surfaces ([Hicks, et. al, 1990](#)). It is thought that, in the case of Pt catalyst, two different types of the Pt particles exist on the surface of the support. One is well dispersed and relatively smaller Pt particles, and the other is relatively bigger crystallites of Pt. In the former case, oxygen makes Pt change to PtO_2 . However, in the latter case, the oxygen is absorbed on the crystallite surface of Pt providing absorbed oxygen with high reactivity. It is concluded that, reactivity of larger Pt particles (crystallites of Pt) is higher than the reactivity of smaller Pt particles ([Hicks, et. al, 1990](#)).

A similar explanation is proposed for the Pd-based catalysts. In the case of Pd based catalysts, oxidizing the Pd catalyst in the excess

amount of oxygen will reduce the particle size of Pd. Oxidizing of small crystallites of Pd will result in formation of dispersed PdO on the support while, oxidizing large crystallites of Pd will result in formation of dispersed PdO on the crystallites of Pd.

It is believed that small crystallites of Pd which are completely oxidized, are catalytically less active than large crystallites of Pd whose external surfaces are partially oxidized, so the large crystallites of Pd is believed to be catalytically more active than small Pd crystallites (Hicks, et. al, 1990).

However, in clear contrast with the above mentioned results, some researchers reported that in the case of supported Pd catalyst, there was no clear relationship between the activity of the catalyst and the particle size of Pd once the rate was measured in terms of specific rate constants (Baldwin and Burch, 1990).

d) The effect of pretreatment conditions

It is widely believed that, the activity of supported Pt and Pd based catalysts significantly depend on the gases which are used for the pretreatment of the catalyst. The effect of pretreatment with gases such as H₂, O₂ and He on the activity of Pt and Pd based catalysts was studied. In the case of pretreatment with H₂, the activity of the catalyst increased however, in the case of pretreatment with O₂, the activity of the catalyst decreased significantly (Cullis, and Willatt, 1983, Otto, 1989).

The reactant gas mixture was also used for the pretreatment of the supported catalyst (Briot and Primet, 1991). For the sake of simplicity, in the following paragraphs, the catalyst only pretreated and reduced by H₂ is called State I catalyst, while the catalyst pretreated with O₂/CH₄ mixtures (100% conversion of methane) after reducing with H₂ is called State II catalyst. In the case of Pd/Al₂O₃ catalyst, the activity of the State II catalyst is reported to be significantly higher than the activity of the State I catalyst (Briot and Primet, 1991, Baldwin and Burch, 1990, and Hicks, et.al, 1990).

The catalytic combustion of CH₄ for State II catalysts started at significantly lower temperatures and the light-off temperatures were also much lower than the light off temperatures of the State I catalyst (Briot and Primet,1991, Baldwin and Burch, 1990, and Hicks, et. al, 1990).

Several explanations for the increase in the activity of the supported Pd based catalysts as a result of pretreatment with O₂/CH₄ mixture (after reducing with H₂) were proposed. One possible explanation is that, when the pretreatment happens, the PdO crystallites will experience some kind of reconstruction resulting in the increase of the catalytic activity (Baldwin and Burch, 1990).

The other possible explanation is based on the probable significant changes in the reactivity of adsorbed oxygen because of the change in the size of the particles of the noble metals during the pretreatment (Baldwin and Burch, 1990). In addition, the increase in the metal particle size could also result in a corresponding decrease in the chemisorptions heat of oxygen as has been observed for large metal particles (Lee and Trimm, 1995). This explanation is somehow similar to the explanation given for the structure sensitivity of the Pd based catalyst (Hicks, et. al, 1990). In the case of Pt/Al₂O₃ catalyst, the supported Pt catalyst in the State II was more active than the State I supported Pt catalyst at temperatures between (300 to-550 °C) (methane conversions was less than 30 %), For the temperatures greater than 550 °C both catalysts had almost the same activity (Briot, et. al,1990). All in all, pretreatment with reactant mixture (O₂-CH₄-carrier gas) will result in more active catalyst than those catalyst pretreated only with H₂.

e) The effect of supports and doping

Noble metals are usually dispersed on an appropriate support to increase the cost efficiency. In addition, as stated before, supports can greatly help to stabilize the catalyst thermally.

For the methane catalytic combustion applications the natures of the support and the support-catalyst interactions have a significant effect on the thermal stability and the activity of the catalyst. The effect of catalyst-support interactions on the activity of Pd and Pt based catalysts has been investigated extensively when different metal oxides are used as support (Cullis, et. al, 1983, Niwa, et. al, 1983). When the catalytic combustion of methane was performed over Pt based catalyst on SiO₂, Al₂O₃, and SiO₂-Al₂O₃ supports, the results showed that the activity of the supported Pt based catalyst decreased in the following order : Pt/SiO₂-Al₂O₃ > Pt/Al₂O₃ > Pt/SiO₂ (Niwa, et. al, 1983). However, in the case of the Pd based catalyst reduced with hydrogen, reduced Pd/SiO₂ was more active than reduced Pd/Al₂O₃ (Hoyos, et. al, 1993). For Pd and Pt catalysts supported on γ -Al₂O₃, ThO₂, and TiO₂, the activity of the both catalysts decreased in the following order: γ -Al₂O₃>TiO₂> ThO₂ (Cullis, et. al, 1983).

As it is stated before, support has a significant effect on the life time of a catalyst, when the catalytic combustion of methane was studied over Pt based catalyst supported on γ -Al₂O₃ and α-Al₂O₃ fibers, it was observed that the activity of Pt/ γ -Al₂O₃ was stable and constant for at least 100 h , On the other hand, in the case of methane combustion over Pt/ α-Al₂O₃ product composition varied after only 40 h of operation and CO was produced (in the first 40 h of the operation, CO₂ was the only product of the catalytic combustion on Pt/ α-Al₂O₃) (Trimm, et.al, 1980). It is thought that alumina supported catalysts can last longer than silica supported catalysts under the catalytic combustion operating conditions (Baldwin, et.al, 1990). This observation was explained on the basis that sintering of silica supported catalyst can happen more easily under common catalytic reaction conditions than does the sintering of alumina supported catalyst.

f) Poisons

Poisons are considered to be the one of the most important causes of catalyst deactivation. Sulphur containing compounds are the

most common poison for supported Pd based catalysts because of the irreversible adsorption of sulphur compounds on Pd.

Catalyst activity decreased by 90% and the ignition temperature was raised by about 150 K with the presence of only 100 ppm of H₂S in the feed (Arrosio, et.al, 2007). Although having a different poisoning mechanism than sulphur, chlorine is another possible poison for supported Pd based catalyst. The other important poison is water which is present in all exhaust streams because it is a product of combustion reactions (which is commonly the case for catalytic combustion). Water can cause a significant inhibition to the catalyst activity when present in the feed stream. Deactivation with water is only partially reversible (Cullis, et.al, 1972). This observation has been confirmed by several investigators. For example, when the catalytic stability of Pd/ γ -Al₂O₃ (5wt %) was tested in the presence of water vapor, the inhibition effect was clearly observed (Persson, et.al, 2007). In these experiments the temperature was kept constant at 500 °C and the water concentrations in the feed stream were 1.25, 2.5, 5, and 10 volume percent. It was seen that in the absence of water, the methane conversion dropped from 100 % to 88% in one hour, however, when 5% water vapor was present in the feed, the conversion decreased drastically from 88% to 40% in only 20 minutes of operation. Only part of the activity was recovered when the water was stopped. In another set of experiments on Pd/Al₂O₃ (7.3wt %), the apparent activation energy of methane catalytic combustion was measured between 200-320°C for dry feed and the feed at the presence of 2 volume percent of water. In the case of the dry feed, the activation energy was 86 kJ/mol; however, in the case of the wet feed, the activation energy increased to 151 ± 15 kJ/mol (van Giezen, et.al, 1999). The inhibition effect of water can be influenced by other parameters. Supports with high oxygen mobility might have the potential to hinder the inhibition effect of water, for example, it is reported that the activity loss caused by water can be removed in 1 hour by cutting off the water stream if the (HSA γ -Al₂O₃) is replaced by (LSA α -Al₂O₃) which has higher oxygen mobility (Ciuparu, et.al, 2002). It is also suggested that,

adding additives like Pt to Pd catalyst can also mitigate the activation inhibition caused by water (Cullis, et.al, 1972).

g) The effect of temperature

The reaction temperature has a significant effect on the level of the activity of the supported Pd catalyst in two ways. Firstly, there is an apparent shift in the activation energy of methane catalytic combustion on Pd catalyst as the temperature increases. The temperature where this transition happens has been reported to be a function of catalyst starting composition (Hayes, et.al, 2001).

Although it is crucial to differentiate changes in apparent activation energy occurring as a result of the onset of mass and heat transfer effects, there is sufficient evidence in the literature indicating that there is indeed a genuine activation energy shift in the reaction. Cullis and Willatt, (1983), studied the methane combustion over supported Pd catalysts in the temperature range of 500-800 K and they observed a sharp change in the values of reaction activation energy. Depending on the catalyst structure, catalyst loading, supporting material, and the reactant composition, the transition temperature changed from 625-720 K. Below the transition temperature, the activation energy varied from 75 to 95 kJ/mol. Above the transition temperature, the activation energy decreases to a value in the range 23-45 kJ/mol. Sakai et.al (1991) studied the performance of a catalytic convertor attached to a natural gas fueled engine, they reported that the performance of Pd catalysts underwent a transition as temperature increased. They reported a value of 690 K for the transition temperature. Below the transition temperature, the value of activation energy was 76.5 kJ/mol. However, above the transition temperature the value of activation energy dropped to 61 kJ/mol. Liu et.al (2001b) studied the catalytic convertor for a natural gas/diesel dual fueled engine. They also found that apparent activation energy changed as temperature increased. In their investigation all mass and heat transfer steps were included explicitly in their model, so the shift in activation energy was not a result of heat and mass transfer effects. Secondly,

the activity of the supported Pd catalyst will also change with the temperature elevation because of the fact that transformation between Pd and PdO will take place. The activity of the catalyst will increase with temperature increase up to around 975 K, then because of the thermal decomposition of PdO to Pd, the activity falls continuously with increasing the temperature up to 1050 K where the PdO is completely converted to Pd. Further increase in temperature will again increase the activity because of the increase in the rate constant of reaction (Datye, et.al, 2000).

2.3.4 Pt-Pd bimetallic catalyst

Because of the excellent activity for methane oxidation, supported Pd based catalysts are used frequently in industry, however Pd based catalysts have some major clear drawbacks. Depending on the nature of the support and oxygen concentration, PdO will usually decompose to Pd at temperatures in range 900-1200 K, when the catalyst is cooled, PdO will be reformed at a lower temperature than the decomposition temperature. This will result in inherent instabilities in the performance of the catalytic convertor. Another disadvantage of the Pd based catalysts is that, even at temperatures lower than the decomposition temperature of PdO, although having high initial activity at these temperatures, the catalyst will lose some of its activity during extended time periods resulting in instability of the activity level of the catalyst. For this reason, the catalytic combustion of methane will become increasingly difficult with time of use. Because of the high initial activity of the supported Pd-based catalysts, one of the important challenges and goals is to increase the stability level of the catalytic activity of the Pd based catalysts. It is suggested that one can greatly improve the stability of supported Pd catalysts by adding a second metal resulting in forming a bimetallic catalyst. Bimetallic catalysts have been used extensively in the field of catalysis and they have been proved to promote both the selectivity and activity level of a great number of catalytic reactions. To produce the desirable effect, the bimetallic catalyst must have the right combination of metals. It is thought that, the change of the

behavior of a bimetallic catalyst results from factors like, geometric effects, electronic effects or the presence of the mixed sites. Nevertheless, how a bimetallic catalyst works is not fully understood yet. Most of the reports about the use of bimetallic catalysts for catalytic combustion applications consider Pd/Pt catalysts. It is reported that, by addition of Pt to a Pd catalyst, the resulted bimetallic catalyst can maintain the high activity level for methane combustion for longer times than does the monometallic supported palladium catalyst. It is also reported that Pd/Ag is also capable of prolonging the activity of the catalyst for methane combustion applications. The excellent stability of Pd/Pt bimetallic catalyst for catalytic combustion of methane has been attributed to suppression of the particle growth and high dispersion of supported particles. Whether the activity is higher for Pd/Pt bimetallic catalyst compared with monometallic Pd catalyst is still a debatable question ([Persson, et. al., 2005](#)).

Another important characteristic of a bimetallic catalyst is the effect of water on the activity of it. It is reported that, when additional water is added to the reaction system, Pd/Al₂O₃ catalysts will lose their activity relatively quickly and even when the water is removed, the activity is not completely recoverable. Although the activity of Pd/Pt bimetallic catalyst is also harmed by the presence of the extra water in the feed, this activation loss is less severe and the activity loss is completely recoverable when the water is removed ([Persson, et. al., 2007](#)). It is suggested that, the improvement caused by addition of Pt to the Pd catalyst might be because of the interaction between Pt and Pd, although the resistance of the bimetallic Pt/Pd catalyst to sulfur poisoning did not improve in comparison to Pd monometallic catalyst ([Larpisardi, et. al, 2007](#)). Based on the above interesting observations, the bimetallic Pt/Pd catalyst can be a viable alternative for monometallic Pd catalyst for low temperature combustion of methane.

Chapter 3 Experiments and procedures

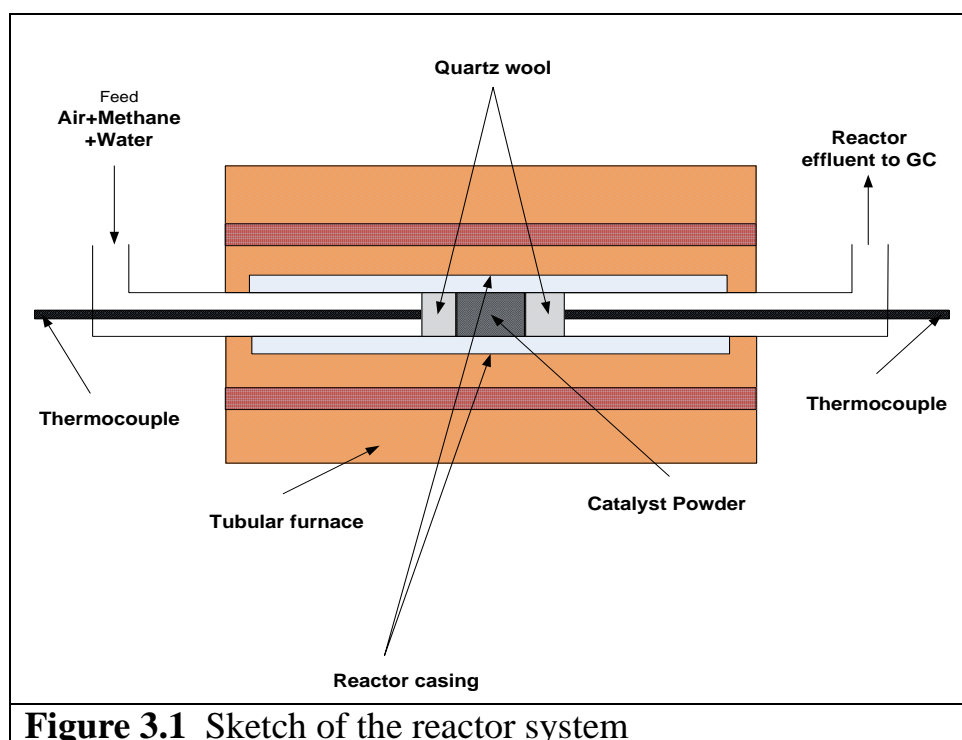
As discussed in the second chapter, although having excellent activity, supported Pd based catalysts do have some major drawbacks (instabilities in the performance of the catalytic convertor, losing the activity with increasing time on stream, and negative effect of water on the activity of the catalyst). To handle these inherent drawbacks of the supported Pd based catalysts, especially to increase the stability, adding a second metal to form a bimetallic catalyst is highly recommended. Moreover, although Pd catalysts are widely used in industrial applications, there is still a lot of disagreement over the general behavior of supported Pd based catalysts and the mechanism of methane combustion over them. The main focus of the experimental part of this project is on four topics.

- 1- Investigating the general performance of monolith Pt, and Pt-Pd catalysts for methane combustion.
- 2- Investigating the effect of parameters such as: temperature and feed composition (i.e. water vapor and methane concentration) on the activity of supported Pt and Pd-Pt catalyst.
- 3- Investigating the effect of different pretreatments on the activity level of the catalysts.
- 4- Characterization of the catalysts to analyze and categorize the reasons for probable different behavior of the catalysts.

The description of experimental devices, materials, experimental procedures, and characterization methods used in this project are given in this chapter. The next chapter shall cover the detailed results of experiments.

3.1 Experimental apparatus and materials

An appropriate reaction system was designed and constructed for experimental purpose of this project. The reaction system includes a micro-reactor, an oven, several gas and water supplies, and analyzers (gas chromatograph (GC), flow meters, and thermocouples). [Figure 3.1](#) presents a diagram of the reaction system, while [Figure 3.2](#) is a photograph of it.



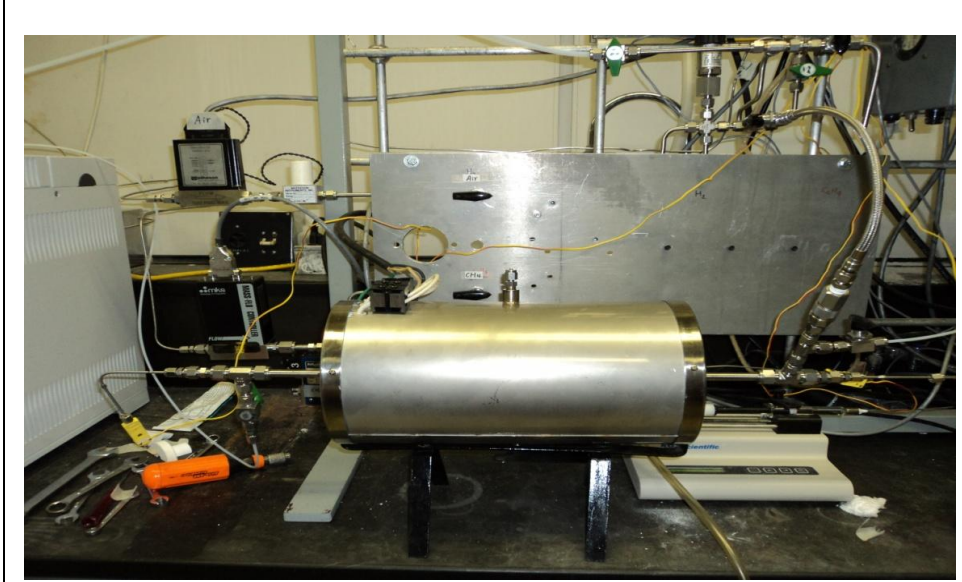


Figure 3.2 Photograph of the reactor system



Figure 3.3 Photo of micro-reactor

Micro-reactor: The micro-reactor is comprised of two parts, the inner tube and outer sleeve. The inner tube is a standard wall 3/8" diameter tube made from 316 stainless steel. The length of the tube is 20 inches. The outer sleeve is also made of 316 stainless steel with an outside diameter of 7/8". A hole is machined through the center of sleeve with a diameter of 3/8". The inner tube was inserted in the hole of the sleeve. A thermocouple well of 1/8" diameter is also drilled to a depth of 5" in the outer sleeve. The outer sleeve serves as a large thermal mass with good heat conducting in order to achieve relatively constant temperature along the wall of the reactor. A photograph of the micro-reactor can be seen in [Figure 3.3](#). During the reaction the micro-reactor (inner tube and outer sleeve) are placed inside an oven. A desired amount of the catalyst (of the order of 0.5 g) was placed inside the reactor. Layers of quartz wool were placed before and after the catalyst bed to prevent the catalyst powders from leaving the reactor. An Opto-22 system was connected to the reaction system so that all of the experimental conditions were recorded on a computer (every 30 s) by software called Lab-view, although these parameters are set manually and are controlled by a temperature controller and a gas flow meter.

Catalysts: The catalysts used in the experiments, were provided by Umicore group. The catalysts were supported Pt and bimetallic Pt-Pd catalysts. These catalysts are low temperature oxidation catalysts designed for catalytic convertors. To fit in the reactor, the monolith cores were crushed, ground, and screened to the particles of size 300-420 μm . A photo of the crushed catalysts used in this project is shown in [Figure 3.4](#).



Figure 3.4 Catalyst samples; Pt-Pd and Pt catalyst(left to right)

Sensors and analyzers: Temperature in the reaction system was monitored by means of three thermocouples (TC, K-type from Omega). TC1 and TC2 were placed in the reactor (i.e. inner tube), at the upstream (before the catalyst sample), and at the downstream (after the catalyst sample), respectively. The average of temperatures recorded by TC1 and TC2 is reported as reaction temperature. The third temperature controller TC3 was placed in the 1/8" diameter hole drilled in the outer sleeve. TC3 was connected to the temperature controller for temperature control. Finally, at the outlet of the reactor, a part of the reactor exhaust stream was imported in to a gas chromatograph (GC) for composition analysis. This GC is HP-7890-A type (Agilent Technologies incorporation) with a HP-Plot capillary column (30 m long, 40 μm in diameter) and the carrier gas flow (helium) rate was set at 15 cm^3/min .

Gas and water supply: All of the gases used in the experiments were taken from high pressure cylinders purchased from Praxair. The gases were 10 % methane in nitrogen mixture, 2 % methane in

nitrogen mixture, hydrogen (ultra high purity, UHP, 5), nitrogen (UHP, 5), helium (carrier gas for GC, UHP 5) and dry air (extra dry). The feed to the reactor consisted of the methane in nitrogen mixture and air, in order to investigate the effect of water in some runs water is added by a syringe pump (5 cm³ in volume) in to the inlet of the reactor where water was evaporated by a heat gun and then carried in to the reactor by other feed gases. Two gas supply lines, both with a flow meter, were used, Line 1 for air only and Line 2 for methane in nitrogen mixture. The flow meter used to measure the air flow was Matheson Modular DYNA-blender model 8250 and the flow meter used for methane was MKS Type 1479. Both of the flow meters were calibrated before using in the experiments. It is worth mentioning that, the calibration of both flow meters were checked every week. In addition, the flow rates of air and methane were measured and compared at beginning and end of each experiment to become sure that the flows rates were constant during each experiment.

3.2 Experimental procedures

It is important to mention that experimental procedures were fixed after the exploratory tests, which were done to find the appropriate experimental procedures needed for reproducibility and repeatability of experiments; the exploratory tests are explained in the next chapter ([Chapter 4 Results and Analysis](#)), their procedure and conditions will be discussed individually. For more detailed information see the run list in the [Appendix A](#).

3.2.1 Reactant compositions:

In the experiments in the absence of water, the flow rate of air was fixed at 225 ± 0.8 cm³/min, and the flow rate of methane in nitrogen streams (10 % and 2% methane in nitrogen) were adjusted to give nominal methane concentrations of 837 ± 4 , 1524 ± 33 , 2122 ± 14 , 4067 ± 20 and 5931 ± 102 ppm.

In the experiments with the presence of additional water, the flow rate of air was fixed at $213.7 \pm 0.8 \text{ cm}^3/\text{min}$. water was added to the feed stream to achieve a water concentration of 5 % (mole basis) in the feed. The flow rate of methane in nitrogen streams (10 % and 2% methane in nitrogen) were adjusted to get methane concentrations of 836 ± 4 , 1526 ± 33 , 2122 ± 14 , and 4064 ± 20 ppm.

Experiments were done using 2 different catalysts (Pt/Pd bimetallic catalyst and Pt based catalyst) with the same total precious metal weight loading. A detailed list of experiments is given in [Appendix A](#).

3.2.2 Ignition and extinction curves of methane catalytic combustion:

The main goal of Ignition-Extinction tests was to realize the effects of experimental conditions on the behavior of methane catalytic combustion. The effect of different experimental conditions such as catalyst pretreatment, methane concentration, reaction temperature and presence of water on the performance of 2 different catalysts (Pt/Pd bimetallic catalyst and Pt based catalyst) were studied. A series of exploratory experiments were done to determine experimental procedures resulting in reproducible results; these procedures are discussed below:

a) Reduction pretreatment:

Reduction pretreatment was done before some of the experiments to investigate the effect of reduction on the performance of catalysts. First, hydrogen flow was started ($40\text{-}50 \text{ cm}^3/\text{min}$). Then the reactor temperature was raised to 500°C to reduce the catalysts. After reaching 500°C , the temperature was kept constant for 30 minutes. After that the hydrogen flow was cut off and the reactor was flushed with nitrogen and the catalysts were cooled down in nitrogen flow until the temperature reached room temperature. After that nitrogen flow was cut off and the reactor was left over night in flowing air ($50 \text{ cm}^3/\text{min}$).

b) Ignition-Extinction experiments

The experiments consisted primarily of steady-state ignition and extinction (IE) curves. In these tests, the temperature was increased or decreased stepwise. The operation parameters were held constant during at least one hour for each temperature step. At least two gas analysis were performed at each temperature stage.

During ignition curve, the experiment started at a temperature between 300 °C and 500 °C (depending on the activity of catalyst), then the temperature was raised stepwise by 40 or 50 °C at a time up to 650 °C or the temperature at which 100% CH₄ conversion was reached. During extinction curve, the temperature was decreased stepwise from the methane full conversion temperature (or 650 °C) to analyze the reaction behavior during cooling at different temperatures. The extinction curve and the whole experiment were ended at temperature region at which the ignition curve was started.

3.3 Catalyst characterization:

Characterization tests are crucial to get a clear understanding of the morphology and composition of the catalyst samples. This understanding gained by the help of the characterization methods might greatly help us to analyze the behavior of the catalyst. Three analytical methods were used for characterization: instrumental neutron activation analysis, X-ray diffraction, and X-ray photo electron spectroscopy.

3.3.1 Instrumental neutron activation analysis (INAA):

Instrumental neutron activation analysis is an analytical technique used for determining the elemental concentrations of solids. The great advantage of this method is that, there is no need for catalyst dissolution in this method. This method is considered to be one of

the most accurate characterization methods used for determining the elemental composition of solids. This method is able to detect elemental concentrations as low as sub-ppm ranges. (http://archaeometry.missouri.edu/naa_overview.html , "Overview of Neutron Activation Analysis", last visited January 27, 2011). In this method, the catalyst sample is first made radioactive by bombardment with suitable nuclear particles, and then by counting the gamma rays emitted from the radioactive isotopes, the elemental concentrations are determined. In this project, INAA is used to measure the elemental concentrations of Pd and Pt in the catalysts.

Four samples, two from each of the two different types of the catalysts used in this project, were sent to Slowpoke Nuclear Reactor facility at the University of Alberta for INAA.

3.3.2 X-Ray diffraction (XRD):

X-ray diffraction is one of the oldest and the most frequently used characterization methods in the field of catalysis. This method is frequently used to identify crystalline phases present inside catalyst samples by means of lattice structural parameters, and to obtain an indication of crystal size. XRD depends on the constructive interference of radiation scattered by relatively large parts of the catalyst sample, so this characterization technique requires long range order. Having wave lengths in the angstrom range, X-rays have sufficient energy to penetrate solids therefore X-ray emissions are well suited to probe internal structure of solids. X-ray diffraction is the elastic scattering of X-ray photons by atoms in a periodic lattice structure. The scattered monochromatic X-rays which are in phase give constructive interference. The lattice spacing can be derived by using Bragg relation:

$$n\lambda = 2d \sin(\theta) , n = 1,2, \dots \quad (3.1)$$

In the above equation: λ is X ray wavelength, d is the distance between two lattice planes, θ is the angle between incoming X rays and the normal to the reflecting lattice plane, and n is an integer which is called reflection order.

By measuring the angle under which constructively interfering X-rays leave the crystal lattice, one can use the Bragg relation to determine the corresponding lattice spacing which are characteristics of compounds and allow the identification of phases present in the catalysts sample. XRD pattern of the powdered samples are usually measured with a stationary X-ray source (usually Cu-K α) and a movable detector that scans the diffracted radiation intensity as a function of angle 2θ between the incoming and diffracted beams. When working with powdered polycrystalline samples, an image of diffraction lines happens because only a small fraction of the powdered particles will be oriented in such a way that by chance a certain crystal plane is at the right angle θ with the incident beam to produce constructive interference. Mainly in catalyst characterization, diffraction patterns are used to determine the crystallographic phases present in the catalyst sample. XRD has an important limitation: clear diffraction peaks can only be observed when the catalyst sample possess sufficient long range order. The clear advantage of this limitation is that the shape or the width of diffraction peaks can be used to obtain information on the dimensions of the reflecting planes. Diffraction lines of perfect crystals are narrow; however, for crystallite sizes below 100 nm peak broadening happens because of incomplete destructive interference in scattering directions where the X-rays are out of phase. The Scherer formula can be used to relate crystal size to peak width:

$$d_{avg} = \frac{0.9\lambda}{(FWHM)\cos(\theta)} \quad (3.2)$$

Where d_{avg} is the average particle size, λ is the wave length of the $\text{CuK}\alpha$ radiation (0.1543 nm), FWHH is the width at half height of the diffracted peak in radians, and θ is half of the diffraction angle.

All in all, XRD has advantages and weaknesses for catalyst investigation: this method gives clear information about the crystalline phase present inside the catalyst sample; in addition, it gives us an indication of crystal size. On the other hand, because of the fact that XRD rests on the interference between reflecting X-rays from lattice planes, it requires samples possessing sufficient long range order, so particles which are either amorphous or crystals which are too small give either broad and weak diffraction lines or no diffraction lines at all, therefore, if catalysts samples contain crystals of varying size, XRD might only be able to detect the large ones (Niemantsverdriet, 2000). XRD facilities in the Department of chemical and materials engineering were used to examine the catalysts used in this study.

Eight samples were examined by XRD. All samples were examined as finely ground powders with particles of size 300-420 μm . The first four samples were: fresh Pt and Pt-Pd catalysts (fresh Pt and Pt-Pd catalysts were used for ignition-extinction experiments in the absence of water), stabilized steam-aged Pt and Pt-Pd catalysts (the steam-aged catalysts were mainly used for ignition-extinction experiments in the presence of water). The next four samples were obtained by reducing the first four samples with hydrogen pretreatment as described in Part a, section 3.2.2 in this chapter). This was done to investigate the effect of reduction on the structure of fresh and steam-aged Pt and Pt-Pd catalysts. XRD patterns were recorded over the 30-50 $^{\circ}$ 2θ range in the step scan mode. The step size was 0.05 $^{\circ}$ per step at a step time of 8 s.

3.3.3 X-ray photo electron spectroscopy (XPS)

Photoemission spectroscopy is based on photoelectric effect. A sample irradiated with light of sufficiently small wavelength will emit electrons. These emitted photoelectrons can be used to obtain information about the surface of catalyst. XPS is among the most

frequently applied techniques in characterization of the solid surfaces, it provides surface sensitive information. XPS yields valuable information about elemental composition, and the oxidation state of the elements. As mentioned before, XPS is based on the photo electric effect, in which an incident X-ray photon is absorbed; next a photoelectron will be emitted. Measuring the kinetic energy of the photoelectron allows the calculation of the binding energy of photoelectron in XPS. Measuring the intensity of photoelectrons $N(E)$ as a function of their kinetic energy, allows the drawing of the XPS spectrum (a plot of $N(E)$ versus binding energy E_b). By consulting binding energy tables, different elements present on the surface can be determined. Moreover, binding energies are not only element specific but also they contain valuable chemical information, because energy levels of core electrons also depend on the chemical state of the atom. For example, the binding energy usually increases with increasing oxidation state, and for a fixed oxidation state the binding energy usually increases with the electro negativity of the ligands, so XPS can provide one with the surface region composition and it can help to distinguish between different chemical states of one element (Niemantsverdriet, 2000). XPS facilities available at Alberta Centre of Surface Engineering and Science were used to determine the oxidation state of surface metal species after various pre-treatments and exposure to various reacting environments.

Chapter 4: Results and Analysis

4.1 Preliminary tests

Different experiments were performed at the beginning of the study to:

1. Get a general idea about the catalyst behavior, and
2. Find appropriate pretreatments required to make the catalyst behavior reproducible. Ageing or high temperature pretreatment in air can often stabilize the performance of the catalysts. It should be noted that “Umicore” company, the manufacturer of these catalysts employed ageing process to produce stable catalysts. They heated catalyst samples in air flow at 650°C for 10 hours.

4.1.1. Pt-Pd bimetallic catalyst

Three exploratory tests were performed on the catalyst to obtain preliminary understanding of catalyst behavior. In the first two tests, the catalyst was reduced following the procedure described in [Chapter 3](#). The results from reduced samples can be seen in [Figure 4.1](#) and [Figure 4.2](#). In the third test, the catalyst was not reduced; the results of this test can be seen in [Figure 4.3](#) (all exploratory tests were done at constant methane concentration of 5931 ppm).

Several interesting observations can be made from these figures. First of all, although the general trend does follow the classic pattern of ignition-extinction curves (i.e. at low temperatures the catalyst is not active, hence the conversion is zero. The conversion starts to increase with a temperature increase and then as the reaction ignites the conversion rises to 100 percent). There appears to be a change in the slope of ignition curve at about 550 °C which might be a result of changes in the surface structure of the catalyst at this temperature.

Secondly, the performance of the catalyst in the tests after reduction pretreatment is very similar, indicating that the reduction pretreatment stabilized catalyst activity.

Thirdly, the ignition and extinction curves are almost identical in all three experiments, showing that the performance of Pt-Pd catalyst has not been influenced by reduction pretreatment.

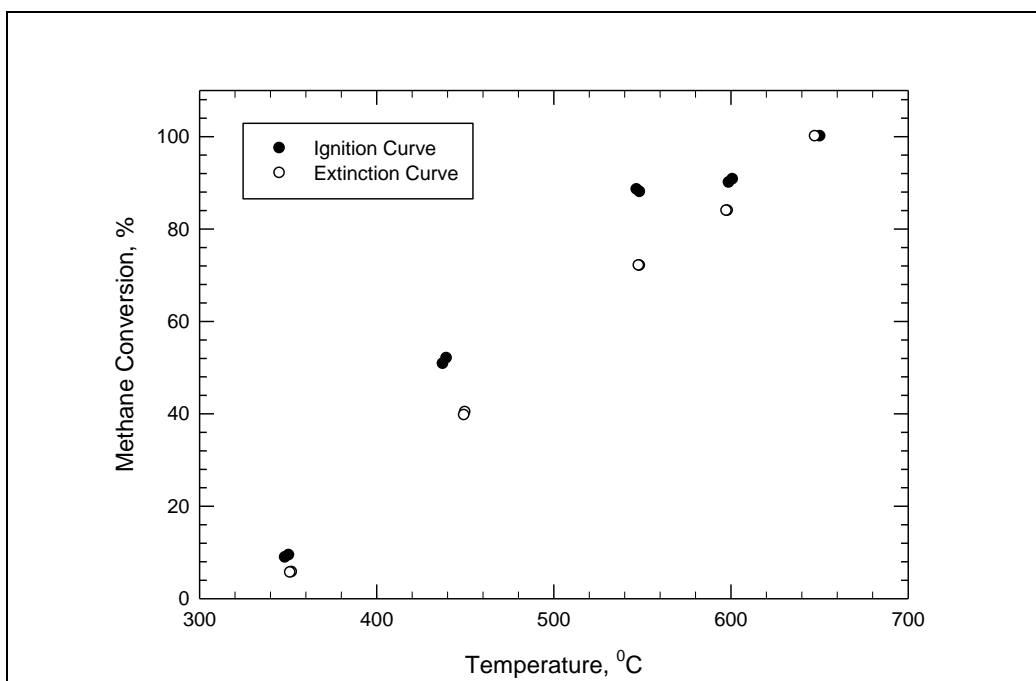


Figure 4.1 Ignition and extinction curves of methane combustion: Run # Pt-Pd-01-12; Pt-Pd catalyst reduced; 2% methane in nitrogen= $95 \pm 2 \text{ cm}^3/\text{min}$, Air= $225 \pm 0.8 \text{ cm}^3/\text{min}$, $5931 \pm 102 \text{ ppm}$.

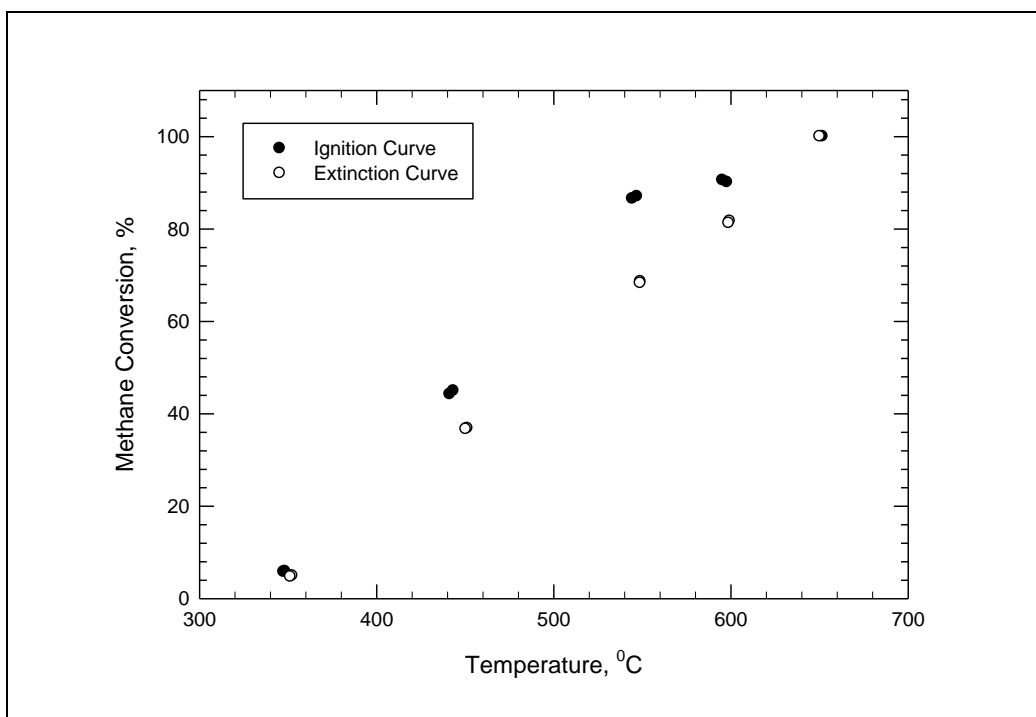


Figure 4.2 Ignition and extinction curves of methane combustion: Run # Pt-Pd-01-13, Pt-Pd catalyst reduced. 2% methane in nitrogen= $95 \pm 2 \text{ cm}^3/\text{min}$, Air= $225 \pm 0.8 \text{ cm}^3/\text{min}$, $5931 \pm 102 \text{ ppm}$.

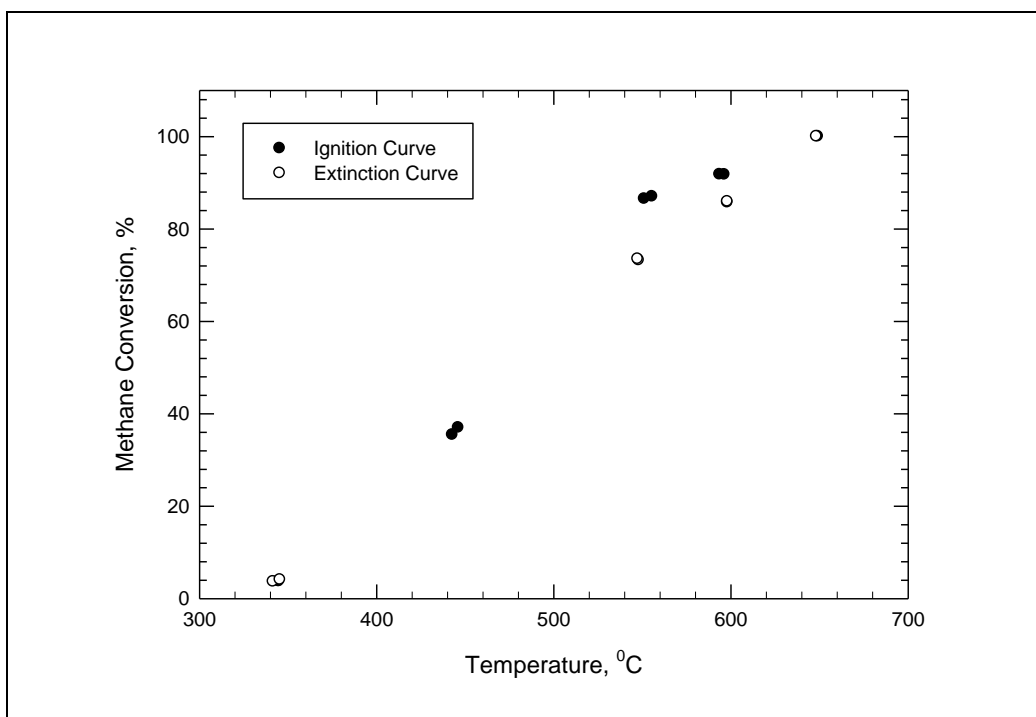


Figure 4.3 Ignition and extinction curves of methane combustion: Run # Pt-Pd-01-14, Pt-Pd catalyst not reduced. 2% methane in nitrogen= 95 ± 2 cm³/min, Air= 225 ± 0.8 cm³/min, 5931 \pm 102 ppm.

4.1.2. Pt catalyst:

Three tests were done on the Pt catalyst to investigate the catalyst behavior, using the procedure described in [Chapter 3](#), in the first two tests the Pt catalyst was first reduced, and then the ignition-extinction experiments were done (all exploratory tests were done at constant methane concentration of 5931 ppm). As can be seen from [Figure 4.4](#) and [Figure 4.5](#), the ignition extinction curves are very similar to each other, hence it can be concluded that reduction pretreatment has stabilized the Pt catalyst performance. [Figure 4.6](#), shows the ignition-extinction experiment done on Pt catalyst without reduction pretreatment, by comparing the ignition and extinction curves in [Figures 4.4, 4.5](#) and [4.6](#), one can realize that that the ignition and extinction curves are almost identical in all three experiments showing that just like Pt-Pd catalyst; reduction pretreatment had no noticeable impact on the catalyst performance.

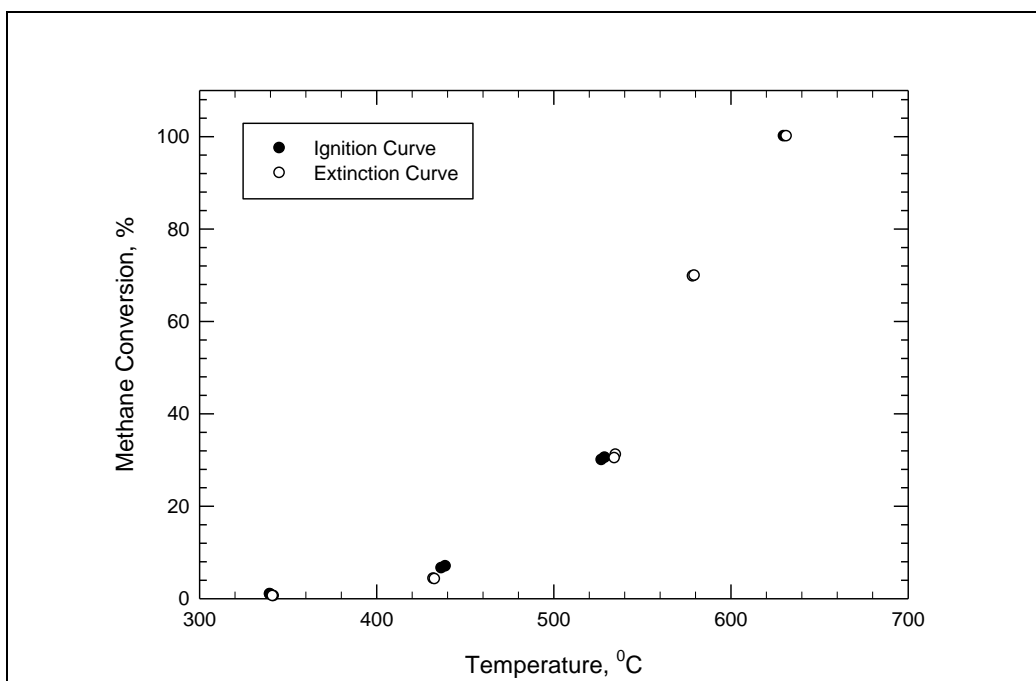


Figure 4.4 Ignition and extinction curves of methane combustion: Run # Pt-01-12, Pt catalyst reduced; 2% methane in nitrogen= $95 \pm 2 \text{ cm}^3/\text{min}$, Air= $225 \pm 0.8 \text{ cm}^3/\text{min}$, $5931 \pm 102 \text{ ppm}$.

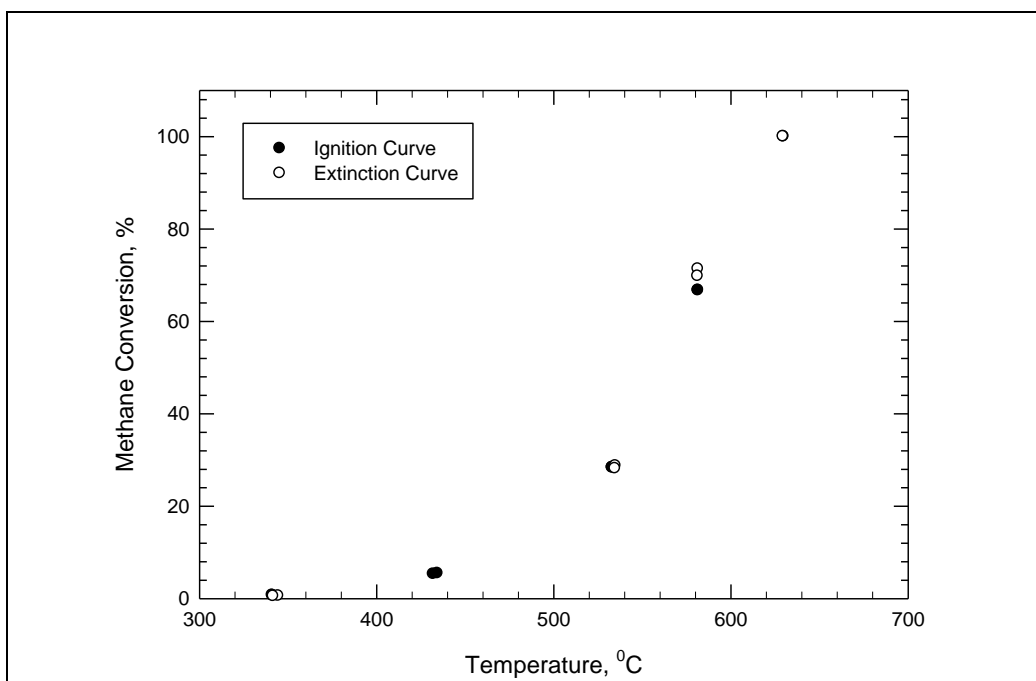


Figure 4.5 Ignition and extinction curves of methane combustion: Run # Pt-01-13; Pt catalyst reduced; 2% methane in nitrogen=95 ±2 cm³/min, Air=225±0.8 cm³/min, 5931±102 ppm.

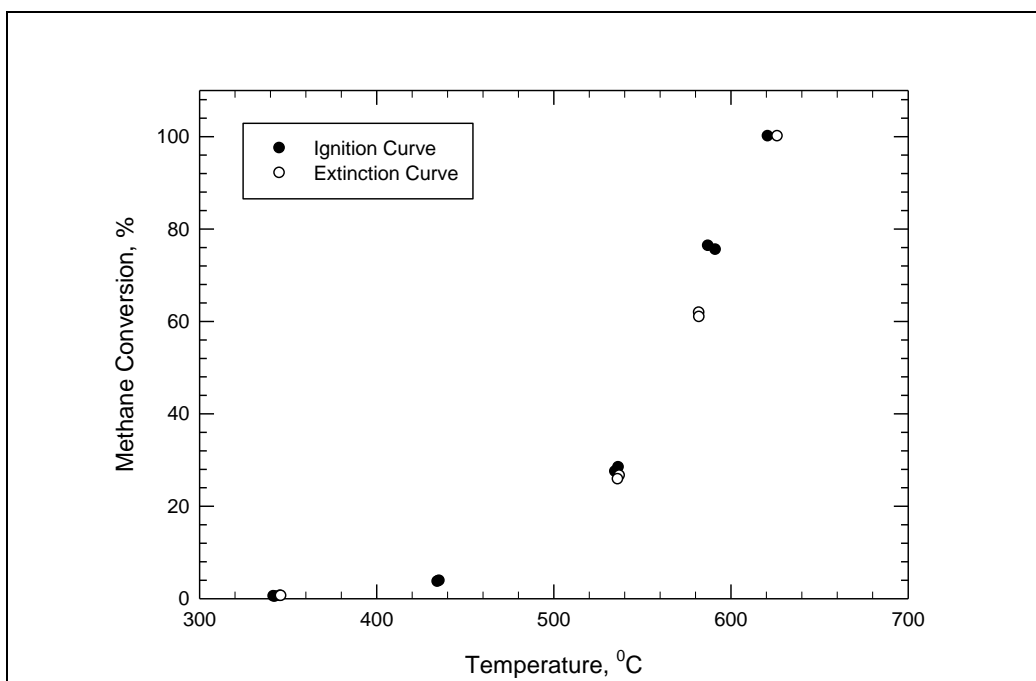


Figure 4.6 Ignition and extinction curves of methane combustion: Run # Pt-01-14, Pt catalyst not reduced; 2% methane in nitrogen= $95 \pm 2 \text{ cm}^3/\text{min}$, Air= $225 \pm 0.8 \text{ cm}^3/\text{min}$, $5931 \pm 102 \text{ ppm}$.

4.2 Ignition and extinction experiments

After completing the preliminary experiments and obtaining an understanding of the catalyst behavior, a series of ignition and extinction experiments were done. The main propose of these experiments was to investigate the general ignition-extinction patterns of methane catalytic oxidation on different types of catalyst. The experiments were done on two different catalysts namely Pt and Pt-Pd, with the same total precious metal loading, under a variety of different conditions to probe the influence of reaction temperature, methane concentration, and the presence of additional water on the performance of the different catalysts.

Depending on the activity of different catalyst samples, the initial operating temperature was chosen (between 300°C and 450°C). Then the temperature was raised by 40 °C or 50 °C or 100 °C increments. At least two steady state tests were performed at each temperature stage. After reaching 100 % conversion (or 650°C for tests on steam-aged catalysts) , the reactor was gradually cooled with at least two steady state tests made at each temperature step, until the final temperature reached the initial operating temperature.

4.2.1 Methane concentration effects

4.2.1.1 Pt-Pd bimetallic catalyst

In this part, ignition extinction tests were done at four different methane concentrations; 837 ± 4 , 1524 ± 33 , 2122 ± 14 , and 4067 ± 20 ppm on Pt-Pd bimetallic catalyst to investigate the effect of methane concentration on the activity of this catalyst.

The results can be seen in [Figures 4.7 to 4.12](#). [Figure 4.7 to 4.10](#) show individual ignition and extinction curves at different concentrations of methane. [Figures 4.11 and 4.12](#) show comparisons of the four ignition and extinction curves for tests done over fresh Pt-Pd catalyst. The primary interesting result observed in this set of experiments was that; ignition temperature increases with increasing methane concentration. In other words, by increasing methane concentration, the ignition and extinction

curves shifted to the right and as a result a higher temperature was required to achieve the same value of conversion. This behavior is a clear indication of self-inhibition caused by methane. Self-inhibition is considered to be a common behavior in catalytic combustion applications such as oxidation of CO or C₃H₆ over Pt catalyst (Voltz et.al, 1973). However, for methane catalytic combustion over Pt and Pd, the general consensus in the literature is that the reaction order with respect to methane is positive (roughly about one) as discussed in Chapter 2 and the self-inhibition effect has not been reported on Pt or Pd monometallic catalysts. Hence, it is clear that the performance of Pt-Pd bimetallic catalyst differs significantly from the performance of Pt or Pd monometallic catalysts which are reported in the literature.

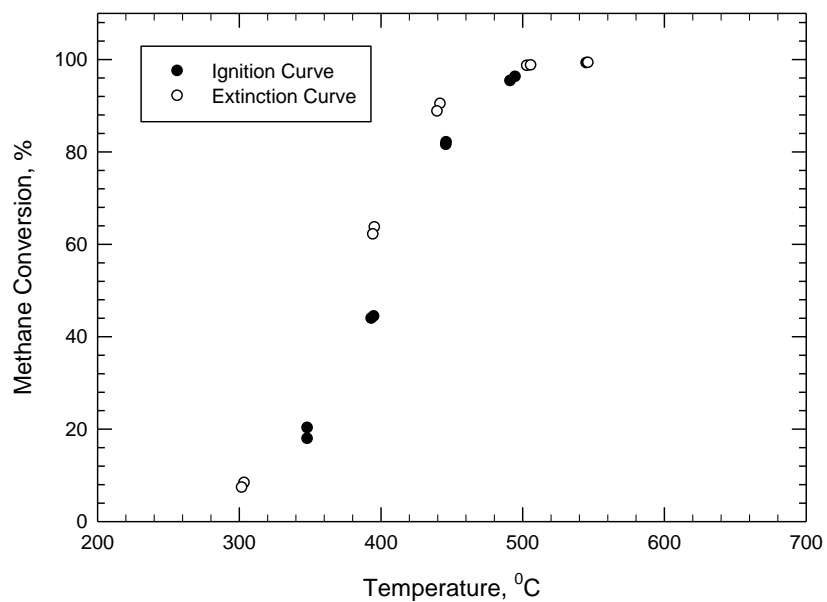


Figure 4.7 Ignition and extinction curves of methane combustion: Run # Pt-Pd-01-15, Pt-Pd catalyst reduced. 10% methane in nitrogen= 9.55 ± 0.14 cm³/min, Air= 225 ± 0.8 cm³/min, 4067 ± 20 ppm

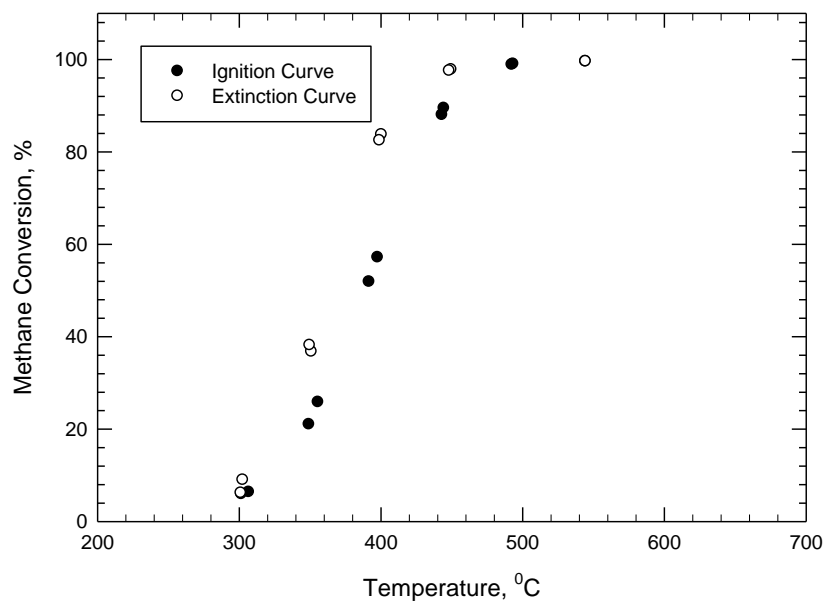


Figure 4.8 Ignition and extinction curves of methane combustion: Run # Pt-Pd-01-16, Pt-Pd catalyst reduced. 10% methane in nitrogen= 4.88 ± 0.01 cm³/min, Air= 225 ± 0.8 cm³/min, 2122 ± 14 ppm.

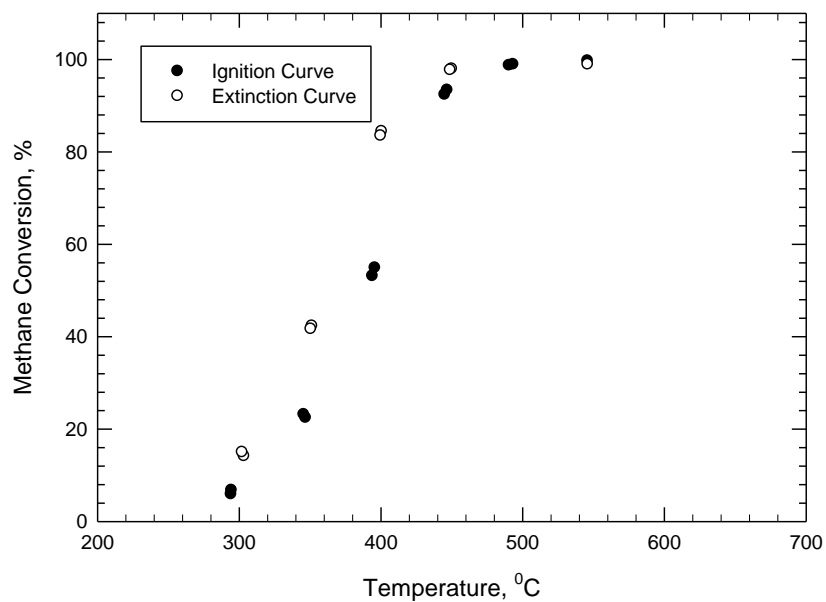


Figure 4.9 Ignition and extinction curves of methane combustion: Run # Pt-Pd-01-18, Pt-Pd catalyst reduced. 10% methane in nitrogen= 3.48 ± 0.06 cm³/min, Air= 225 ± 0.8 cm³/min, 1524 ± 33 ppm.

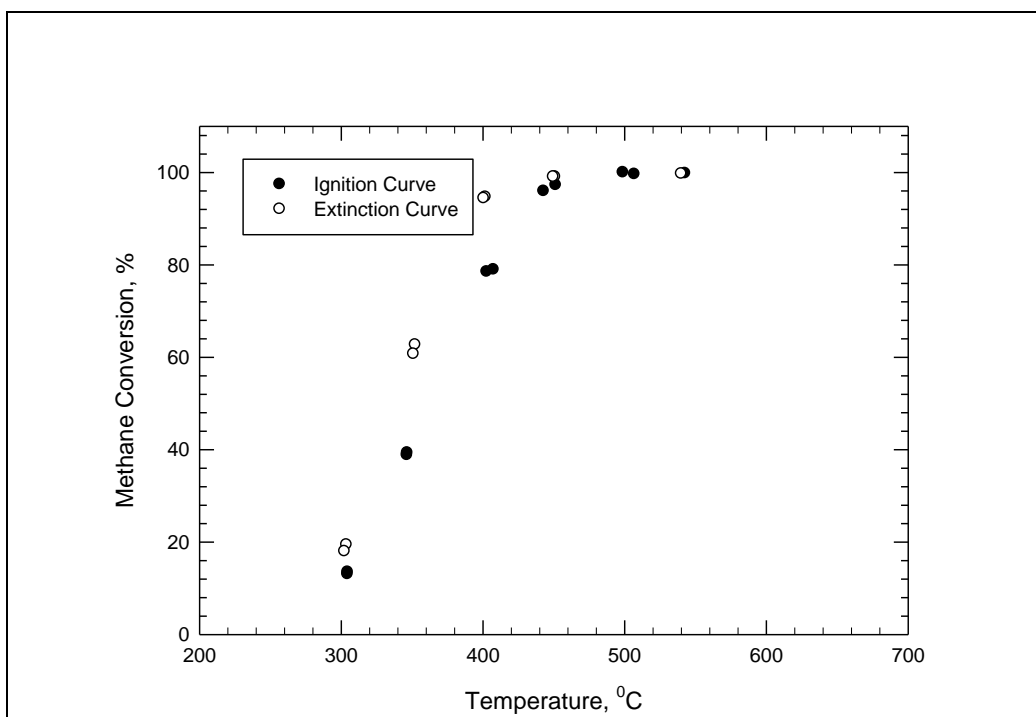
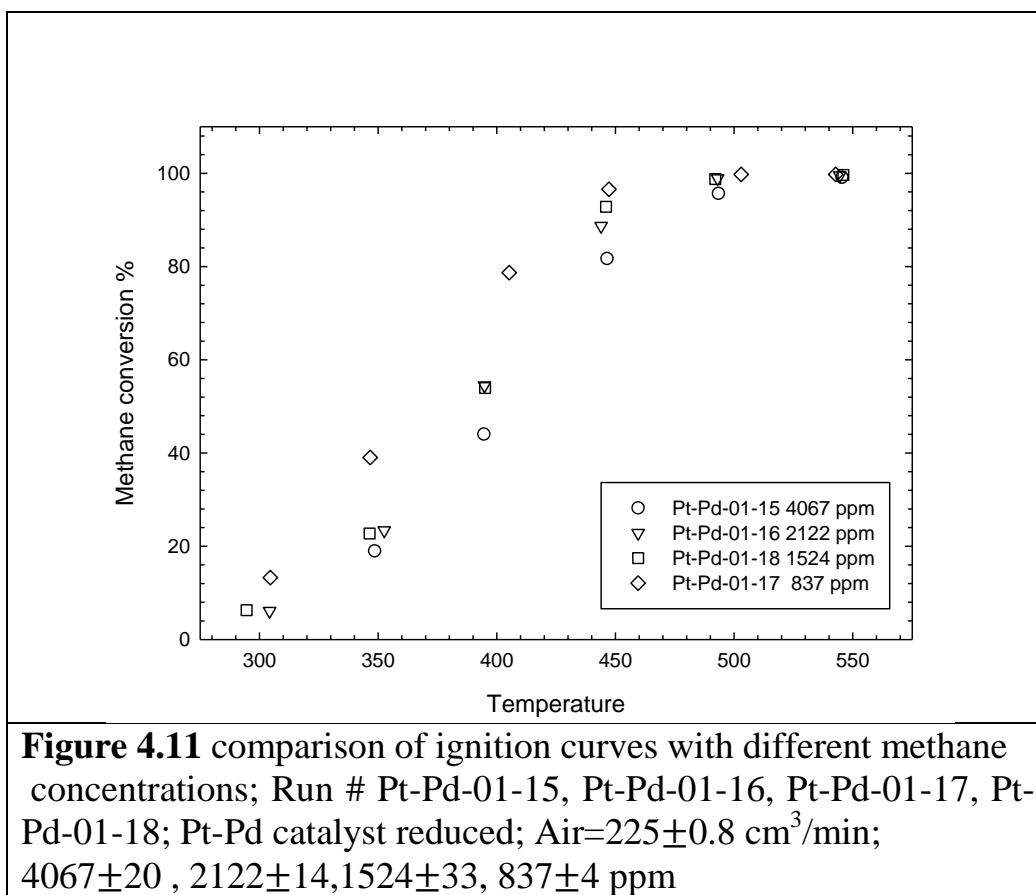
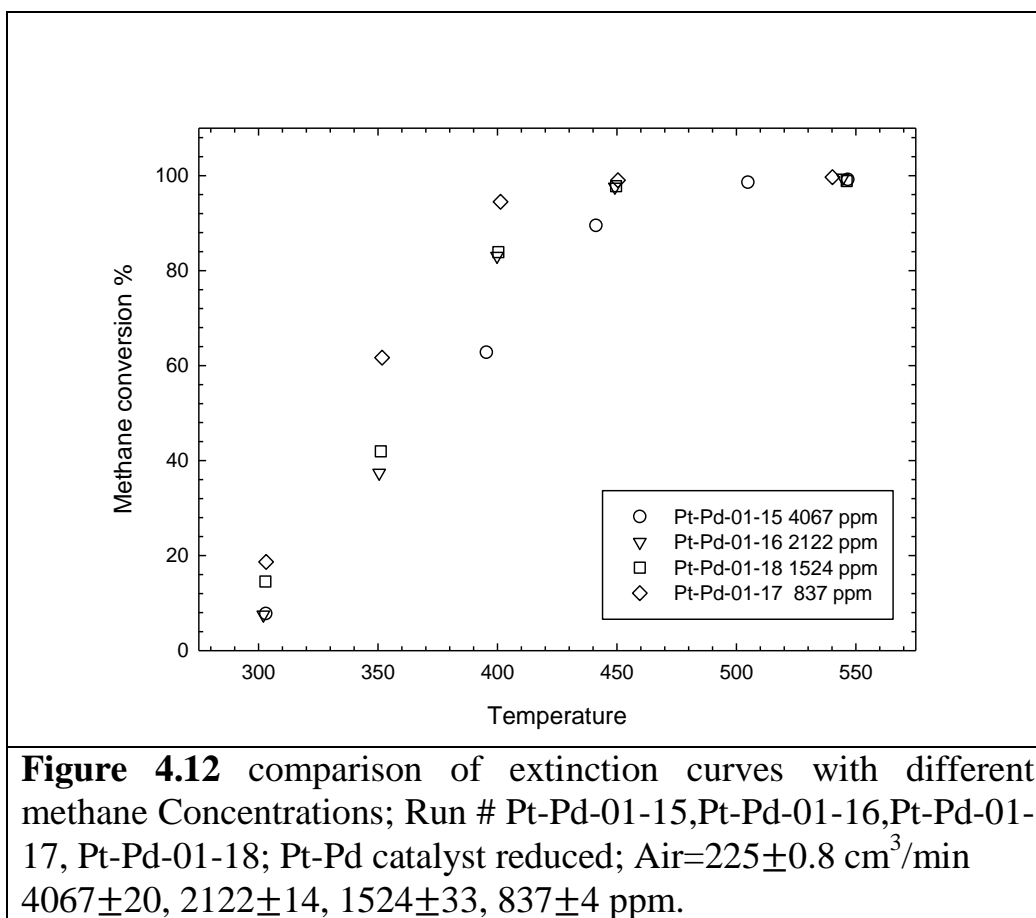


Figure 4.10 Ignition and extinction curves of methane combustion: Run # Pt-Pd-01-17, Pt-Pd catalyst reduced. 2% methane in nitrogen= $9.8 \pm 0.01 \text{ cm}^3/\text{min}$, Air= $225 \pm 0.8 \text{ cm}^3/\text{min}$, $837 \pm 4 \text{ ppm}$.

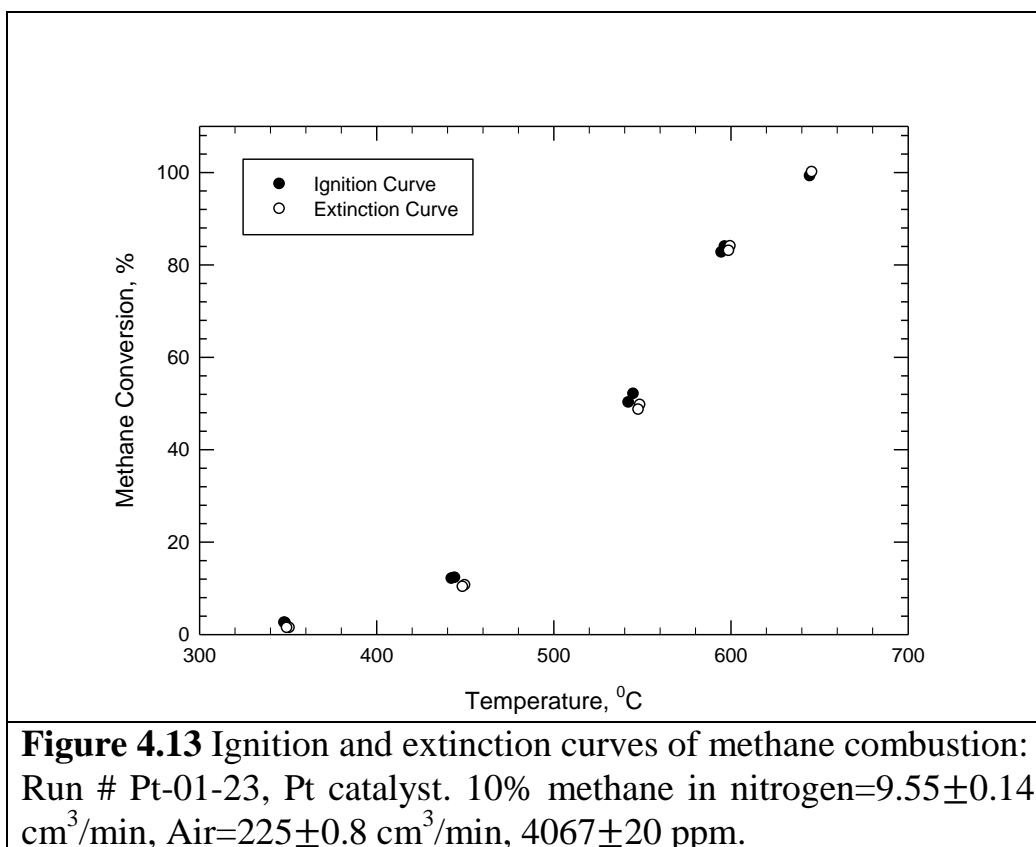


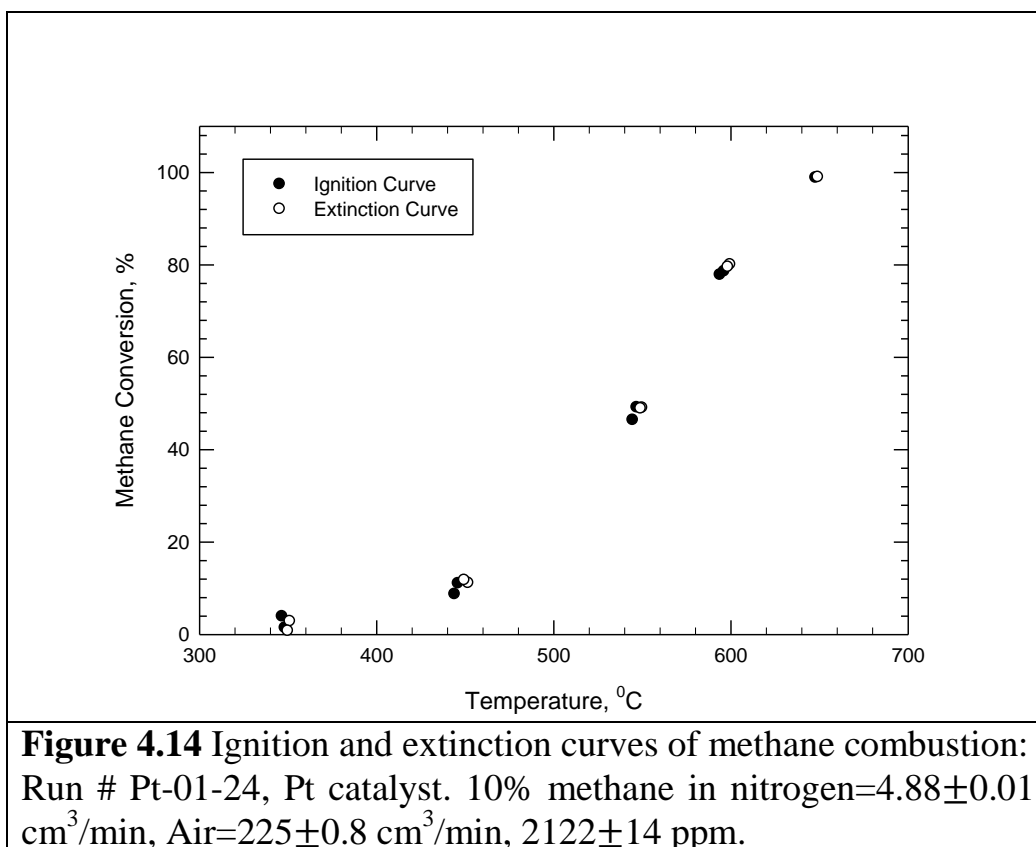


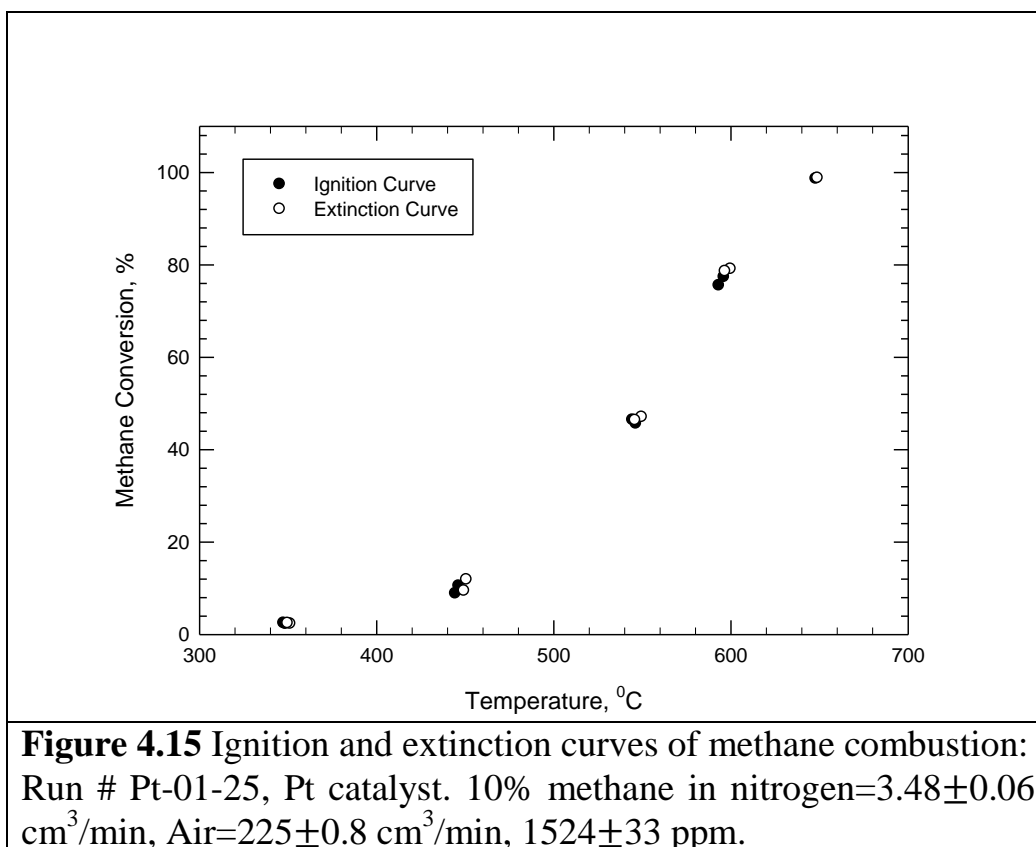
4.2.1.2 Pt catalyst

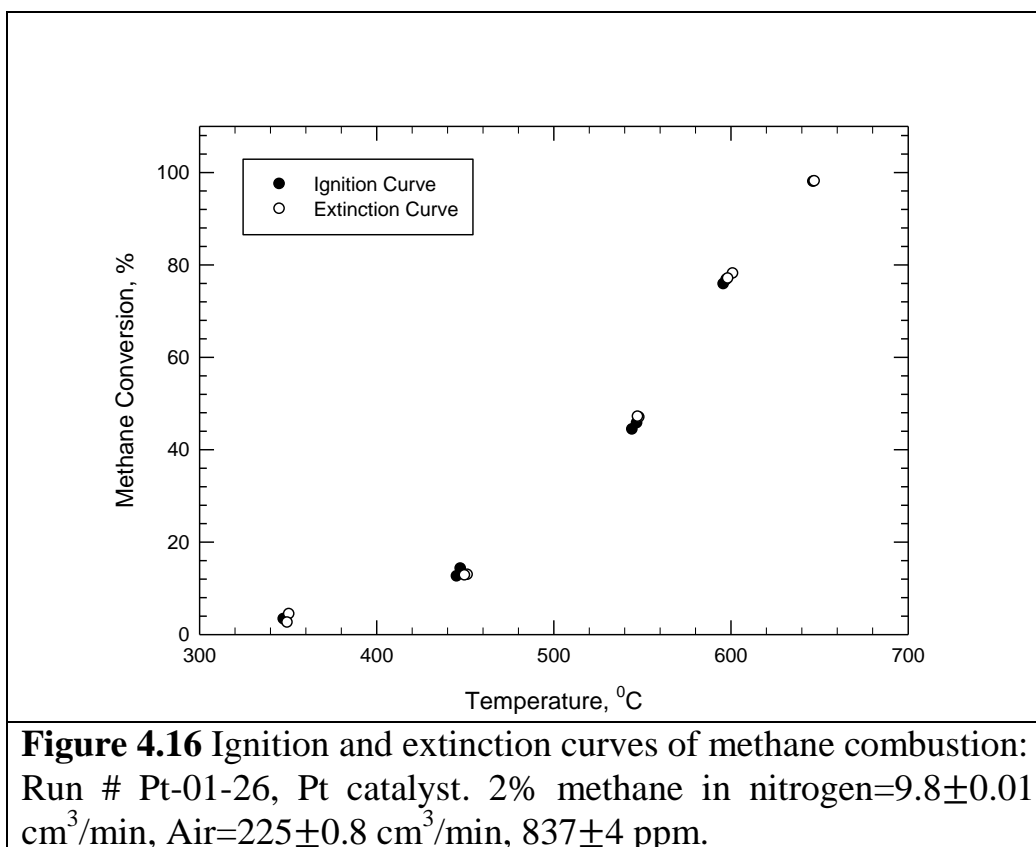
The results of individual ignition-extinction experiments on monometallic Pt catalyst at different methane concentrations (837 ± 4 , 1524 ± 33 , 2122 ± 14 , and 4067 ± 20 ppm) can be seen in [Figures 4.13 to 4.16](#). [Figures 4.17 and 4.18](#) show comparisons of the four ignition and extinction curves for tests done over fresh Pt catalyst.

The first interesting observation obtained from ignition-extinction tests was that ignition and extinction curves are almost identical at each methane concentration (i.e. there is no hysteresis effect) , in addition, it can be seen that the ignition and extinction curves are almost the same at different methane concentrations indicating that the reaction rate is approximately first order with respect to methane concentration , which is in agreement with general results reported in the literature for methane catalytic oxidation on Pt monometallic catalyst.









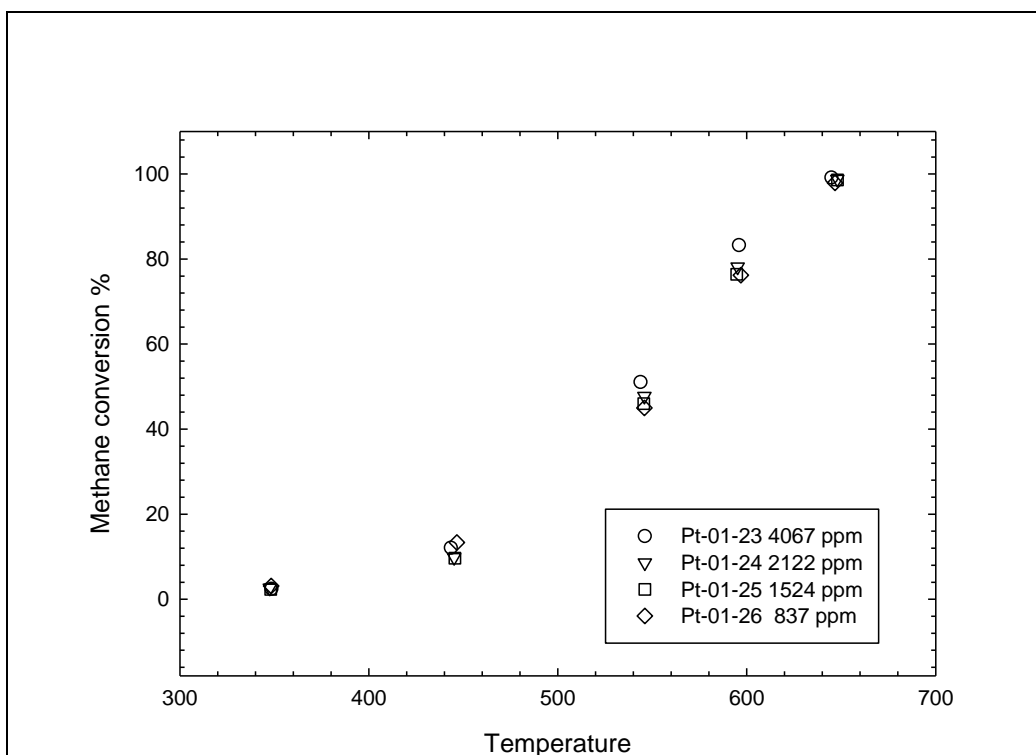
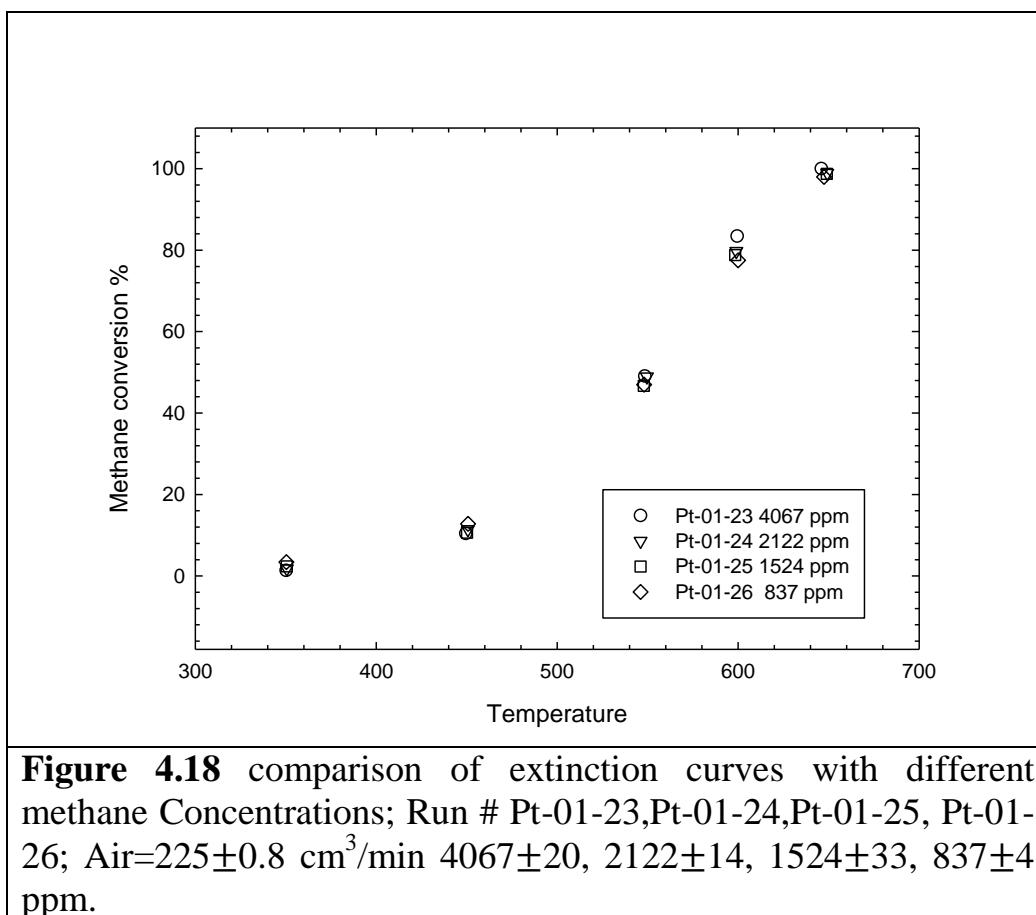


Figure 4.17 comparison of ignition curves with different methane concentrations; Run # Pt-01-23, Pt-01-24, Pt-01-25, Pt-01-26; Air= $225 \pm 0.8 \text{ cm}^3/\text{min}$; 4067 ± 20 , 2122 ± 14 , 1524 ± 33 , 837 ± 4 ppm



4.2.2 The effect of added water

Water is well known to inhibit methane catalytic oxidation as described in [Chapter 2](#). As an example, [Hayes et.al \(2001\)](#) showed that not only addition of water can cause significant reduction in the activity of Pd catalyst, but even the water produced by reaction itself can also inhibit methane catalytic oxidation over Pd based catalyst. As discussed in [Chapter 2](#), although water also inhibits methane oxidation over Pd/Pt bimetallic catalysts, the catalyst activity lost is less severe than Pd catalyst and upon removing the water, the activity comes back to its dry feed level. As up to 10 mol % water might be present in the exhaust gas of natural gas fueled vehicles, in order to simulate the performance of catalysts under the presence of water 5 mol % water was added to the reactor feed using a syringe pump.

4.2.2.1 The effect of added water on Pt-Pd bimetallic catalyst

Activity test and steam aging

To investigate the performance of Pt-Pd bimetallic catalyst in the presence of added water, an activity test was carried out. [Figure 4.19](#) shows the evolution of Pt-Pd catalyst activity versus time on stream after 5 mol % water was added to the feed stream at 442°C. The temperature was chosen to give a conversion of about 80% in dry feed. Then water was added to the reactor feed and catalyst activity was measured with time for eight hours. Water injection was then halted and Pt-Pd catalyst activity was recorded for eight hours in dry feed condition.

As can be seen from [Figure 4.19](#), the methane conversion decreases from about 80% to about 40% quickly upon addition of water. Methane conversion further decreased to about 25% after 1.5 hours exposure to the wet feed. In the next six hours, methane conversion was fluctuated somewhat; however, on average, the methane conversion was about 30% during the remaining six hours under wet feed condition.

Upon suppression of water supply to the feed, methane conversion increased to about 35% quickly and it remained almost constant for 40 minutes. After that, methane conversion rapidly increased to about 55% and it kept increasing with time to about 60% in the next one hour. Then methane conversion further increased to about 70% quickly and, finally after that it increased to 72% gradually during the next six hours.

The sharp decrease in the activity level of bimetallic Pt-Pd catalyst upon addition of water to the feed stream shows the strong inhibition effect of water on Pt-Pd bimetallic catalyst. The fact that Pt-Pd catalyst activity did not fully recover after suppression of water to the reactor feed, suggests a slight slow irreversible deactivation because of water presence.

To simulate long term aging in real exhaust conditions, the bimetallic Pt-Pd catalyst was steam aged at 648 °C in the presence of 5 mol% water, after about 4 hours at 648 °C, the reactor was cooled to 492 °C and it was kept constant at 492 °C for 1 hour to become stabilized, then the conversion of methane was recorded at 492 °C. The reactor was then heated again to 648 °C and the same procedure was repeated. [Figure 4.20](#) shows the methane conversion at 492 °C versus time on stream. As shown in [Figure 4.20](#), the catalyst activity reduced from about 50% to about 10% after about 20 hours of steam aging, and the activity of the catalyst stabilized at about 10%. The stabilized Pt-Pd bimetallic catalyst was then used to perform a series of ignition-extinction experiments.

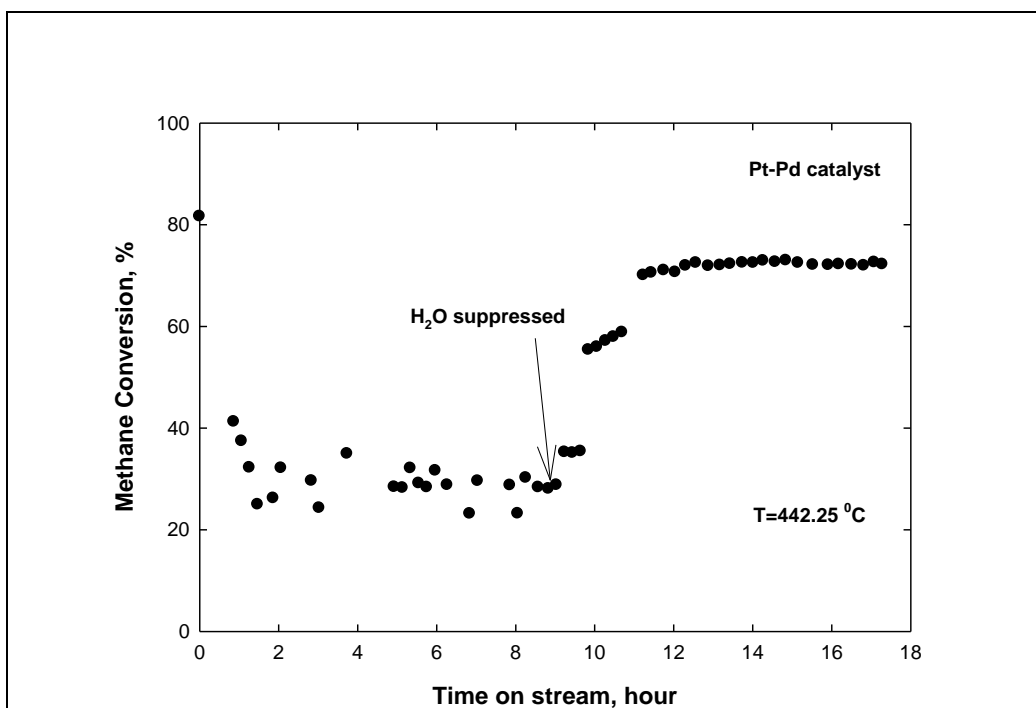
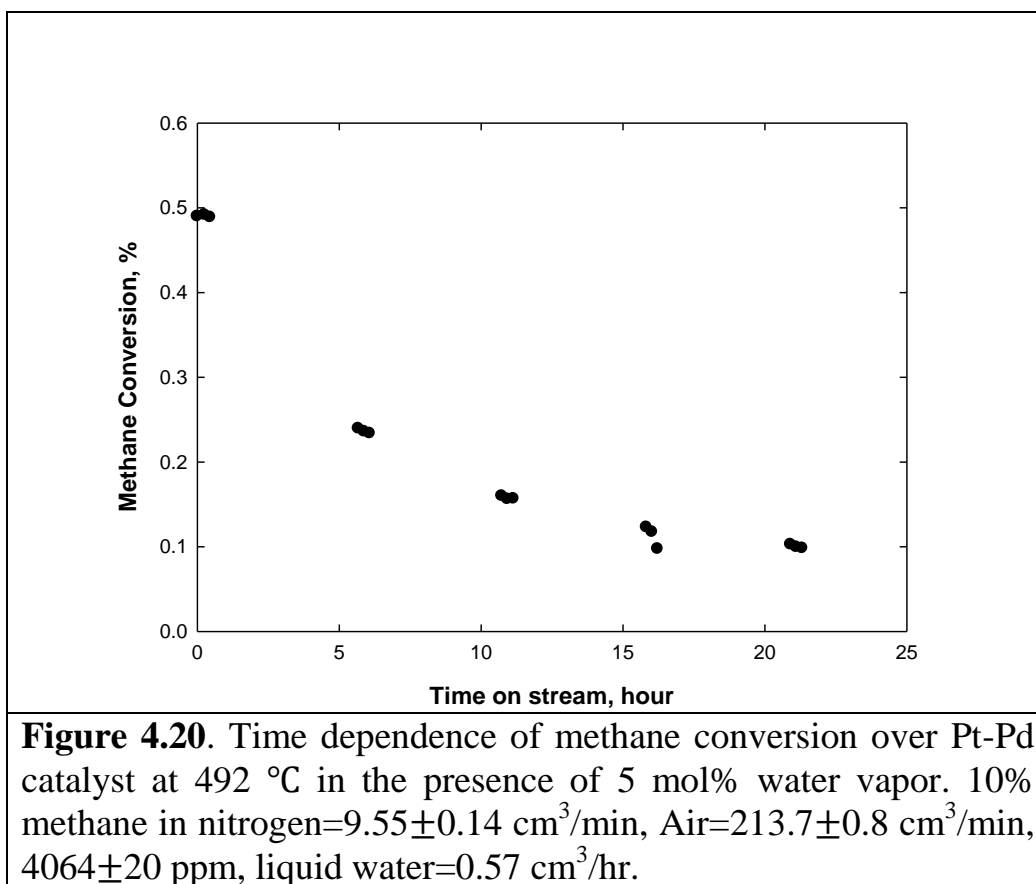


Figure 4.19 influence of 5 mol% water addition on conversion of methane over Pt-Pd bimetallic catalyst versus time on stream. (Note: the first point at about 80% conversion corresponds to dry feed)

Feed composition (in the presence of water) 10% methane in nitrogen=9.55±0.14 cm³/min, Air=213.7±0.8 cm³/min, 4064±20 ppm, liquid water=0.57 cm³/hr.

Feed composition (in the absence of water) 10% methane in nitrogen=9.55±0.14 cm³/min, Air=225±0.8 cm³/min, 4067±20 ppm.



The effect of methane concentration on the activity of steam aged Pt-Pd catalyst in the presence and absence of 5 mol % water

In this part the ignition-extinction tests were performed at different methane concentrations; (837±4, 1524±33, 2122±14, and 4067±20 ppm in the absence of water) and (836±4, 1526±33, 2122±14, and 4064±20 ppm in the presence of water) on the Pt-Pd bimetallic catalyst to investigate the effect of methane concentration on the activity of steam-aged catalyst in the presence and absence of water in the feed stream (Note that no reduction procedure was used at anytime for these runs). The results can be seen in [Figure 4.21](#) to [Figure 4.32](#) ([Figures 4.25 and 4.26](#) show comparisons of the four ignition and extinction curves for tests done over steam-aged Pt-Pd catalyst in the presence of water, [Figures 4.31 and 4.32](#) show comparisons of the four ignition and extinction curves for tests done over steam-aged Pt-Pd catalyst in the absence of water).

First of all, the effect of methane concentration on the ignition-extinction curves for steam-aged Pt-Pd catalyst is negligible to non-existent in the presence of water. Furthermore, the extinction curves are almost the same at different methane concentrations for tests over the steam-aged Pt-Pd in the presence of water. However, as can be seen from [Figure 4.27](#) to [Figure 4.30](#), in the absence of water, the ignition temperature increases with increasing methane concentration, in other words, ignition and extinction curves shifted to the right with increasing methane concentration which is a clear indication of methane self-inhibition. In addition, as can be seen from [Figure 4.27](#) to [Figure 4.30](#), the steam-aged Pt-Pd catalyst is more active in the absence of water; in other words, steam-aged Pt-Pd catalyst regained some of its activity with cutting off the water in the feed stream. However, by comparing ignition-extinction experiments on the steam-aged and fresh Pt-Pd in the absence of water, one realizes that, steam-aged Pt-Pd is still much less active than fresh Pt-Pd. This indicates that Pt-Pd permanently lost some of its activity as a result of exposure to excess water in the feed stream at elevated temperature.

Secondly, for the ignition-extinction experiments in the presence of water, the steam-aged Pt-Pd catalyst shows a reproducible

significant slope change at about 550 °C ,and there is a significant hysteresis present at each methane concentration (i.e. the activities during ignition are markedly higher than during extinction).

However, for the ignition-extinction experiments in the absence of water, interestingly the ignition and the extinction curves are the same at each methane concentration (i.e. the hysteresis is negligible to non-existence in the absence of water for steam-aged Pt-Pd catalyst). In addition, there is no observable slope change at 550 °C for the tests in the absence of water ,unlike the tests in the presence of water.

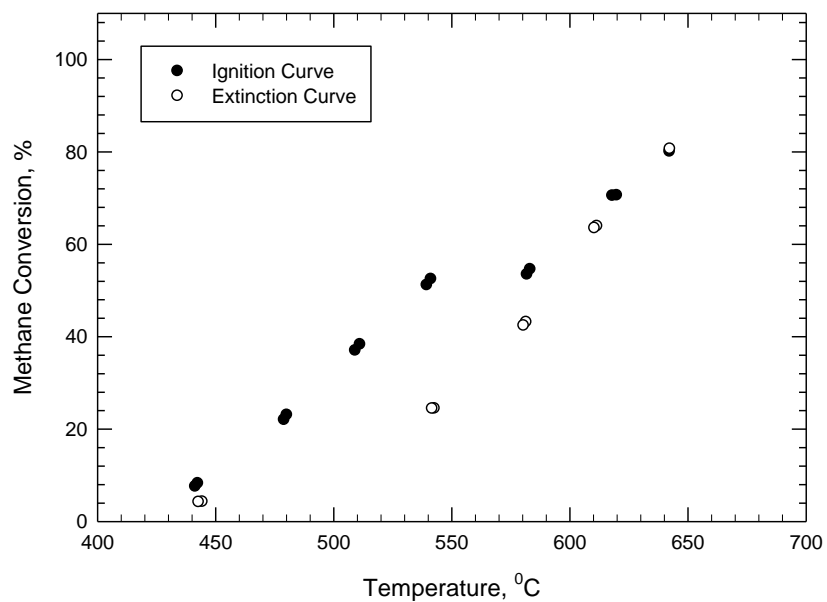
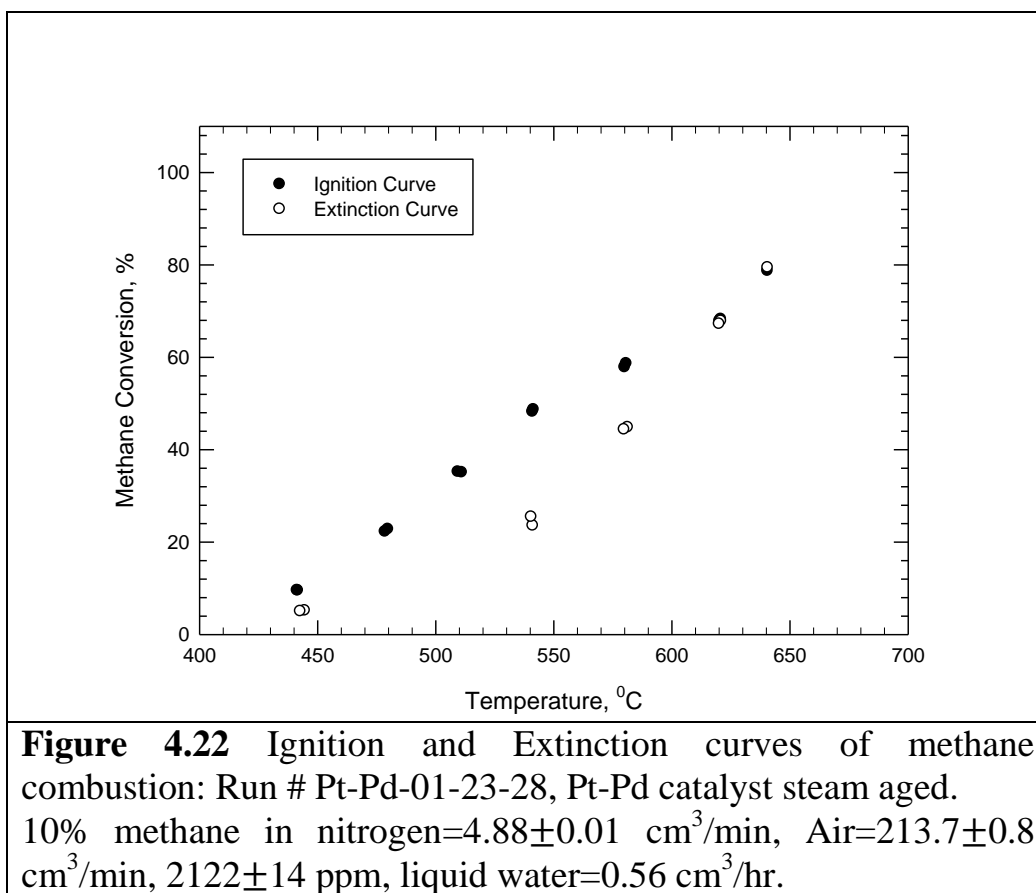
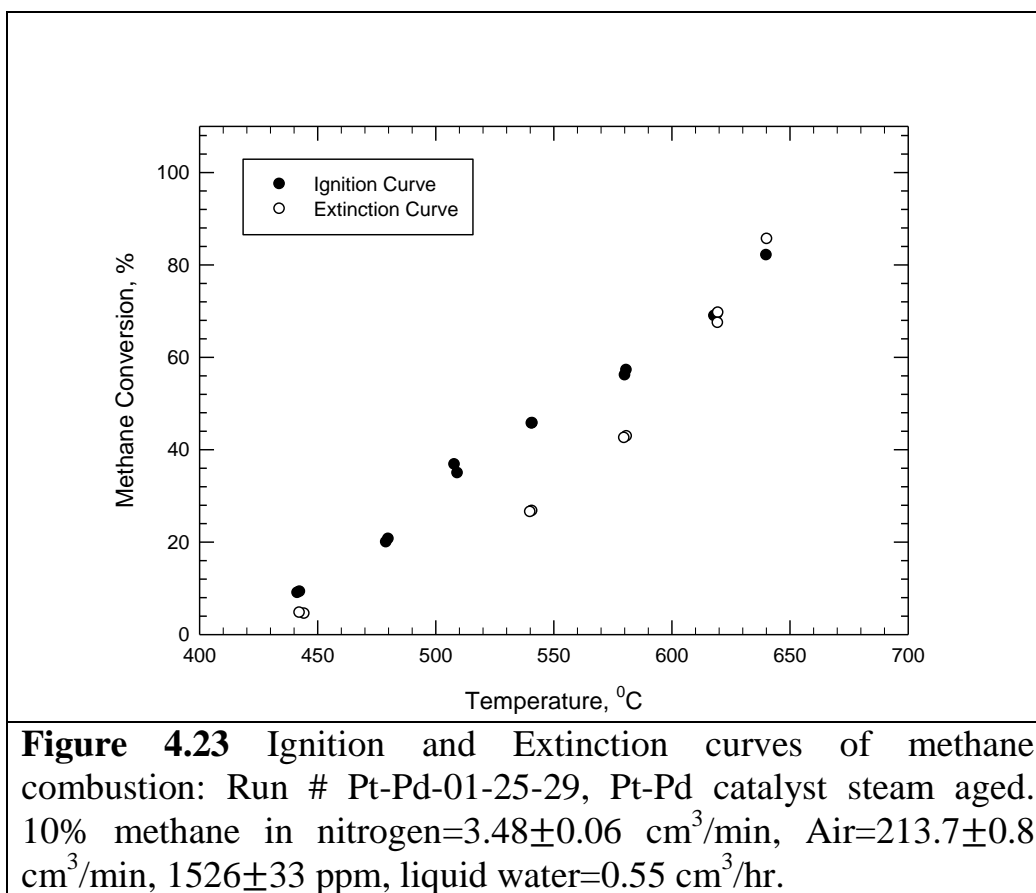


Figure 4.21 Ignition and Extinction curves of methane combustion: Run # Pt-Pd-01-22-26, Pt-Pd catalyst steam aged. 10% methane in nitrogen= 9.55 ± 0.14 cm³/min, Air= 213.7 ± 0.8 cm³/min, 4064 ± 20 ppm, liquid water= 0.57 cm³/hr.





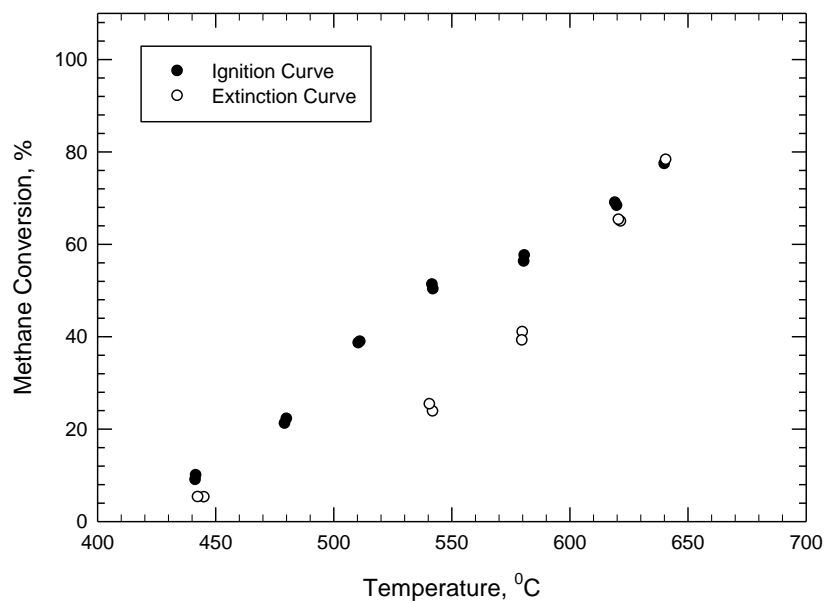


Figure 4.24 Ignition and Extinction curves of methane combustion: Run # Pt-Pd-01-24-27, Pt-Pd catalyst steam aged. 2% methane in nitrogen= $9.84 \pm 0.01 \text{ cm}^3/\text{min}$, Air= $213.7 \pm 0.8 \text{ cm}^3/\text{min}$, $836 \pm 4 \text{ ppm}$, liquid water= $0.57 \text{ cm}^3/\text{hr}$.

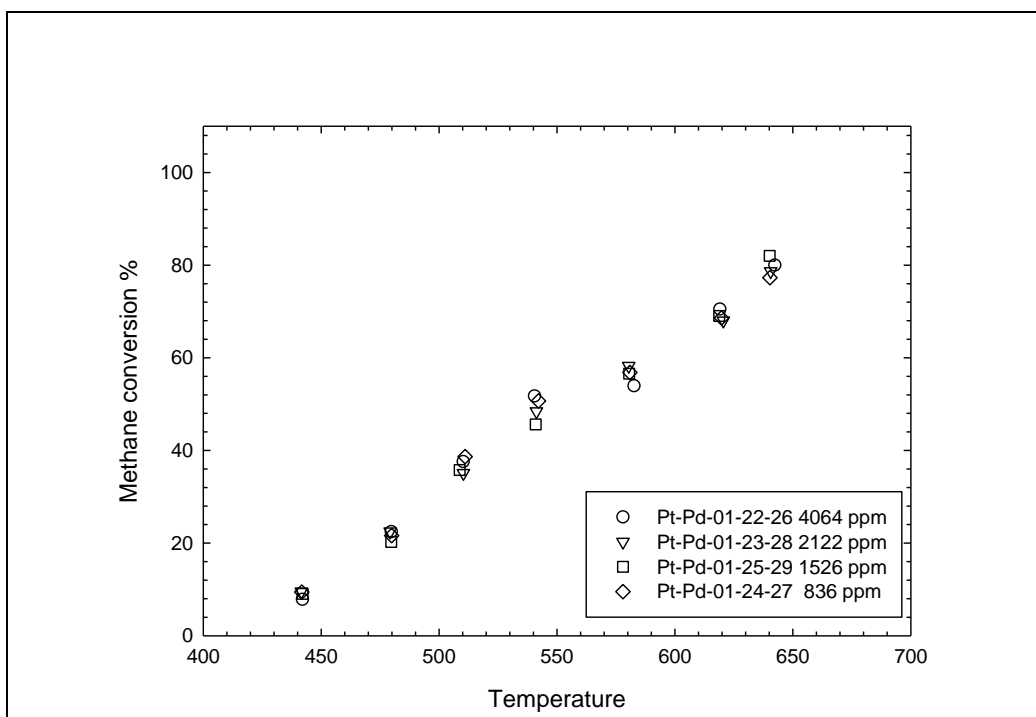


Figure 4.25 comparison of ignition curves with different methane concentrations; Run # Pt-Pd-01-22-26, Pt-Pd-01-23-28, Pt-Pd-01-25-29, Pt-Pd-01-24-27; Pt-Pd catalyst steam aged; Air= 213.7 ± 0.8 cm^3/min , 5 mol% water in the feed. 4064 ± 20 , 2122 ± 14 , 1526 ± 33 , 836 ± 4 ppm

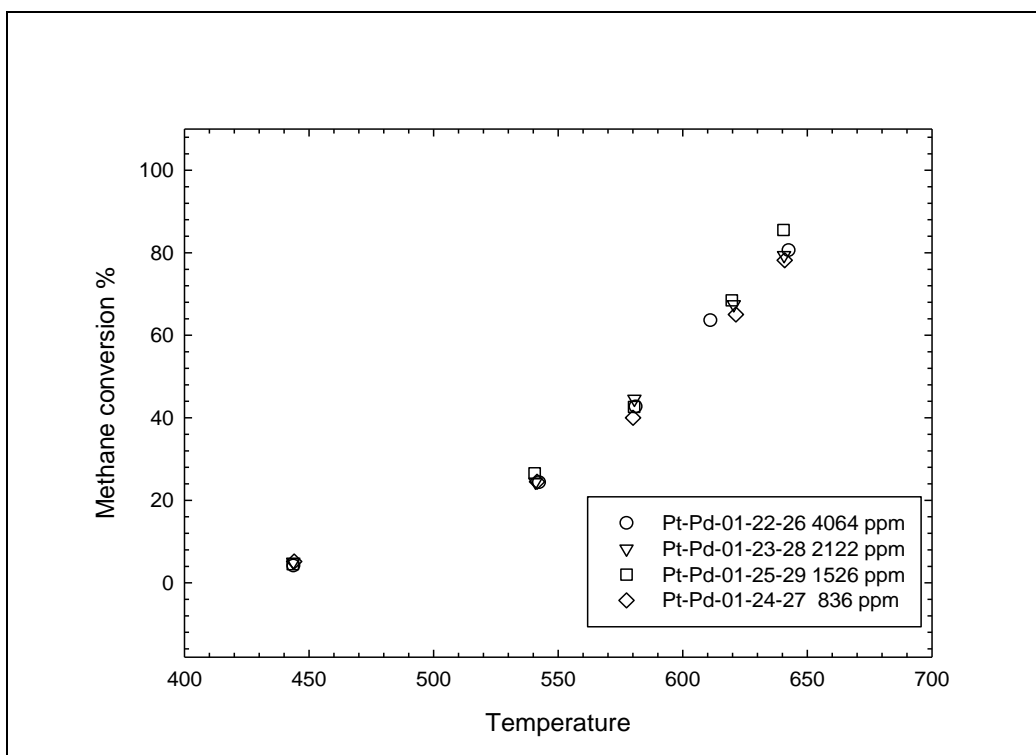
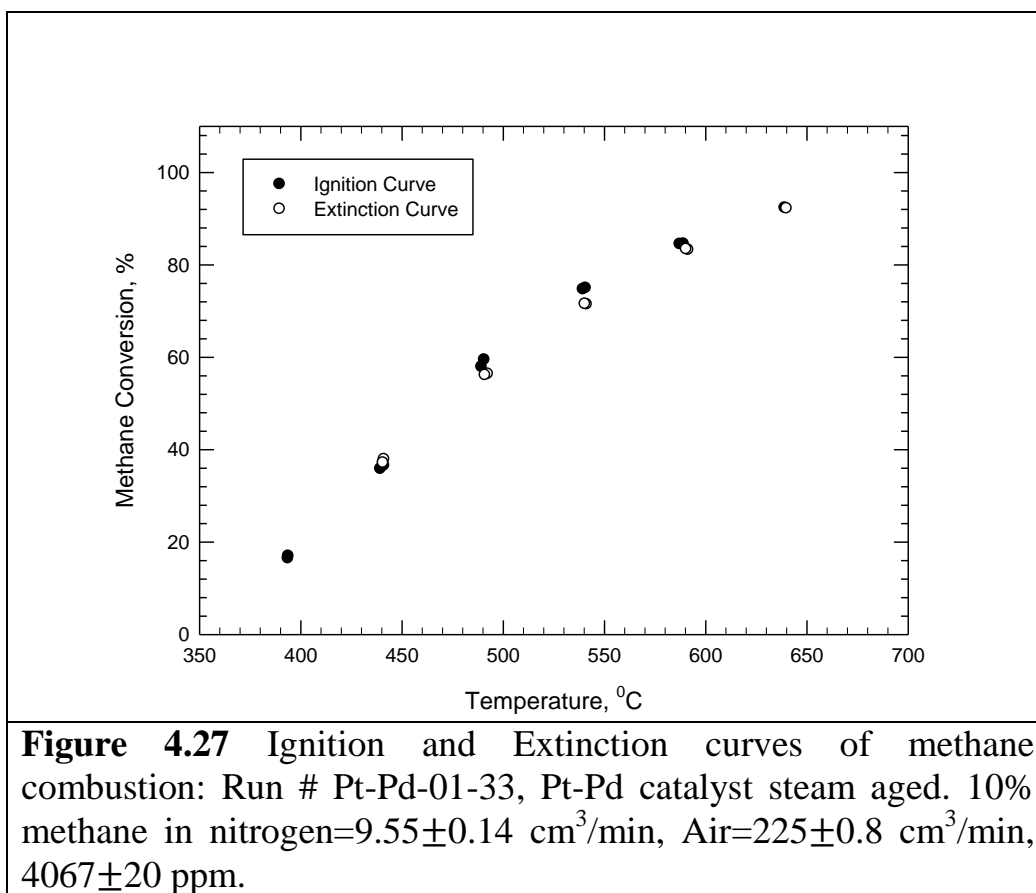
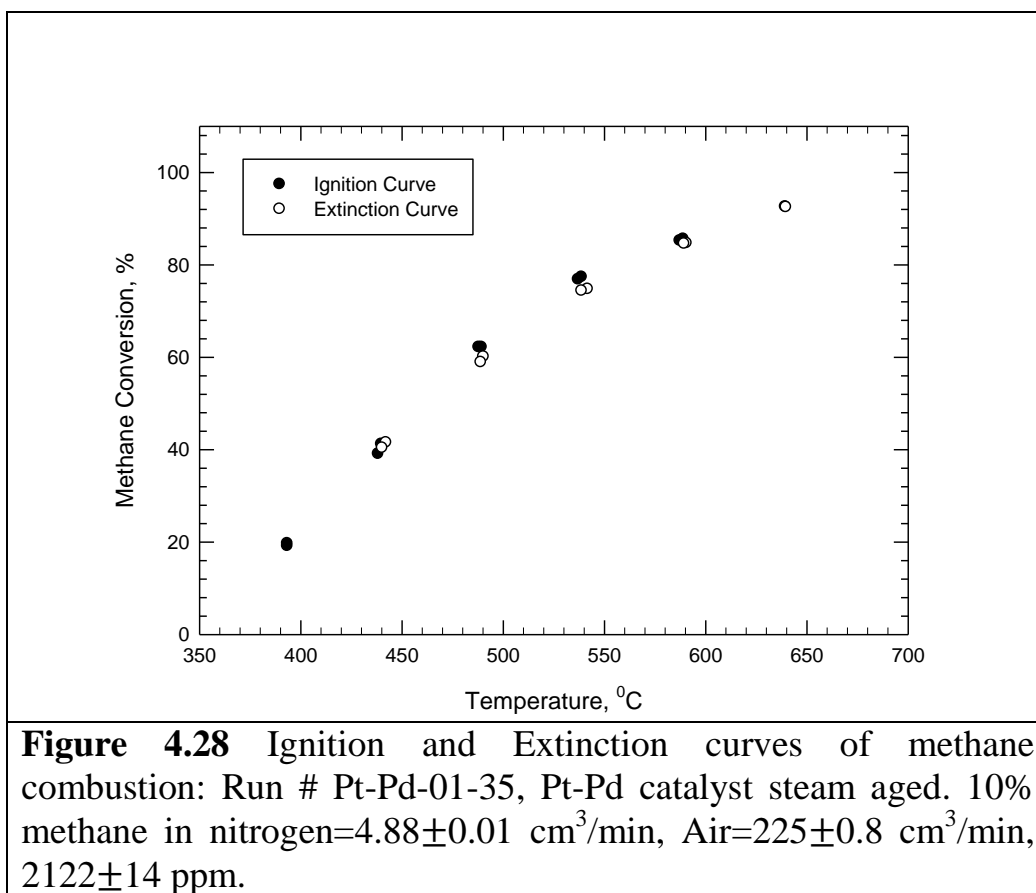


Figure 4.26 comparison of extinction curves with different methane concentrations; Run # Pt-Pd-01-22-26, Pt-Pd-01-23-28, Pt-Pd-01-25-29, Pt-Pd-01-24-27; Pt-Pd catalyst steam aged; Air= 213.7 ± 0.8 cm³/min, 5 mol% water in the feed. 4064 ± 20 , 2122 ± 14 , 1526 ± 33 , 836 ± 4 ppm





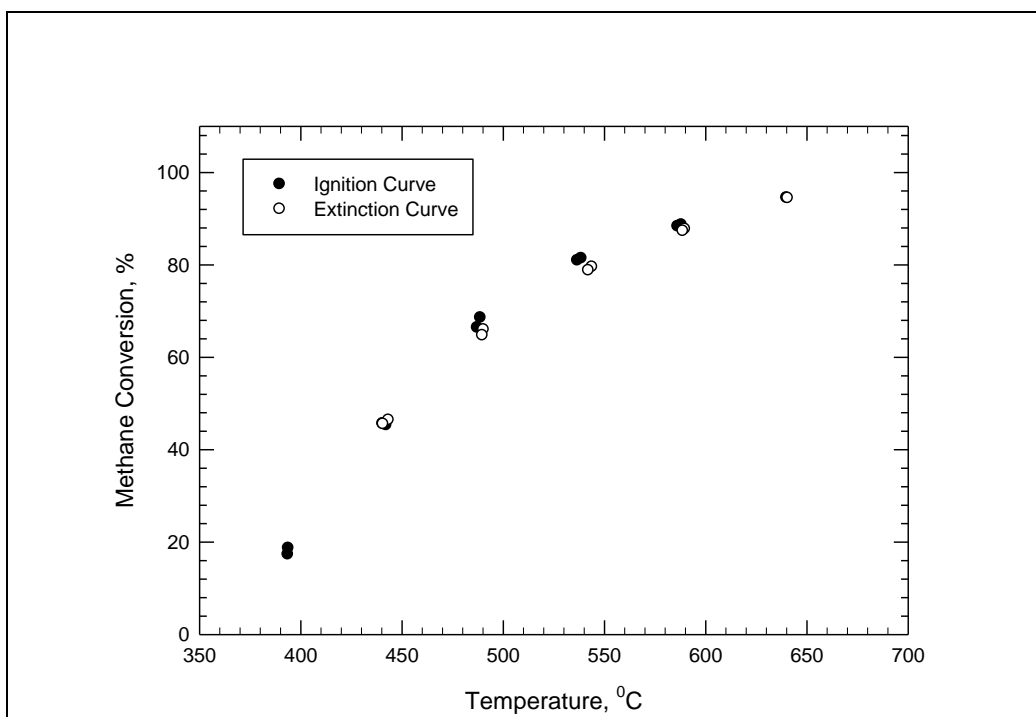


Figure 4.29 Ignition and Extinction curves of methane combustion: Run # Pt-Pd-01-34, Pt-Pd catalyst steam aged. 10% methane in nitrogen= 3.48 ± 0.06 cm³/min, Air= 225 ± 0.8 cm³/min, 1524 ± 33 ppm.

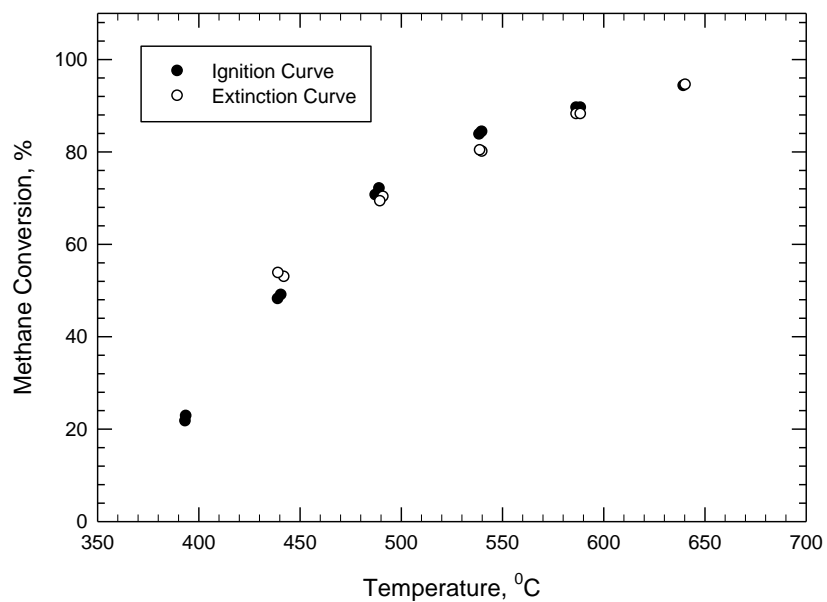


Figure 4.30 Ignition and Extinction curves of methane combustion: Run # Pt-Pd-01-36, Pt-Pd catalyst steam aged. 2% methane in nitrogen= 9.8 ± 0.01 cm³/min, Air= 225 ± 0.8 cm³/min, 837 ± 4 ppm.

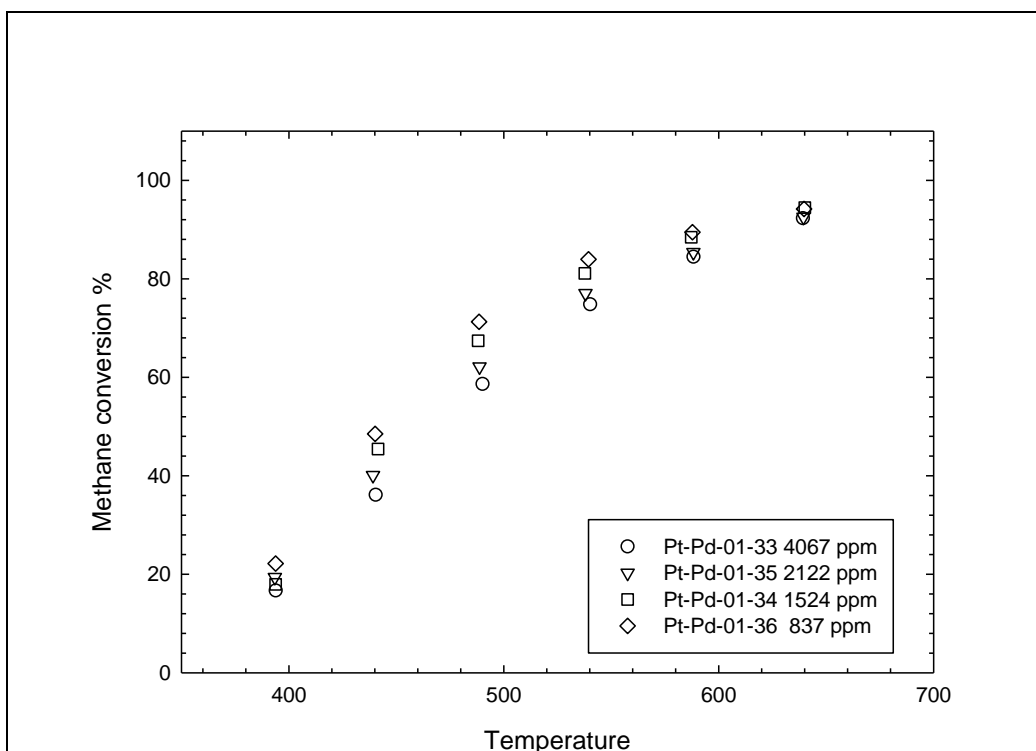


Figure 4.31 comparison of ignition curves with different methane concentrations; Run # Pt-Pd-01-33, Pt-Pd-01-35, Pt-Pd-01-34, Pt-Pd-01-36; Pt-Pd catalyst steam aged; Air= 225 ± 0.8 cm³/min, 4067 ± 20 , 2122 ± 14 , 1524 ± 33 , 837 ± 4 ppm

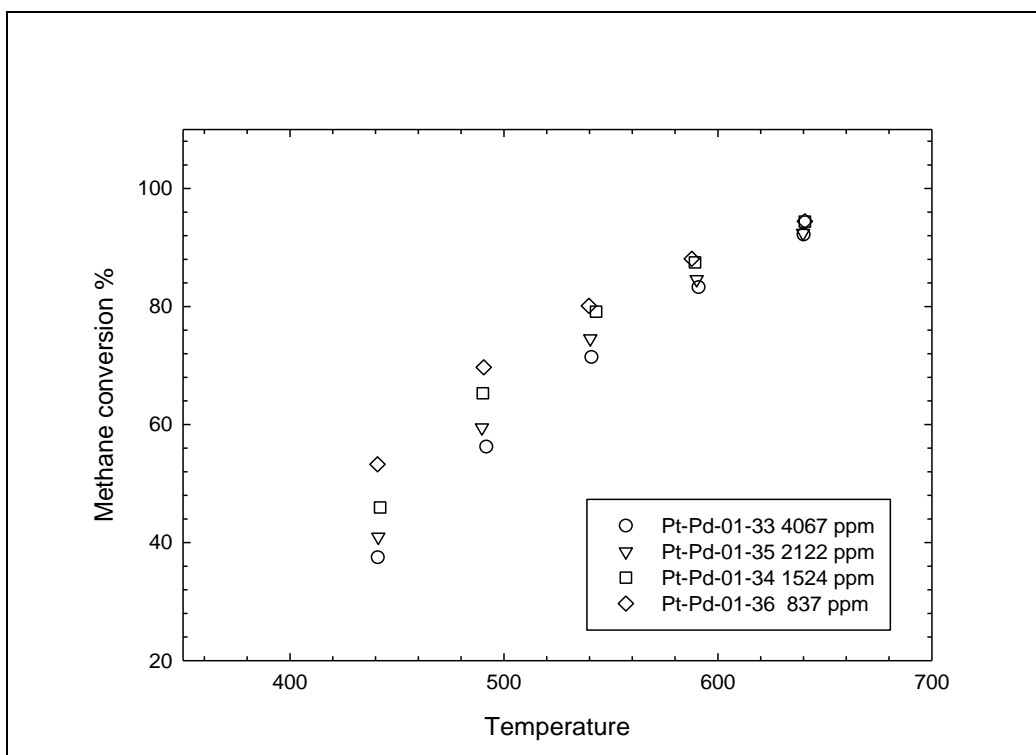


Figure 4.32 comparison of extinction curves with different methane concentrations; Run # Pt-Pd-01-33, Pt-Pd-01-35, Pt-Pd-01-34, Pt-Pd-01-36; Pt-Pd catalyst steam aged; Air= 225 ± 0.8 cm^3/min , 4067 ± 20 , 2122 ± 14 , 1524 ± 33 , 837 ± 4 ppm

4.2.2.2 The effect of added water on Pt catalyst

Activity test and steam aging

A set of experiments was conducted over the Pt catalyst similar to those of the Pt-Pd catalyst to study the performance of Pt catalyst in the presence of water.

[Figure 4.33](#) shows the evolution of Pt catalyst activity versus time on stream after 5 mol % water was added to the feed stream at 547°C. This temperature was chosen to give a conversion of about 50 % in dry feed (the first experimental point represents the activity in dry feed before any exposure to water) ,then water was added to the reactor feed and catalyst activity was measured with time for eight hours. After eight hours the water injection was suppressed and the activity of Pt catalyst was recorded for another eight hours.

As can be seen in [Figure 4.33](#) ,upon addition of water the methane conversion immediately decreased from about 50 % to about 30% ,where it stayed almost constant at 30 % over eight hours of exposure to the wet feed. Upon suppression of water supply to the reactor feed stream , methane conversion slowly increased to about 34 % and it remained almost constant until the end of the activity test. The sharp decrease in the activity level of Pt catalyst which was observed upon addition of water to the reactor feed stream shows the strong inhibition effect of water on Pt catalyst. The fact that Pt catalyst activity was not fully recovered after suppression of water to the reactor feed, suggests a great irreversible deactivation because of water presence.

To simulate long-term ageing in real exhaust conditions, the Pt catalyst was steam aged at 648 °C in the presence of 5 mol% water. After about four hours at 648 °C , the reactor was cooled to 547 °C and it was kept at 547 °C for about an hour to become stabilized, then the methane conversion was recorded at 547 °C. The reactor was then heated again to 648 °C and the same procedure was repeated.

Figure 4.34 shows the methane conversion at 547 °C versus time on stream. As can be seen from Figure 4.34 the catalyst activity was further reduced from about 32 % to 19 % after 20 hours ,and it became stabilized at 19 %. This stabilized catalyst was then used to perform a series of Ignition-Extinction experiments.

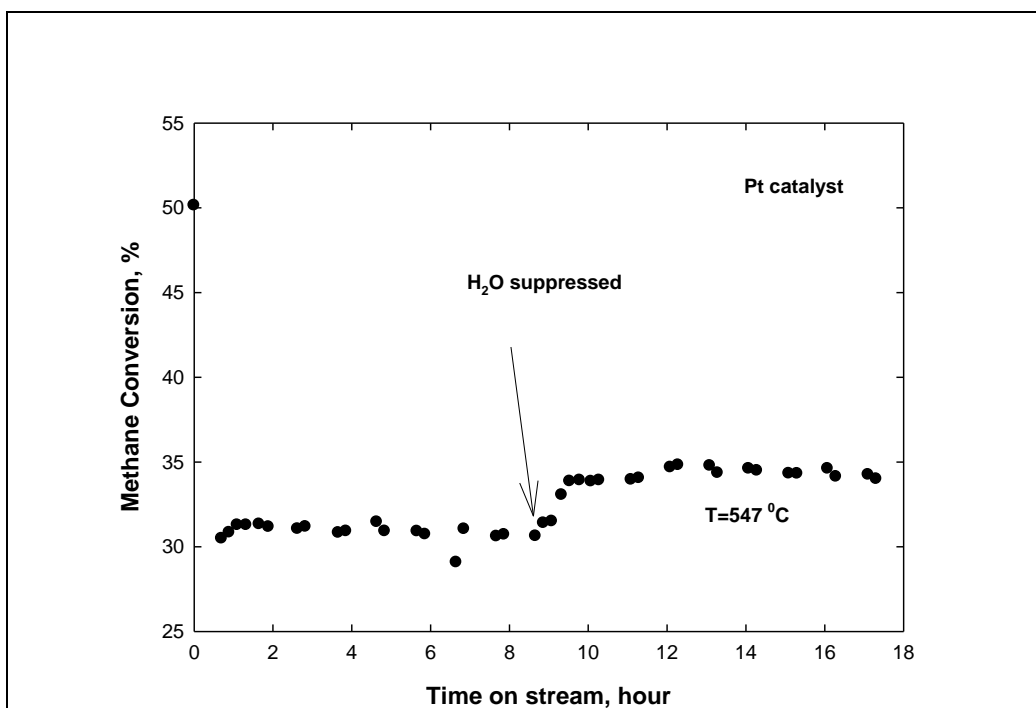
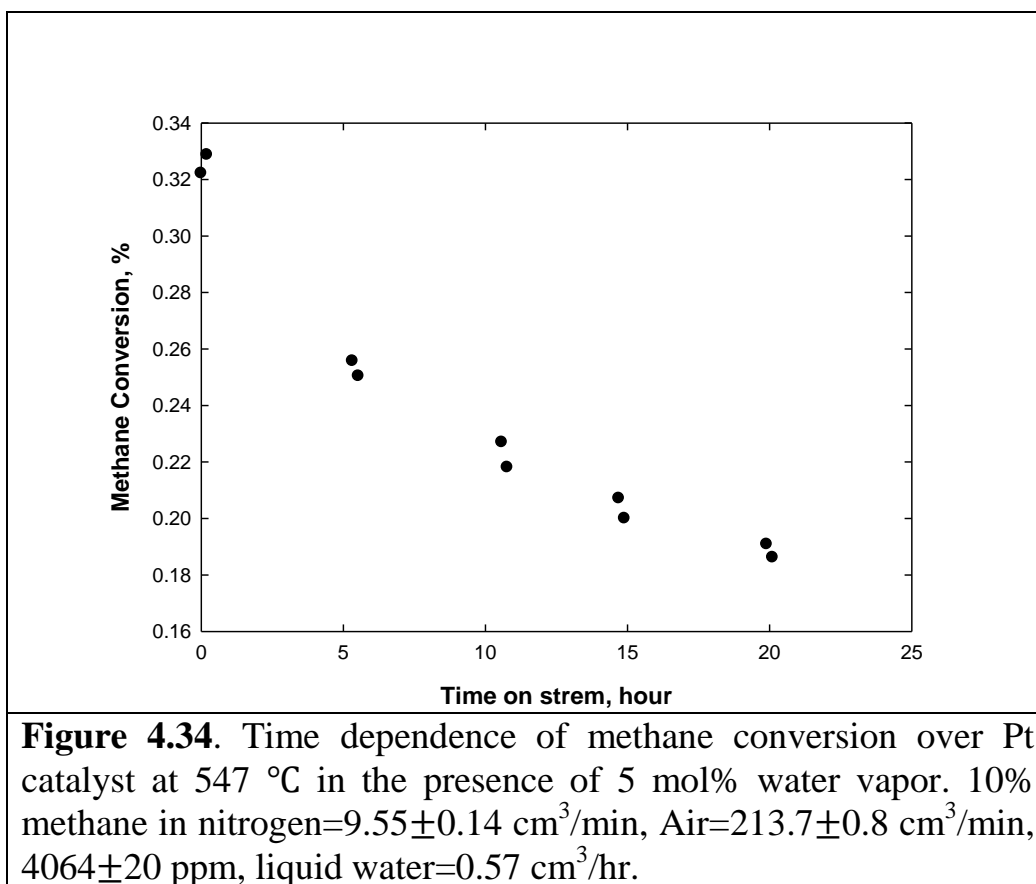


Figure 4.33 influence of 5 mol% water addition on conversion of methane over Pt catalyst versus time on stream.

(Note: the first point at about 50% conversion corresponds to dry feed)

Feed composition (in the presence of water) 10% methane in nitrogen=9.55±0.14 cm³/min, Air=213.7±0.8 cm³/min, 4064±20 ppm, liquid water=0.57 cm³/hr.

Feed composition (in the absence of water) 10% methane in nitrogen=9.55±0.14 cm³/min, Air=225±0.8 cm³/min, 4067±20 ppm.



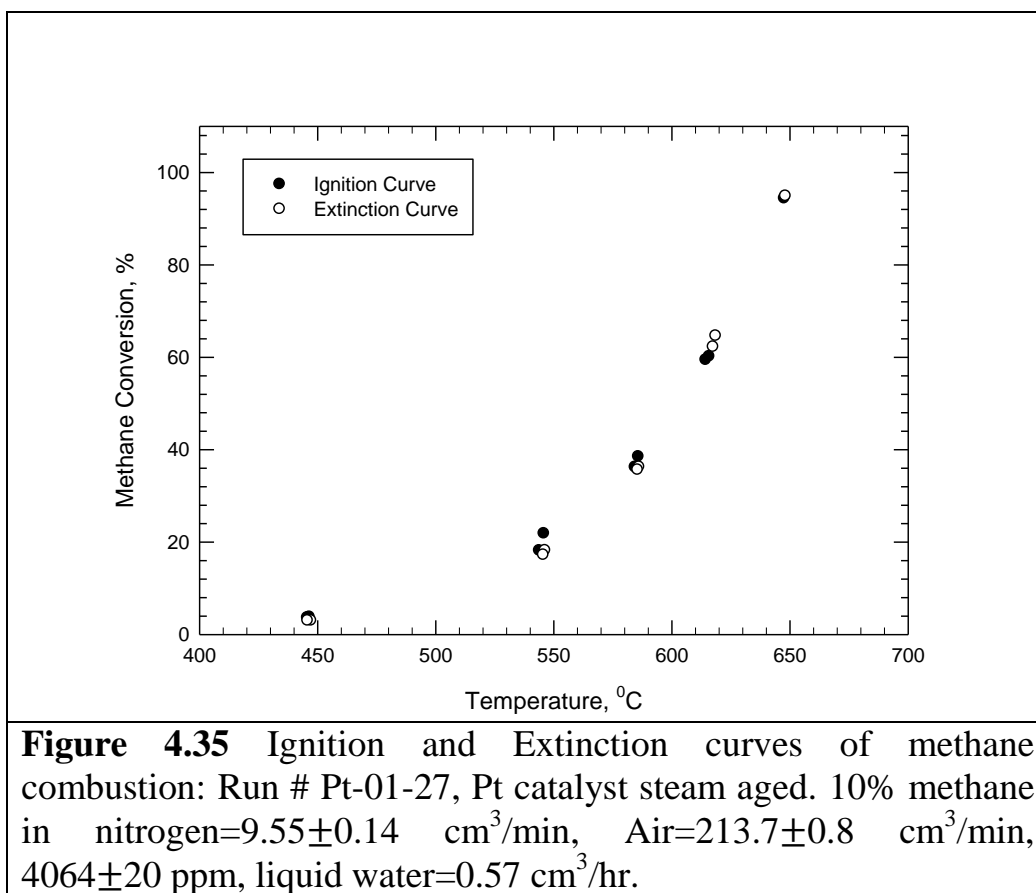
The effect of methane concentration on the activity of steam aged Pt catalyst in the presence and absence of 5 mol % water

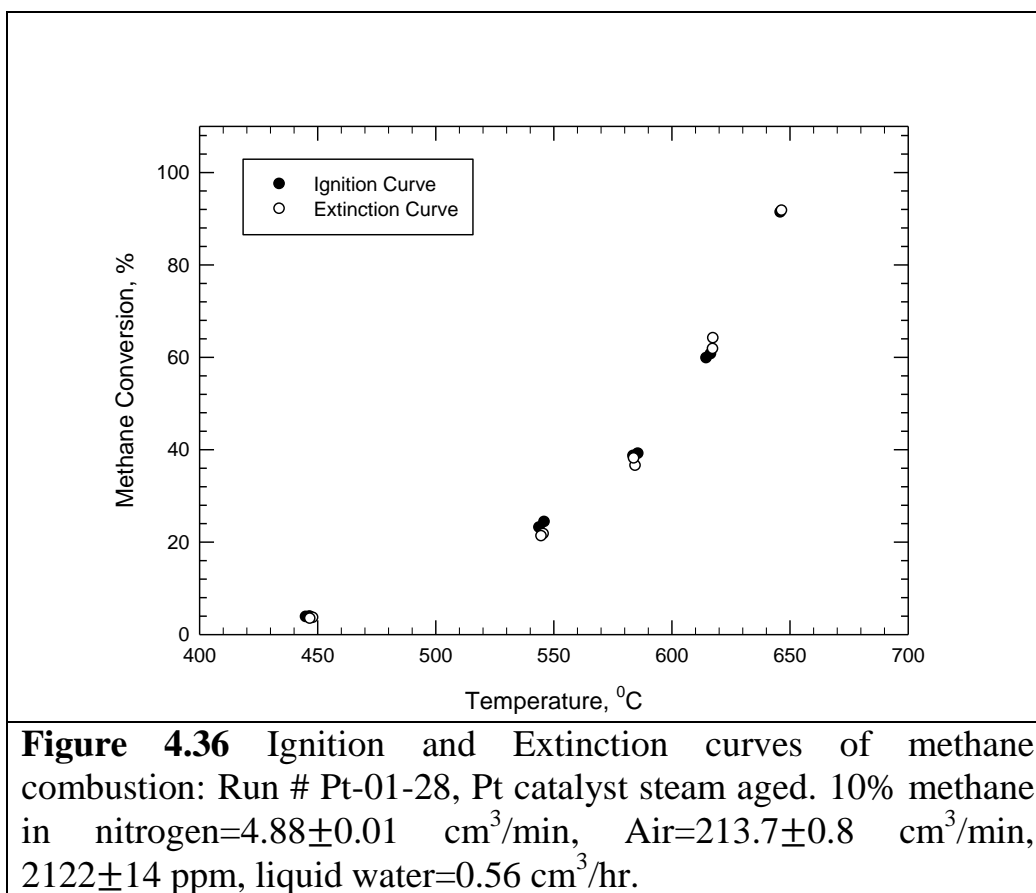
In this part, Ignition-Extinction tests were done at different methane concentrations; (837±4, 1524±33, 2122±14, and 4067±20 ppm in the absence of water) and (836±4, 1526±33, 2122±14, and 4064±20 ppm in the presence of water) on Pt catalyst to investigate the effect of methane concentration on the activity of steam aged Pt catalyst in the presence and absence of added water (Note that no reduction procedure was used at anytime for these runs). The results can be seen in [Figure 4.35](#) to [Figure 4.46](#) ([Figures 4.39 and 4.40](#) show comparisons of the four ignition and extinction curves for tests done over steam-aged Pt catalyst in the presence of water, [Figures 4.45 and 4.46](#) show comparisons of the four ignition and extinction curves for tests done over steam-aged Pt catalyst in the absence of water).

Several interesting observations can be made from these figures. First of all, the activity of steam-aged Pt catalyst is the same in the presence and absence of water for different concentrations of methane; this indicates that reversible inhibition effect caused by the presence of water is almost negligible over steam-aged Pt catalyst.

Second of all, all ignition-extinction curves are almost identical in the presence of water. The same observation can be made in the absence of water. In other words, there is no methane concentration effect over pure Pt catalyst indicating that the overall reaction order with respect to methane concentration is about one.

Finally, there is no hysteresis in the ignition-extinction curves in the presence and absence of water. This is significant, especially for the tests with water, because it shows that the steam aging at 648 °C stabilized the Pt catalyst activity in the presence of water.





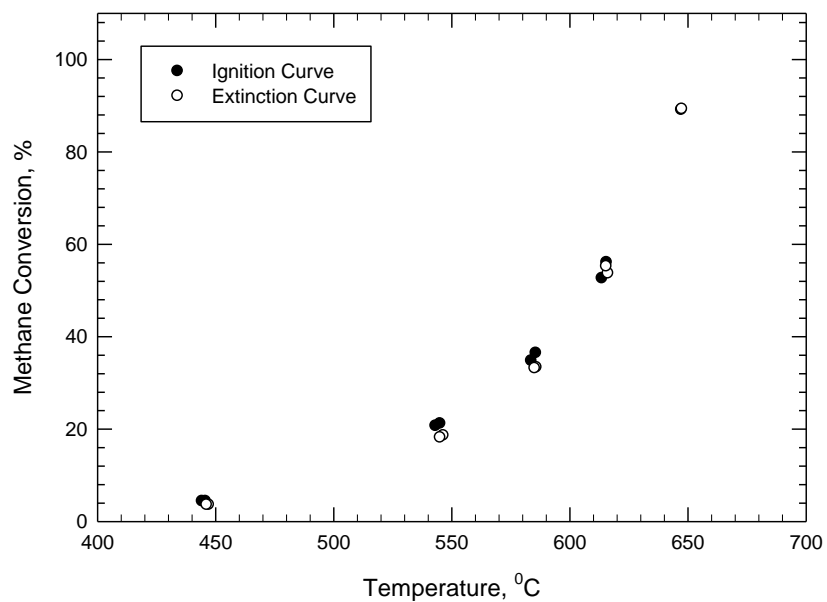


Figure 4.37 Ignition and Extinction curves of methane combustion: Run # Pt-01-29, Pt catalyst steam aged. 10% methane in nitrogen= 3.48 ± 0.06 cm³/min, Air= 213.7 ± 0.8 cm³/min, 1526 ± 33 ppm, liquid water= 0.55 cm³/hr.

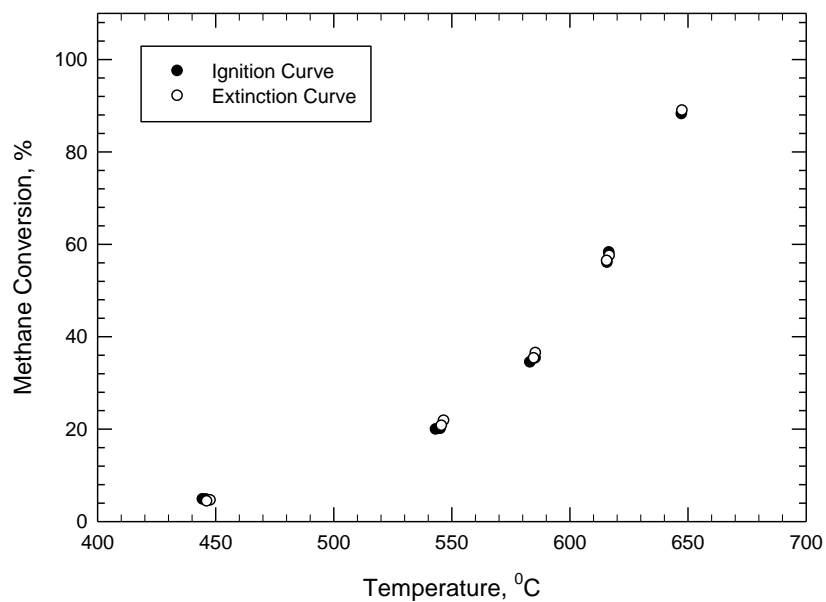
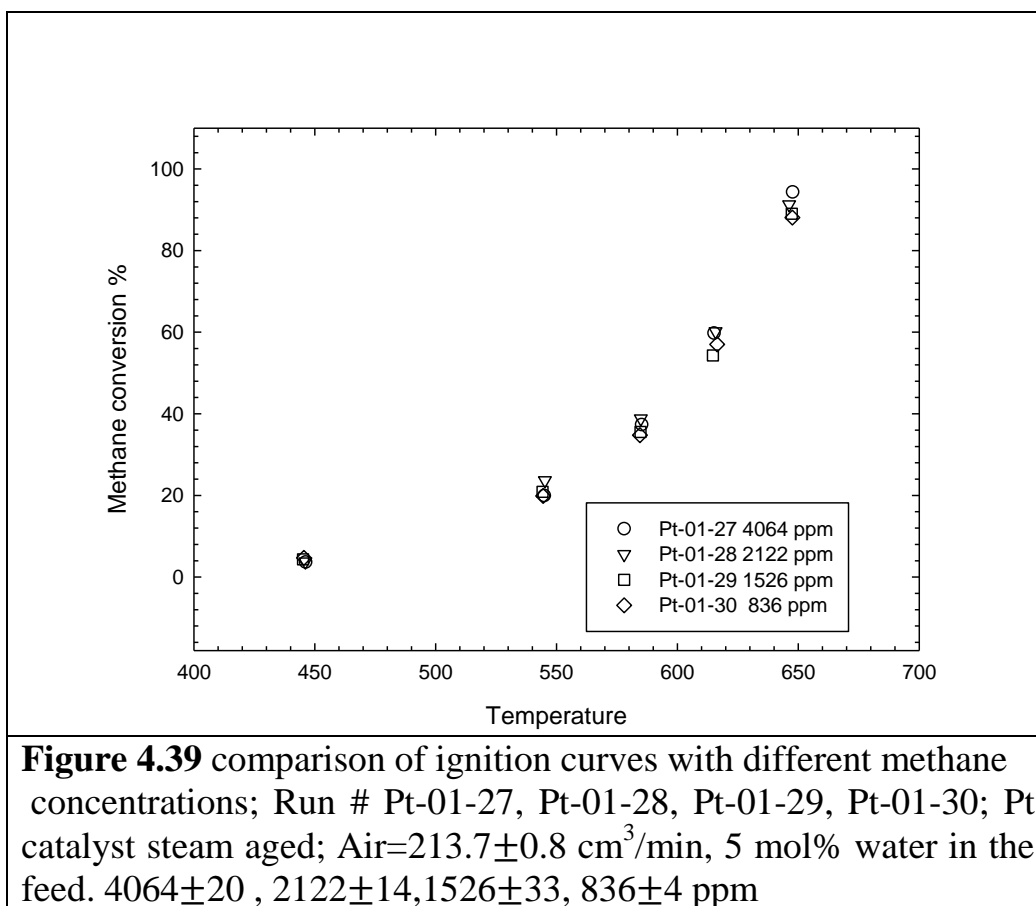


Figure 4.38 Ignition and Extinction curves of methane combustion: Run # Pt-01-30, Pt catalyst steam aged. 2% methane in nitrogen= $9.84 \pm 0.01 \text{ cm}^3/\text{min}$, Air= $213.7 \pm 0.8 \text{ cm}^3/\text{min}$, $836 \pm 4 \text{ ppm}$, liquid water= $0.57 \text{ cm}^3/\text{hr}$.



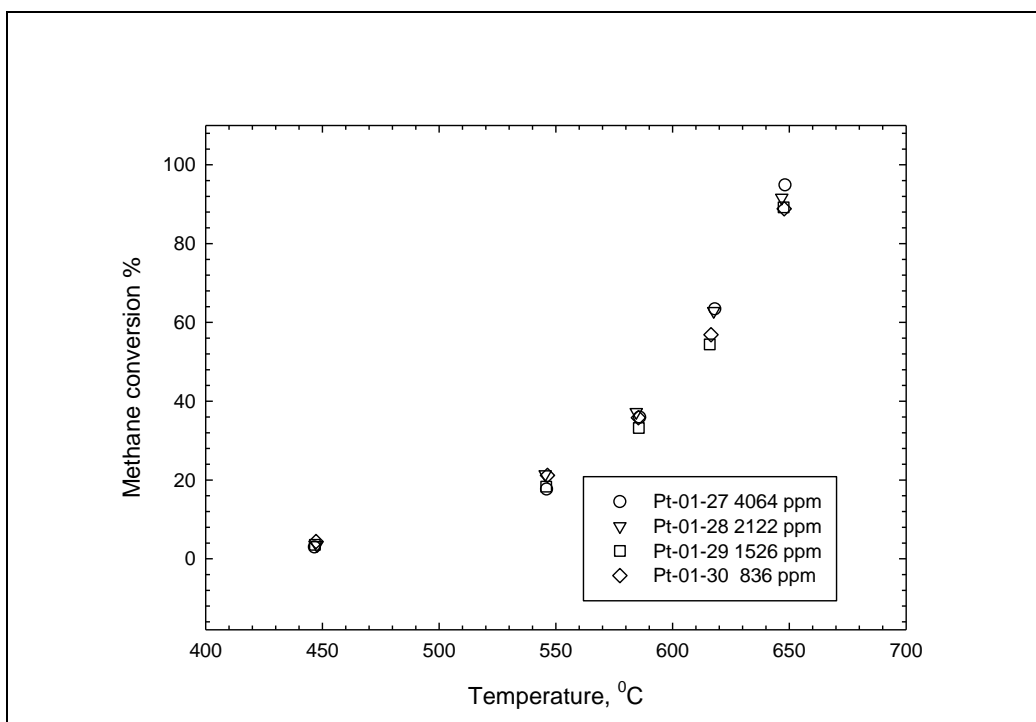


Figure 4.40 comparison of extinction curves with different methane concentrations; Run # Pt-01-27, Pt-01-28, Pt-01-29, Pt-01-30; Pt catalyst steam aged; Air= 213.7 ± 0.8 cm³/min, 5 mol% water in the feed. 4064 ± 20 , 2122 ± 14 , 1526 ± 33 , 836 ± 4 ppm

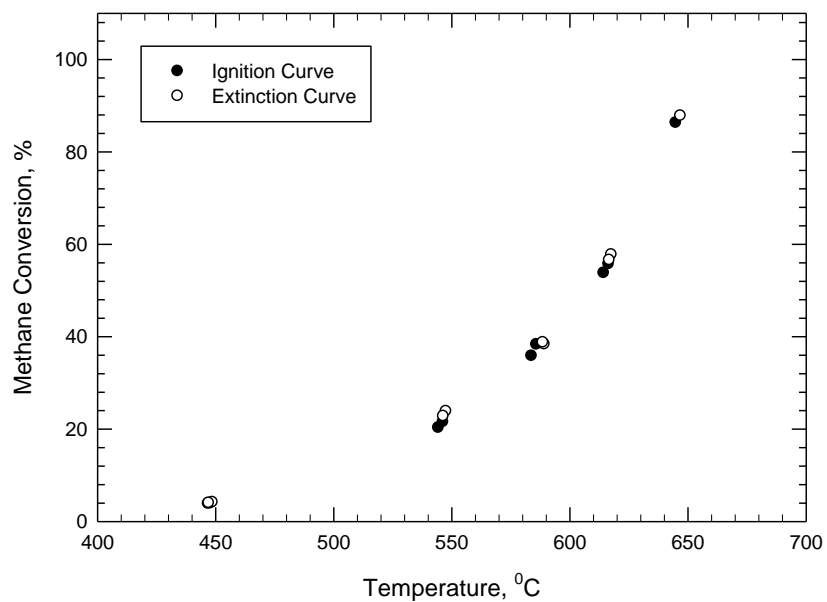


Figure 4.41 Ignition and Extinction curves of methane combustion: Run # Pt-01-32, Pt catalyst steam aged. 10% methane in nitrogen= $9.55 \pm 0.14 \text{ cm}^3/\text{min}$, Air= $225 \pm 0.8 \text{ cm}^3/\text{min}$, $4067 \pm 20 \text{ ppm}$.

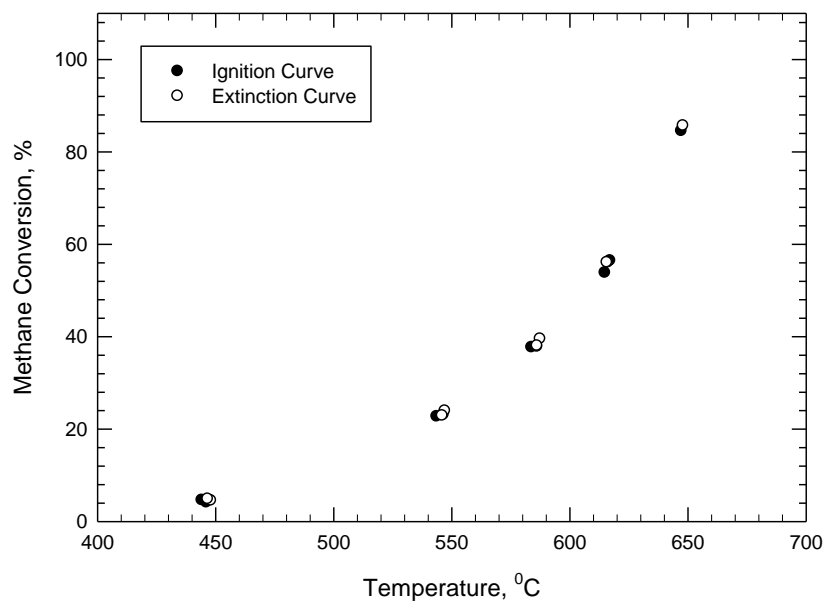


Figure 4.42 Ignition and Extinction curves of methane combustion: Run # Pt-01-33, Pt catalyst steam aged. 10% methane in nitrogen= 4.88 ± 0.01 cm³/min, Air= 225 ± 0.8 cm³/min, 2122 ± 14 ppm.

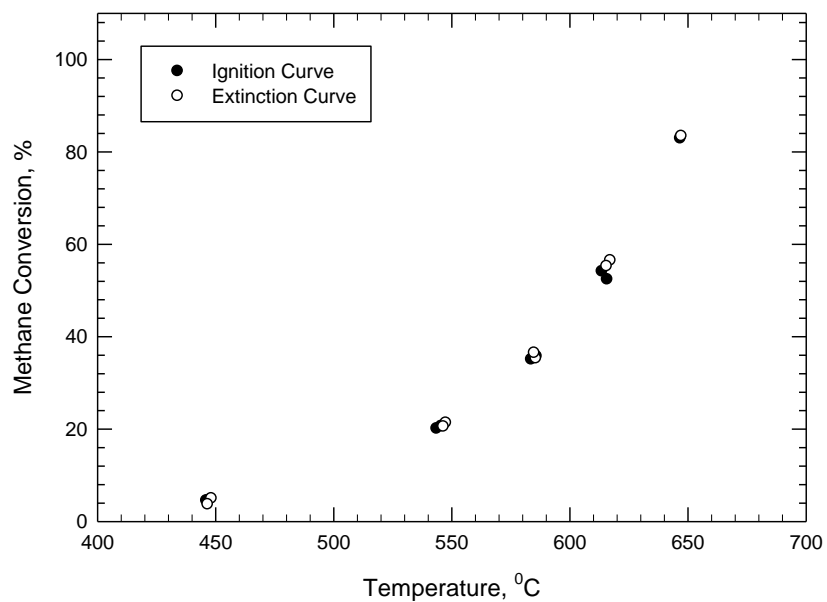


Figure 4.43 Ignition and Extinction curves of methane combustion: Run # Pt-01-34, Pt catalyst steam aged. 10% methane in nitrogen= 3.48 ± 0.06 cm³/min, Air= 225 ± 0.8 cm³/min, 1524 ± 33 ppm.

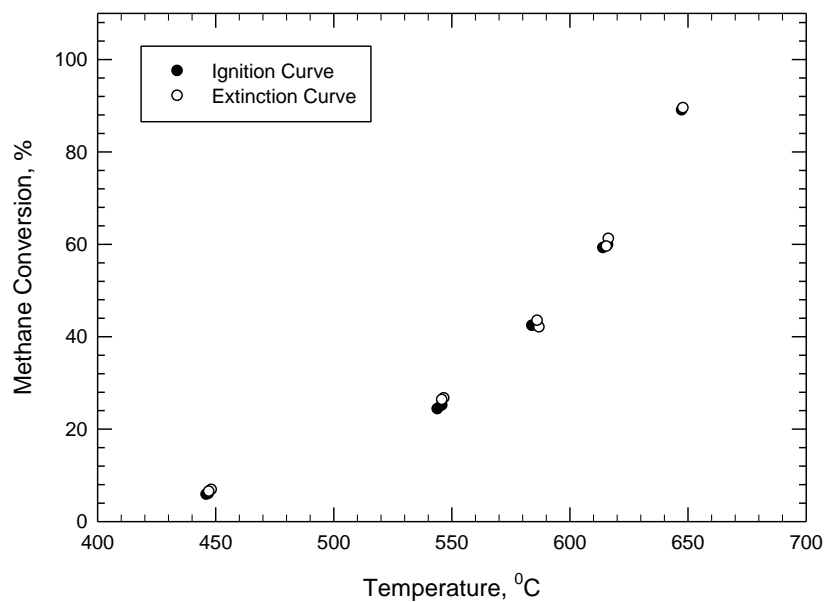


Figure 4.44 Ignition and Extinction curves of methane combustion: Run # Pt-01-31, Pt catalyst steam aged. 2% methane in nitrogen= 9.8 ± 0.01 cm³/min, Air= 225 ± 0.8 cm³/min, 837 ± 4 ppm.

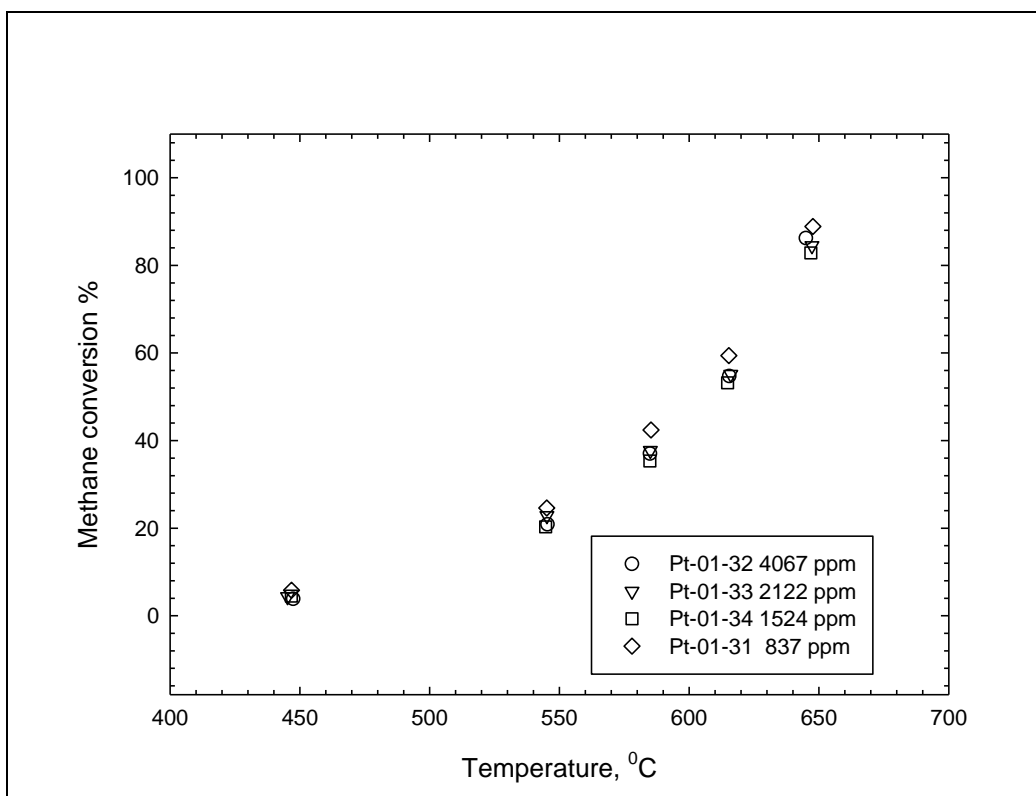


Figure 4.45 comparison of ignition curves with different methane concentrations; Run # Pt-01-32, Pt-01-33, Pt-01-34, Pt-01-31; Pt catalyst steam aged; Air= 225 ± 0.8 cm³/min, 4067 ± 20 , 2122 ± 14 , 1524 ± 33 , 837 ± 4 ppm

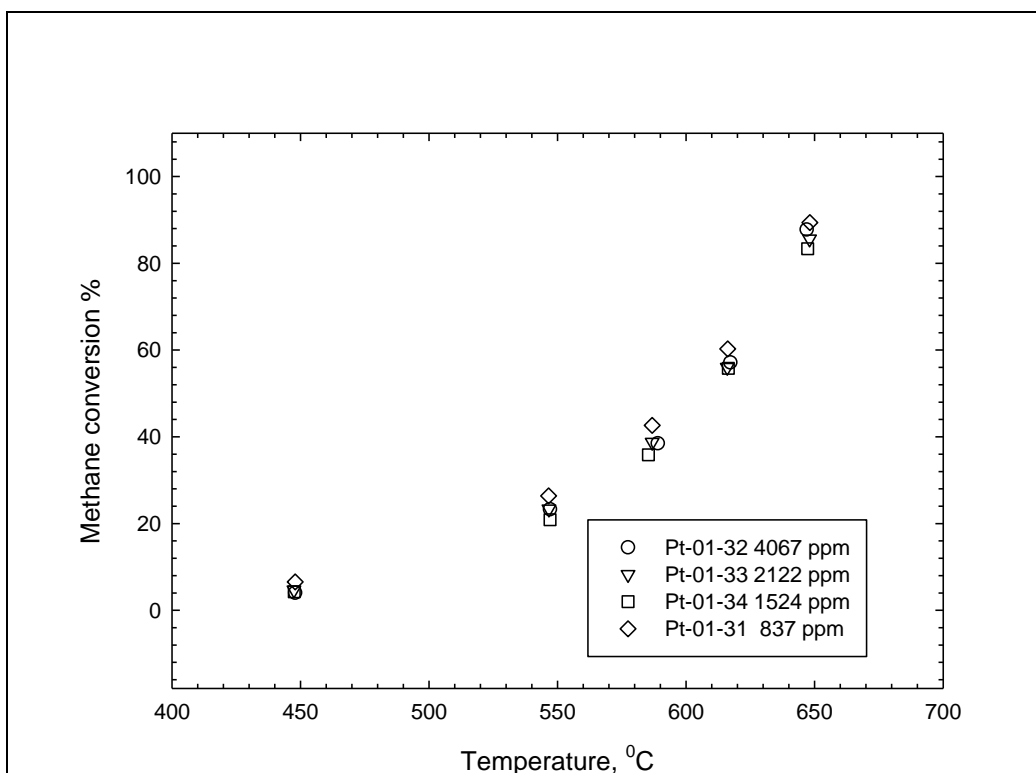


Figure 4.46 comparison of extinction curves with different methane concentrations; Run # Pt-01-32, Pt-01-33, Pt-01-34, Pt-01-31; Pt catalyst steam aged; Air= 225 ± 0.8 cm³/min, 4067 ± 20 , 2122 ± 14 , 1524 ± 33 , 837 ± 4 ppm

4.3 Characterization of catalysts and analysis

4.3.1 Instrumental Neutron Activation Analysis (INAA)

The mass fractions of Pt and Pd in the catalysts were determined by INAA. Two samples from the same catalyst batch were analyzed. The results can be seen in [Table 4.1](#). First of all, the mass fraction of Pt in the catalyst with 95 g/ft³ Pt loading is about 0.41 wt%. Secondly, the weight percent of Pt and Pd are about 0.41% and 0.14% respectively for the Pt-Pd bimetallic catalyst. Interestingly, the ratio of Pt to Pd in the bimetallic Pt-Pd catalyst is about three which looks to be in conflict with the reported ratio of four by the manufacturer. The results from INAA partially explain why Pt-Pd catalyst is more active than Pt catalyst for methane combustion. By comparing the weight percent of Pt and Pd in two catalysts, one realizes that Pt and Pt-Pd catalysts almost have the same Pt loading; however Pt-Pd catalyst contains a considerable amount of additional Pd which probably enhanced the activity of Pt-Pd catalyst in comparison with Pt catalyst.

Table 4.1 Instrumental Neutron Activation Analysis results

Sample ID	Pd (wt %)	1 σ	Pt (wt %)	1 σ
Pt-Pd 95	0.149	0.002	0.429	0.015
Pt-Pd 95	0.132	0.003	0.388	0.015
Pt 95	ND		0.424	0.015
Pt 95	ND		0.391	0.014

- uncertainty $\pm 1\sigma$; 68% confidence limit

- all concentrations in wt %

4.3.2 X-Ray diffraction (XRD)

As stated in [Chapter 3](#), XRD could be used to provide useful information about Pt and Pd crystal phases, as well as to provide other information such as crystal size and the dispersion of catalyst particles. [Figures 4.47](#) to [4.52](#) show the XRD patterns for 8

samples. In [Figures 4.47 to 4.50](#) the unreduced samples are compared with the reduced ones. [Figure 4.51](#) and [4.52](#) compare the XRD patterns of unreduced fresh and steam-aged catalyst samples. The most intense peaks for Pd, PdO and Pt appear at 2θ equal to 40.1° , 33.8° and 39.8° related to reflection planes (1 1 1), (1 0 1), and (1 1 1) respectively.

The detectability of Pd or PdO by XRD strongly depends on the concentration and crystal size of Pd and/or PdO. For example, [Lapisardie et al 2006](#) studied Pd based and Pt-Pd based catalysts (with different Pt to Pd molar ratios) by XRD and they realized that Pd and PdO peaks cannot be detected in catalysts characterized by a Pd loading lower than 2%. They attributed this observation to relatively low Pd content and possibly decreasing size of PdO domains due to Pt mixing with Pd. In a similar study by [Maione et al 2007](#), the Pd or PdO present in Pd/Al₂O₃ system (with a Pd loading equal to 1.54 wt%) could not be detected by XRD.

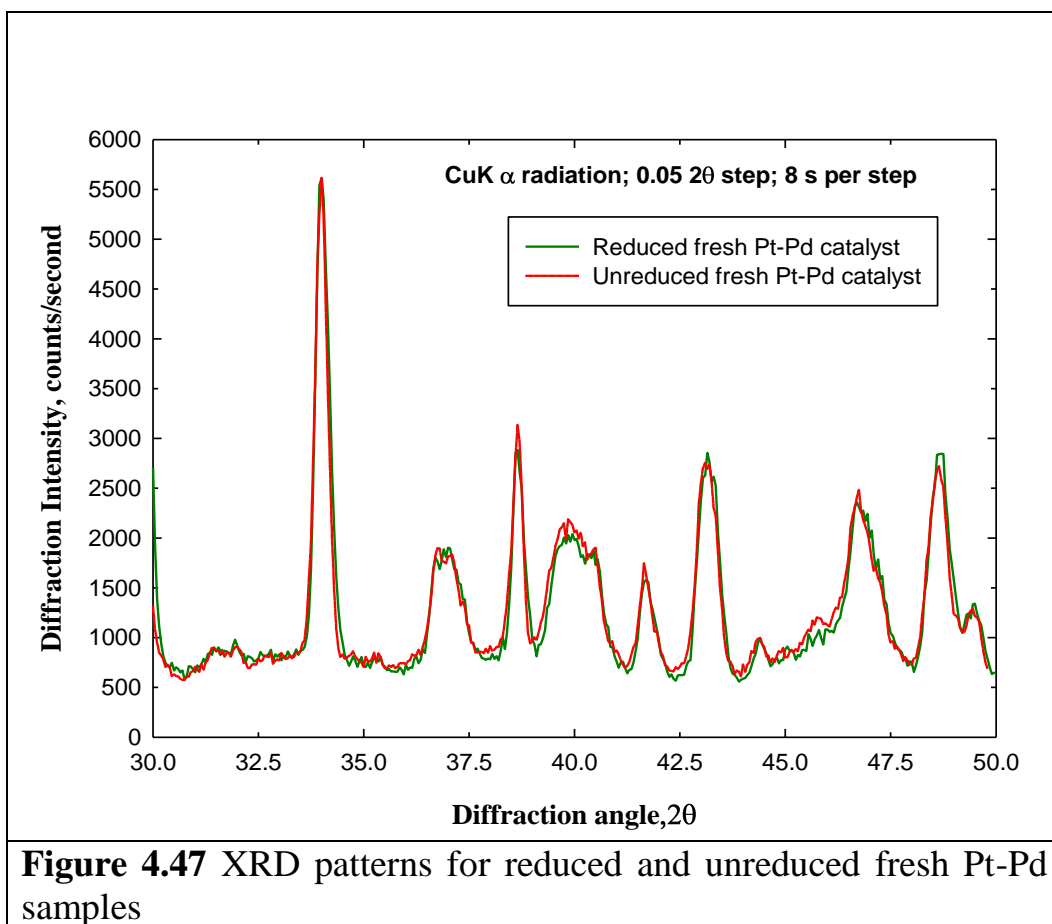
In a similar manner, neither metallic palladium nor palladium oxide were detected in XRD patterns of reduced and unreduced Pt-Pd catalyst samples. It seems that the concentration of Pd and PdO were too low to ensure a meaningful XRD analysis or even to make qualitative comments on Pd dispersion. On the other hand, metallic platinum in all samples were identified by the presence of peaks appearing at 2θ equal to 39.8° related to reflection plane (1 1 1). The Pt peaks were relatively weak and consequently quantification was somehow difficult. However, taking the weakness of Pt peaks in to account, the following observations could be made.

First of all, the weakness of Pt peaks implies that Pt is very well dispersed over the surface of support.

Secondly, the XRD patterns of reduced and unreduced samples are essentially identical, this indicates that reduction pretreatment has almost negligible effect on the structure of catalysts.

Finally, by comparing the XRD patterns of unreduced fresh and steam-aged Pt catalyst in [Figure 4.51](#), one can realize that metallic platinum peak in unreduced steam-aged sample is significantly higher. Consequently, the crystal size of metal particles in

unreduced steam-aged Pt catalyst sample is larger. In other words, steam-aging has resulted in an increase in Pt crystal size. The decrease in Pt dispersion resulting from the increase in Pt crystal size could possibly explain the deactivation of fresh Pt catalyst as a result of high temperature steam-aging. In a similar manner, by comparing the XRD patterns of unreduced fresh and steam-aged Pt-Pd catalyst in [Figure 4.52](#), one can realize that the unreduced fresh Pt-Pd catalyst has much broader peak at 39.8° than the unreduced steam-aged Pt-Pd. This seems to indicate that fresh Pt-Pd catalyst has smaller metal crystallites. Hence, it can be concluded that Pt metal dispersion in Pt-Pd catalyst decreases as a result of high temperature steam-aging. As mentioned before, the decrease in Pt dispersion can partially explain the deactivation of fresh Pt-Pd catalyst as a result of high temperature steam-aging. More interestingly, the area under the Pt peak for the unreduced fresh Pt-Pd sample is much larger than the area under the Pt peak for the unreduced steam-aged Pt-Pd sample. As the area under a peak is proportional to the amount of metal detected by XRD, this indicates that much less metallic Pt is detected in the unreduced steam-aged Pt-Pd sample even if the Pt crystals in this sample are larger. One possible explanation is that the fresh Pt-Pd catalyst contains metal crystals which are a mixture of Pt and Pd. This results in a broad peak. High temperature steam-aging can result in a separation of the Pt and Pd resulting in Pt peaks which are sharper. However, considerably more XRD measurements are required to clearly determine the cause for the changes in the shapes of the peaks.



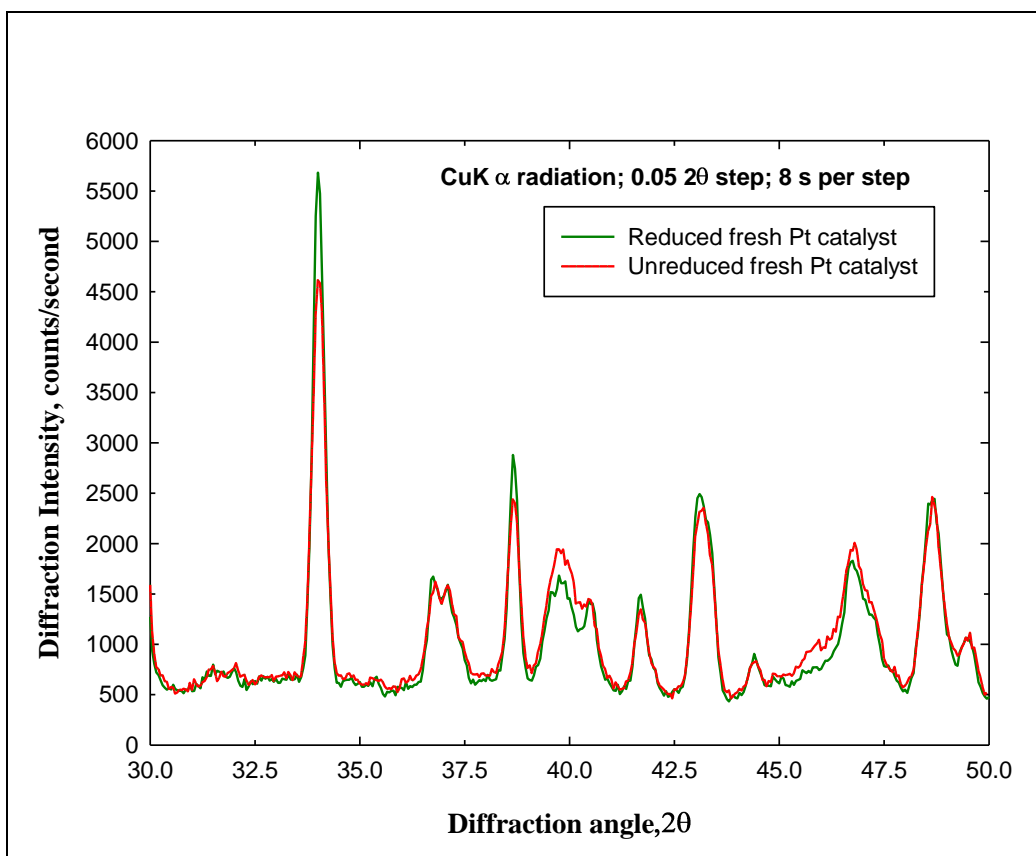


Figure 4.48 XRD patterns for reduced and unreduced fresh Pt samples

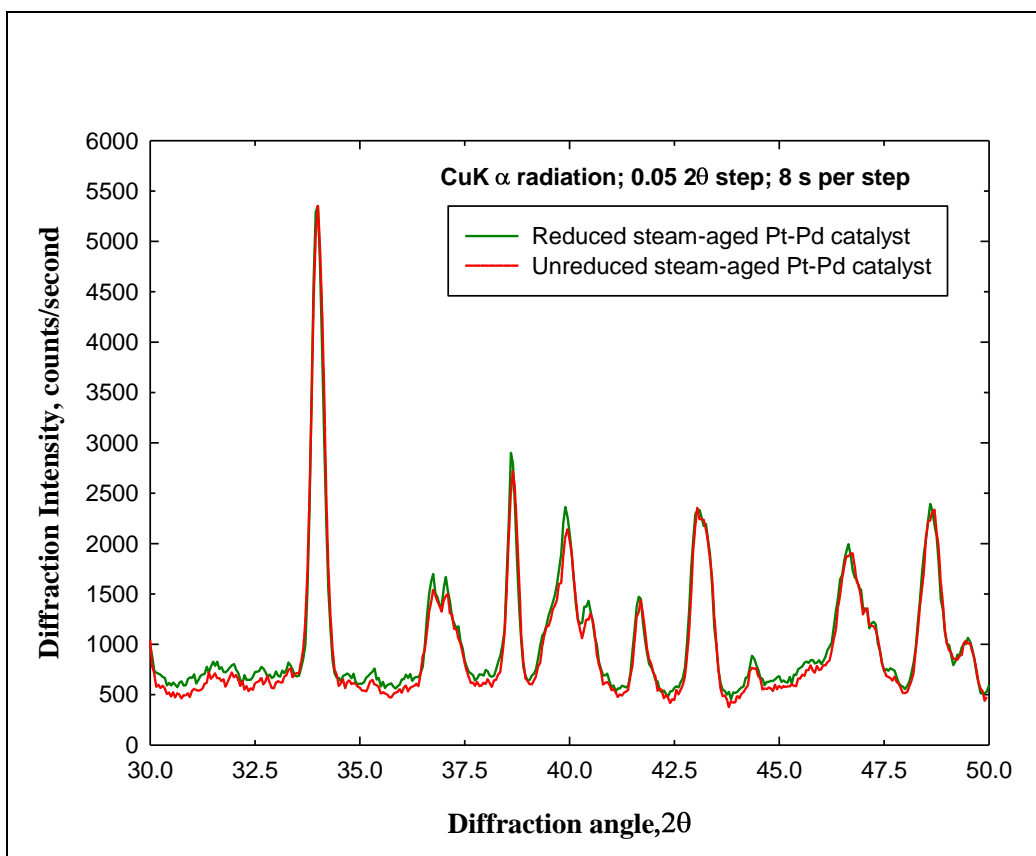


Figure 4.49 XRD patterns for reduced and unreduced steam-aged Pt-Pd samples

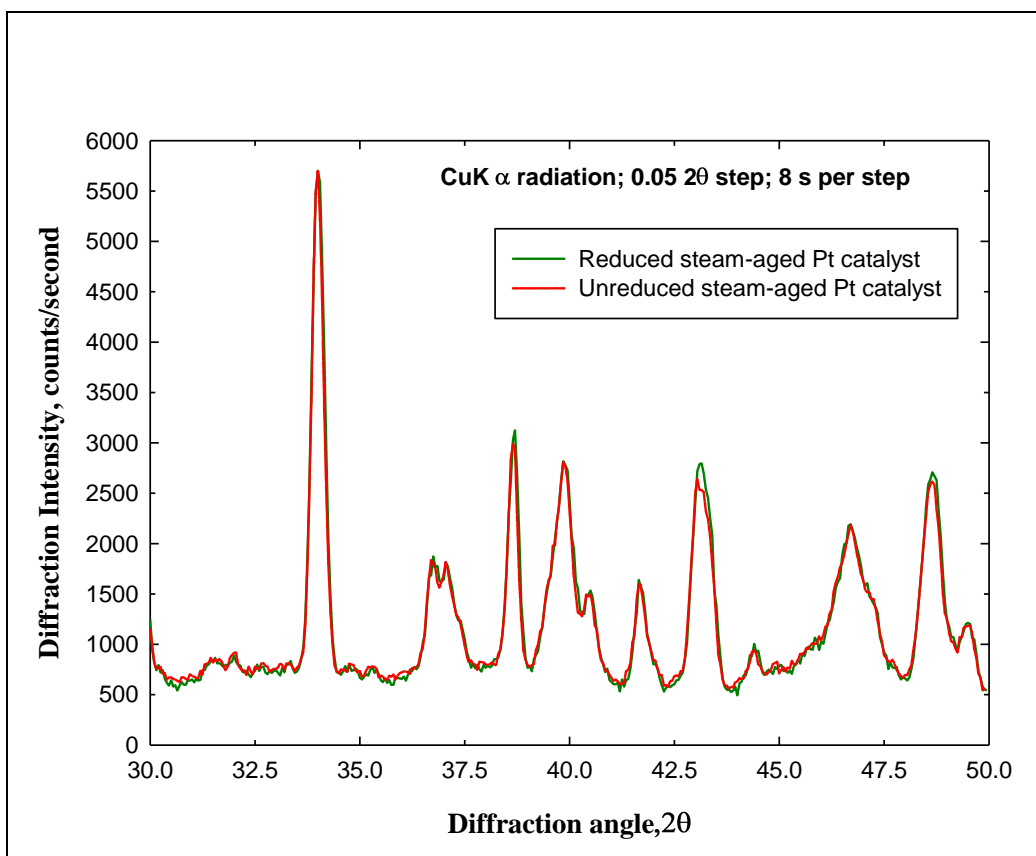


Figure 4.50 XRD patterns for reduced and unreduced steam-aged Pt samples

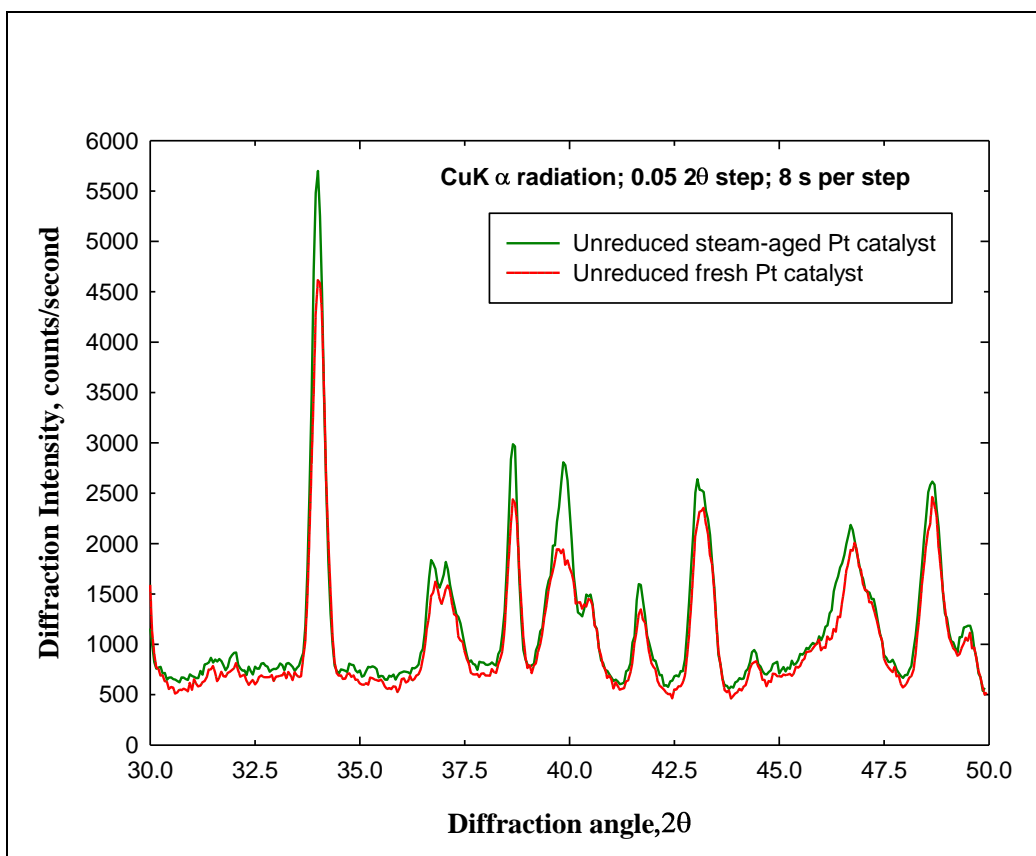


Figure 4.51 XRD patterns for unreduced fresh and steam-aged Pt samples

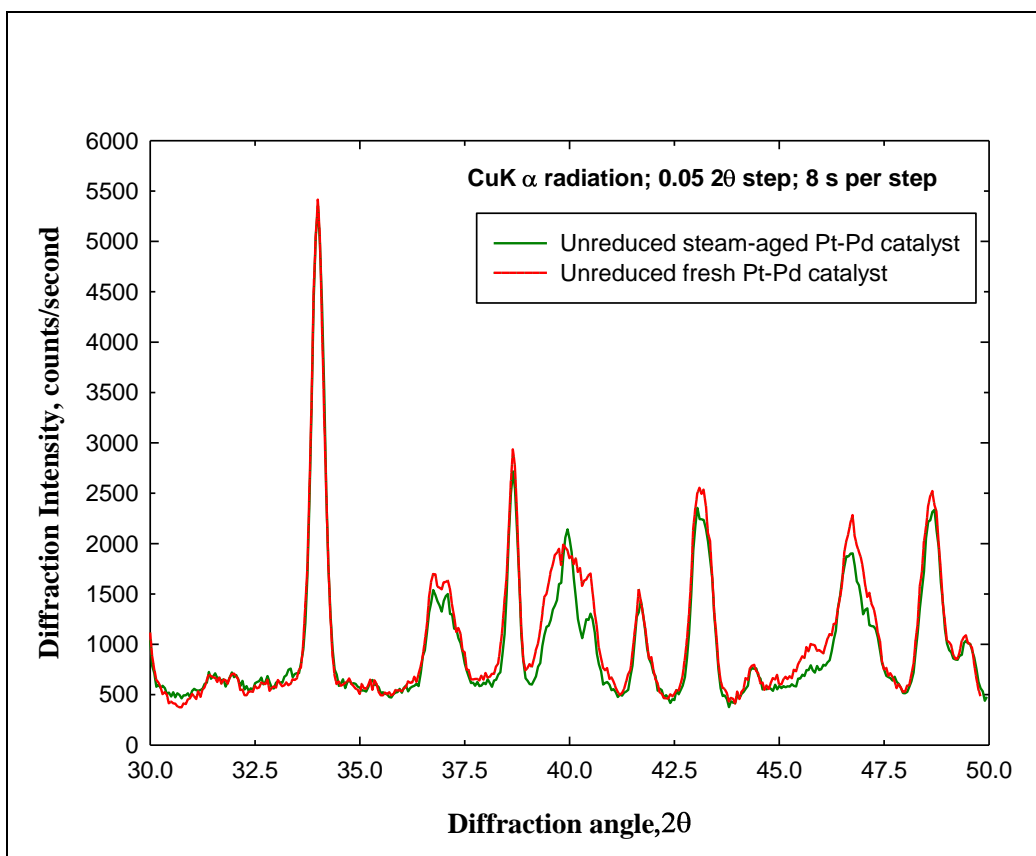


Figure 4.52 XRD patterns for unreduced fresh and steam-aged Pt-Pd samples

4.3.3 X-ray photo electron spectroscopy (XPS)

The XPS measurements were performed on AXIS 165 spectrometer (Kratos Analytical) at the Alberta Centre for Surface Engineering and Science (ACSES), University of Alberta.

The base pressure in the analytical chamber was lower than 3×10^{-8} Pa. Monochromatic Al-K α source ($h\nu = 1486.6$ eV) was used at a power of 210 W. The analysis spot was 400×700 μm . The resolution of the instrument is 0.55 eV for Ag 3d and 0.70 eV for Au 4f peaks. The powders were evenly spread over carbon tape attached to the sample holder.

The survey scans were collected for binding energy spanning from 1100 eV to 0 eV with analyzer pass energy of 160 eV and a step of 0.4 eV. For the high-resolution spectra the pass-energy was 20 eV with a step of 0.1 eV. Number of scans varied from 12 for O1s to 20 for Pt4f_{7/2} and 100 for Pd3d_{5/2}. Charge neutralization was required to compensate the sample charging. The instrument software VISION2 was used for data processing. All binding energies are reported after calibration for C1s peak to match 284.8 eV.

The analysis of palladium, platinum, oxygen and carbon were based on the following photo peaks, Pd3d_{5/2}, Pt4f_{7/2}, O1s and C1s. It is worth mentioning that, the signals of the Pt4f_{7/2} and Pd3d_{5/2} were relatively weak and consequently qualification was somehow difficult. XPS results of various samples can be found in [Table 4.2](#).

As shown in [Table 4.2](#), the binding energy (BE) values of the Pd3d_{5/2} for fresh and steam-aged Pt-Pd catalysts are (337.61 eV) and (337.25 eV) respectively. These values of binding energy for the Pd3d_{5/2} peak indicate that, the surface of palladium particles is in the oxidized state. (The BE values for Pd, PdO, and PdO₂ are 335.1 eV, 336.2 eV, and 338 eV respectively) ([Moulder et al 1995](#)).

Furthermore, as shown in [Table 4.2](#), the binding energy values of the Pt4f_{7/2} for fresh Pt catalyst, steam-aged Pt catalyst, fresh Pt-Pd catalyst, and steam-aged Pt-Pd catalyst are 70.93 eV, 70.54 eV, 71.21 eV, 71.25 eV respectively. Based on literature data, BE

value for metallic Pt $4f_{7/2}$ is 71.2 eV(Moulder et al 1995). This indicates that the surface of Pt particles is in metallic state in every case.

Table 4.2 X-ray photo electron spectroscopy results

Catalyst sample description	BE, Pd 3d_{5/2} (eV)	BE, Pt 4f_{7/2} (eV)
Fresh Pt-Pd catalyst (oxidized at 650°C in air)	337.61	71.21
Steam-aged Pt-Pd catalyst	337.25	71.25
Fresh Pt catalyst (oxidized at 650°C in air)	-	70.93
Steam-aged Pt catalyst	-	70.54

Chapter 5: Summary and future work

5.1 Summary

5.1.1 General behavior of the catalysts

Several interesting phenomena were observed from ignition-extinction patterns of Pt and Pt-Pd catalysts.

- 1) Fresh Pt-Pd catalyst is more active than fresh Pt catalyst by quite a lot at all methane concentrations.
- 2) Fresh Pt-Pd catalyst shows a significant reproducible slope change in ignition curve at about 550°C, however, this slope change was not observed over the fresh Pt catalyst.
- 3) Reduction pretreatment seems to have little if any effect on the activity of Pt and Pt-Pd catalysts.
- 4) The ignition-extinction experiments on fresh Pt and Pt-Pd catalysts are reproducible without reduction.
- 5) It is evident that there is a strong methane concentration effect on ignition-extinction curve for fresh Pt-Pd catalyst; however, there is no methane concentration effect over pure fresh Pt catalyst. The fact that methane conversion is independent of concentration over fresh Pt catalyst indicates that the overall reaction order with respect to methane is about one over fresh Pt catalyst.
- 6) For ignition-extinction experiments where the reaction temperature does not exceed 550°C, the slope change in the ignition curve cannot be observed over fresh Pt-Pd catalyst.
- 7) The extinction curves are more active than the ignition curves for fresh Pt-Pd catalyst. However, the ignition and extinction curves are the same for fresh Pt catalyst.
- 8) Water has a strong negative effect on the activity of Pt and Pt-Pd catalysts. Both catalysts lose a large portion of their activity as a result of exposure to 5 mol% water in the feed stream.

9) After water injection was stopped, both catalysts recovered some of their initial activity, however, Pt catalyst only recovered a small fraction of its initial activity.

10) The activity of both Pt and Pt-Pd catalysts declines exponentially as a result of steam-aging at about 650°C. In addition, steam aging at about 650°C produces stable catalysts with constant catalytic activity.

11) In the presence of water, there was no methane concentration effect over steam aged Pt-Pd catalyst. In addition, there is a significant reproducible slope change at about 550°C and the ignition curves are more active than extinction curves for tests over steam-aged Pt-Pd catalyst in the presence of water.

12) In the absence of water, strong methane inhibition can be observed over steam-aged Pt-Pd catalyst, more interestingly there is no hysteresis under these conditions (the ignition and extinction curves are the same for tests over steam-aged Pt-Pd catalyst in the absence of water). Furthermore, there is no observable slope change at about 550°C in the absence of water.

13) The activity of steam-aged Pt catalyst is insensitive to presence or absence of 5 mol% water in the feed stream.

14) There is no methane concentration effect over steam-aged Pt catalyst. In addition, the ignition and extinction curves are the same for different concentrations of methane; in other words, there is no hysteresis over steam-aged Pt catalyst (there is no methane concentration effect over Pt for fresh and steam-aged samples).

5.2 Future work

5.2.1 Gas constitutes

The gas feeds used in this project are much simpler than real exhaust gases from internal combustion engines containing not only methane and water but also unacceptable levels of carbon

monoxide, and NO_x according to many former researchers (Fino et.al 2007). The catalyst behavior will be a lot different under this complex gas atmosphere because of interaction among different compounds. First of all, some of the gas components may improve or inhibit the reaction (Salaun et al 2009). Secondly, the real exhaust gas will contain water mole fractions as high as 10 percent, which is much higher than the water mole fraction that was used in this project. For example, presence of additional hydrogen in gas feeds is believed to improve methane conversion because of exothermal feature of methane combustion reaction, so it is worthwhile to examine the activity of catalyst in a lean methane environment in the presence and absence of compounds like CO_2 , water, CO, hydrogen, and NO. The catalyst activity study should be performed at different compositions and concentration, over a range of temperatures (550 to 850 K). Also combustion of rich methane streams deserves to be investigated as a comparison to lean methane combustion.

5.2.2 Various pretreatments

In this project three kinds of pretreatments were used. First of all, all catalyst samples were aged in the air for 10 hours at 650°C . In addition, in order to investigate the effect of reduction on catalysts' activity, reduction pretreatment was done on catalyst samples in some experiments. Finally, in order to stabilize the activity of catalysts and in order to get reproducible results for tests in the presence of water, the catalyst samples were steam-aged at about 650°C .

It has been proved that, aging in air will stabilize the performance of Pt and Pt-Pd catalysts (in the absence of water). Furthermore, although the activity of Pt and Pt-Pd catalysts decreases greatly as a result of steam-aging at about 650°C , steam-aging can stabilize the catalysts' activity and it can lead to reproducible results for tests in the presence of water on Pt and Pt-Pd catalysts. Finally, reduction has negligible effect on the activity of Pt and Pt-Pd catalysts.

In a similar manner other pretreatments can possibly influence the performance of catalysts, therefore, the effect of other pretreatments such as pretreatment with O₂-CH₄-Carrier gas mixture or high temperature oxidation on the activity of fresh and steam-aged Pt-Pd catalysts deserves to be investigated.

5.2.3 Catalyst characterization

The state of precious metals on the surface of catalyst has an important effect on the activity of catalyst, so the role of the surface state on the activity of catalyst should be thoroughly studied by comparing reduced, oxidized, used, and deactivated catalysts. In this project metal contents (Pt and Pd) were determined by instrumental neutron activation analysis (INAA) using the Slowpoke reactor facility at the University of Alberta. Furthermore, wide angle X-ray diffraction (XRD) was used to determine the bulk metal phase and metal crystal sizes using XRD facilities. It will be an excellent supplement to investigate catalysts via other characterization methods to gain better understanding of the results from aging, reduction, and oxidation. First of all, energy dispersive X-ray analysis (EDX) can be used to study spatial distribution of active metal on the surface of support. Secondly, transmission electron microscopy (TEM) can be used to determine metal particle sizes which are the key parameter affecting activity of catalyst. Another reason to emphasize the importance of catalyst characterization is to comprehend the catalyst composition which can be used to justify interesting unusual behaviors observed in this project especially methane inhibition effect which is neglected in reported studies. All in all, detailed investigation of catalyst composition via characterization methods can provide important and useful feedbacks on phenomena like catalyst activity, methane and water inhibition effects, etc.

5.2.4 Further study on catalyst formulation

New catalyst formulations should be tested for activity and water resistance. For instance, the effect of Pt ratio on the catalyst activity should be investigated more thoroughly. [Persson et.al \(2006\)](#) investigated catalysts with different platinum and palladium molar ratios. They discovered that in Pt/Pd bimetallic catalyst an alloy between Pt and Pd was formed which was in close contact with PdO phase, with an exception for Pt-rich catalyst where no PdO phase was observed. In addition, they found that molar ratio between platinum and palladium strongly influences both activity and stability of catalysts for methane conversion. They found out that adding relatively small amounts of Pt in to Pd based catalyst can greatly improve activity of Pd based catalyst in comparison with monometallic Pd catalyst. However, higher amounts of Pt should be added to palladium catalysts to stabilize methane conversion. The effect of addition of other co-metals such as Ag, Au, Rh, Co, Ir, Ni, Au, and Cu on the performance of the Pt and Pd based catalysts can also be investigated.

References

- Anderson, R.B., Stein, K.C., Feenan, J.J. and Hofer, L.J.E., 1961. Catalytic oxidation of methane. *Industrial and Engineering Chemistry Research*, 53: 809-812.
- Araya, P., Guerrero, S., Robertson, J., and Gracia, F., 2005. Methane combustion over Pd/SiO₂ catalysts with different degrees of hydrophobicity. *Applied Catalysis A: General*, 283(1-2):225–233.
- Arrosio, F., Colussi, S., Groppi, G., and Trovarelli, A., 2007. Regeneration of S-poisoned Pd/Al₂O₃ and Pd/CeO₂/Al₂O₃ catalysts for the combustion of methane. *Topics in Catalysis*, 42-43 (1-4): 405-408.
- Aryafar, M., Zaera, F., 1997. Kinetic study of the catalytic oxidation of alkanes over nickel, palladium, and platinum foils. *Catalysis Letters*, 48(3-4) :173-183.
- “Automobile Emissions: An overview”,
<http://www.epa.gov/oms/consumer/05-autos.pdf>. Last Visited 20 July 2010.
- Au-Yeung, D., Chen, K., Bell, A., and Iglesia, E., 1999b. Isotopic studies of methane oxidation pathways on PdO catalyst. *Catalysis*, 188:132–139.

Baldwin, T.R. and Burch, R., 1990. Catalytic combustion of methane over supported palladium catalysts: 2. Support and possible morphological effects. *Applied Catalysis*, 66: 359-381.

Baldwin, T.R. and Burch, R., 1990. Catalytic combustion of methane over supported palladium catalysts: 1. Alumina supported catalysts. *Applied Catalysis*, 66: 337-358.

Bird, R. B., Stewart, W. E., and Lightfoot, E. N., 2001. Transport phenomena , Second edition, Wiley.

Bittance, J.C., 1977. Sorting out ceramics. *Machine Design*, 49(28): 176-182.

Bond, T. C., Noguchi, R. A., Chou, C.-P., Mongia, R. K., Chen, J., and Dibble, R. W., 1996. Catalytic oxidation of natural gas over supported platinum: Flow reactor experiments and detailed numerical modeling. *Twenty-sixth Symposium (International) on Combustion /The Combustion Institute*, pages 1771–1778.

Boudart, M., Aldag, A., Benson, J. E., Dougharty, N. A., and Harkins, G. G., J., 1966. On the Specific Activity of Platinum Catalysts, *Journal of catalysis*, 6, 92 (1966).

Briot, P., Auroux, A., Jones, D. and Primet, M., 1990. Effect of particle size on the reactivity of oxygen-adsorbed platinum supported on alumina. *Applied Catalysis.*, 59: 141-152.

Briot, P. and Primet, M., 1991. Catalytic oxidation of methane over palladium supported on alumina. *Applied Catalysis.*, 68: 301-314.

Burch R., Loader P.K., 1994. Investigation of Pt/Al₂O₃ and Pd/Al₂O₃ catalysts for the combustion of methane at low concentrations. *Applied Catalysis B: Environmental*, 5(1-2):149-164.

Burch, R., Urbano, F. J., and Loader, P. K., 1995. Methane combustion over palladium catalysts: The effect of carbon dioxide and water on activity. *Applied Catalysis A: General*, 123(1):173–184.

Chou, C.-P., Chen, J.-Y., Evans, G. H., and Winters, W. S., 2000. Numerical studies of methane catalytic combustion inside a monolith honeycomb reactor using multi-step surface reactions. *Combustion Science and Technology*, 150(1):27–57.

Choudhary, V. and Rane, V., 1992. Pulse micro reactor studies on conversion of methane, ethane, and ethylene over rare earth oxides in the absence and presence of free oxygen. *Journal of Catalysis*, 135(1):310–316.

Choudhary, V. and Rane, V. H., and Chaudhari, S. T., 1997. Surface property of rare earth promoted MgO catalysts and their activity/ selectivity in oxidative coupling of methane. *Applied Catalysis A: General*, 158:121-136.

Choudhary, T.V , Banerjee, S , Choudhary, V.R ., 2002. Catalysts for combustion of methane and lower alkanes. *Applied Catalysis A: General*, 234(1-2) :1-23.

Ciuparu, D. and Pfefferle, L., 2001. Support and water effects on palladium based methane combustion catalysts. *Applied Catalysis A: General*, 209(1-2):415–428.

- Ciuparu, D., Altman, E., and Pfefferle, L., 2001. Contribution of lattice oxygen in methane combustion over PdO-based catalysts. *Catalysis*, 234:64–74.
- Ciuparu, D., Lyubovsky, M. R., Altman E. Pfefferle, L. D., and Datye, A., 2002. Catalytic combustion of methane over palladium-based catalysts. *Catalysis Reviews-Science and Engineering*, 44 (4): 593-649.
- Ciuparu, D., Perkins, E., and Pfefferle, L. D., 2004. In situ DR-FTIR investigation of surface hydroxyls on γ - Al_2O_3 supported PdO catalysts during methane combustion. *Applied catalysis A: General*, 263(2):145-153.
- Cullis, C. F., Nevell, T. G., and Trimm, D. L., 1972. Role of the catalyst support in the oxidation of methane over palladium. *Journal of the Chemical Society, Faraday Transactions 1: Physical Chemistry in Condensed Phases*, 68: 1406-1412.
- Cullis, CF. and Willatt, B.M., 1983. Oxidation of methane over supported precious metal catalysts. *Journal of Catalysis*, 83: 267-285.
- Datye, A., Bravo, J., Nelson, T. R., Atanasova, P., Lyubovsky, M., and Pfefferle, L., 2000. Catalyst microstructure and methane oxidation reactivity during the Pd \leftrightarrow PdO transformation on alumina supports. *Applied Catalysis A:General*, 198 (1-2): 179-196.
- Dragos Ciuparu, Maxim R. Lyubovsky, Eric Altman, Lisa D. Pfefferle, and Abhaya Datye , 2002. Catalytic combustion of methane over palladium-based catalysts, *Catalysis Reviews*, 44, 593–649.
- Demoulin, O., Navez, M., and Ruiz, P., 2005. Investigation of the behavior of a Pd/ γ - Al_2O_3 catalyst during methane combustion

reaction using in situ drift spectroscopy. *Applied Catalysis A: General*, 295(1):59–70.

Deutschmann, O., Behrendt, F., and Warnatz, J., 1994. Modeling and simulation of heterogeneous oxidation of methane on a platinum foil. *Catalysis Today*, 21(2-3):461–470.

Deutschmann, O., Schmidt, R., Behrent, F., and Warnatz, J., 1996. Numerical modelling of catalytic ignition. *The 26th symposium (international) on Combustion/Combustion Institute*, pages 747–1754.

Deutschmann, O., Behrendt, F., and Warnatz, J., 1998. Formal treatment of catalytic combustion and catalytic conversion of methane. *Catalysis Today*, 46(2-3):155–163.

Deutschmann, O., Maier, L. I., Riedel, U., Stroemman, A. H., and Dibble, R. W., 2000. Hydrogen assisted catalytic combustion of methane on platinum. *Catalysis Today*, 59(1-2):141–150.

Deutschmann, O., Schmidt, R., Behrent, F., and Warnatz, J., 1996. Numerical modelling of catalytic ignition. *The 26th symposium (international) on Combustion/Combustion Institute*, pages 747–1754.

Dubien, C., Schweich, D., Mabilon, G., Martin, B., and Prigent, M., 1998. Three-way catalytic converter modeling: Fast- and slow-oxidizing hydrocarbons, inhibiting species, and steam reforming reaction. *Chemical Engineering Science*, 53:471 – 481.

Ebtekar T, 2004, Air pollution, *Sharif Institute of Technology journal* 7: 37-41.

Engel, T. and Ertl, G., 1978. A molecular beam investigation of the catalytic oxidation of CO on Pd(111). *Journal of Chemical Physics*, 69(3):1267–1281.

EPA, 1998. Inventory of U.S. Greenhouse Gas Emissions and Sinks: 1990-1995. Technical report, EPA.

Escandon, L. S., Ordonez, S., Vega, A., and Di'ez, F. V., 2005. Oxidation of methane over palladium catalysts: Effect of the support. *Chemosphere*, 58(1):9–17.

Fino, D., Ruso, N., Saracco, G., and Specchia, V., 2007. Supported Pd-perovskite catalyst for CNG engines' exhaust gas treatment. *Progress in Solid State Chemistry*, 35: 501-511.

Fogler, H.S, 2005. Elements of chemical reaction engineering , third edition, Prentice-Hall.

Froment, G.F., Bischoff, K.B., 1990. Chemical reactor analysis and design, Second edition, New York.

Fujimoto, F., Ribiero, R., Avalos borja, A., and Iglesia, E., 1998. Structure and reactivity of PdO_x/ZrO₂ catalysts for methane oxidation at low temperatures . *catalysis*, 179:431–442.

Garbowski, E., Feumi-Jantou, C., Mouaddib, N., and Primet, M., 1994. Catalytic combustion of methane over palladium supported

on alumina catalysts: Evidence for reconstruction of particles. *Applied Catalysis A: General*, 109(2):277–292.

Gelin, P. and Primet, M., 1999. Modeling heterogeneous and homogeneous reactions in the high-temperature catalytic combustion of methane. *Chemical engineering Science*, 54:5791–5807.

Gelin, P. and Primet, M., 2002. Complete oxidation of methane at low temperature over noble metal based catalysts: a review. *Applied Catalysis B: Environmental*, 39(1):1–37.

Gelin, P., Urfels, L., Primet, M., and Tena, E., 2003. Complete oxidation of methane at low temperature over Pt and Pd catalysts for the abatement of lean- burn natural gas fuelled vehicles emissions: Influence of water and sulphur containing compounds. *Catalysis Today*, 83(1-4):45–57.

Golodets, G. I., 1983. Heterogeneous catalytic reactions involving molecular oxygen. *Studies in Surface Science and Catalysis*, 15:437 – 452.

Griffin, T. A., Calabrese, M., Pfefferle, L. D., Sappey, A., Copeland, R., and Crosley, D. R., 1992. The influence of catalytic activity on the ignition of boundary layer flows. Part III: hydroxyl radical measurements in low-pressure boundary layer flows. *Combustion and Flame*, 90(1):11–33.

Groppi, G., 2003. Combustion of CH₄ over a PdO/ZrO₂ catalyst: an example of kinetic study under severe conditions. *Catalysis Today*, 77(4):335–346.

Han, J., Zemlyanov, D. Y., and Ribeiro, F. H., 2006. Catalytic combustion of methane on palladium single crystals. *Catalysis Today*, 117(4):506–513.

Hayes, R.E, and Kolaczkowski, S., 1997. *Introduction to Catalytic Combustion*. Gordon and Breach Science Publishers, Reading, UK.

Hayes, R.E, Kolaczkowski, S., Lib, P., Awdryb, S., 2001. The palladium catalyzed oxidation of methane: reaction kinetics and the effect of diffusion barriers, *Chemical Engineering Science*, 56:4815–4835.

Hayes, R.E, 2004. Catalytic solutions for fugitive methane emissions in the oil and gas sector. *Chemical Engineering Science*, 59: 4073 – 4080.

Hayes, R.E, Mok, P.K, Mmbaga, J, Votsmeier, M, 2007. A fast approximation method for computing effectiveness factor with non-linear kinetics. *Chemical Engineering Science*, 62: 2209 – 2215.

Hicks, R.F., Qi, H., Young, M.L. and Lee, R.G., 1990. Structure sensitivity of methane oxidation over platinum and palladium. *Journal of Catalysis*, 122: 280-294.

Hicks, R.F., Qi, H., Young, M.L. and Lee, R.G., 1990. Effect of catalyst structure on methane oxidation over palladium on alumina. *Journal of Catalysis*, 122: 295-306.

Hoyos, L.J., Praliaud, H. and Primet, M., 1993. Catalytic combustion of methane over palladium supported on alumina and silica in presence of hydrogen sulfide. *Applied Catalysis A:General*, 98: 125-138.

Hurtado, P., Ordonez, S., Sastre, H., and Diez, F., V., 2004. Combustion of methane over palladium catalyst in the presence of inorganic compounds : inhibition and deactivation phenomena : *Applied catalysis B: Environmental*, 47(2):85-93.

Ibashi, W., Groppi, G., and Forzatti, P., 2003. Kinetic measurement of CH₄ combustion over a 10% PdO/ZrO₂ catalyst using an annular flow micro reactor. *Catalysis Today*, 83:115–129.

Incopera, F. P., and Dewitt, D. P., 1996. Introduction to heat transfer, Third edition, Toronto: Wiley.

IPCC, 2007. Climate change 2007: The physical science basis, summary for policy makers, and contribution of working group to the fourth assessment report of the IPCC. Technical Report 6, IPCC.

Kiehl, J. T., and Trenberth K. E, 1997. Earth's Annual Global Mean Energy Budget. *Bulletin of the American Meteorological Society* 78 (2): 197–208

Lampert, J. K., Kazia, M. S., and Farrauto, R. J., 1997. Palladium catalyst performance for methane emissions abatement from lean burn natural gas vehicles. *Applied catalysis B: Environmental*, 14(3–4):211 – 223.

- Lapisardi, G., Urfels, L., Gelin, P., Primet, M., Kaddouri, A., Garbowski, E., Toppi, S., and Tena, E., 2006. Superior catalytic behaviour of Pt-doped Pd catalysts in the complete oxidation of methane at low temperature. *Catalysis Today*, 117: 564–568.
- Larpisardi, G., G elin, P., Kaddouri, A., Garbowski, E., and Da Costa, S., 2007. Pt-Pd bimetallic catalysts for methane emissions abatement. *Topics in Catalysis*, 42-43: 461–464.
- Lee, J. H. and Trimm, D. L., 1995. Catalytic combustion of methane. *Fuel Processing Technology*, 42(2-3):339–359.
- Li, Z., Xu, G., and Hoflund, G. B., 2003. In situ IR studies on the mechanism of methane oxidation over Pd/Al₂O₃ and Pd/Co₃O₄ catalysts. *Fuel Processing Technology*, 84(1-3):1–11.
- Liu, B., Checkel, M., and Hayes, R., 2001a. Experimental study of a reverse flow catalytic converter for a dual fuel engine. *Canadian Journal of Chemical Engineering*, 79(4):491–506.
- Liu, B., Hayes, R. E., Checkel, M. D., Zheng, M., & Mirosh, E., 2001b. Reversing How catalytic converter for a natural gas-diesel dual fuel engine. *Chemical Engineering Science*, 56(8), 2641–2658.
- L opez-Herce J, Borrego R, Bustinza A, Carrillo A, September 2005. Elevated carboxyhemoglobin associated with sodium nitroprusside treatment . *Intensive Care Med* 31 (9): 1235–8.
- Lyubovsky, M., Karim, H., Menacherry, P., Boorse, S., LaPierre, R., Pfefferle, W. C., and Roychoudhury, S., 2003. Complete and partial catalytic oxidation of methane over substrates with enhanced transport properties. *Catalysis Today*, 83(1-4):183–197.

Maione, A., Andre, F., and Ruiz, P., 2007. Structured bimetallic Pd-Pt/ γ -Al₂O₃ catalysts on FeCr Alloy fibers for total combustion of methane. *Applied Catalysis B: Environmental*, 75: 59–70.

Markatou, P., Pfefferle, L. D., and Smooke, M. D., 1993. A computational study of methane-air combustion over heated catalytic and non-catalytic surfaces. *Combustion and Flame*, 93(1-2):185–201.

Meeyoo, V., Trimm, D. L., and Cant, N. W., 1998. The effects of sulphur containing pollutants on the oxidation activity of precious metals used in vehicle exhaust catalysts. *Applied Catalysis B: Environmental*, 16: L101- L104.

Mezaki, R., Watson, C., 1966. Catalytic oxidation of methane. *I&EC Process Design and Development*, 5, 62-65.

Moallemi, M., Batley, B., Dupont, V., Foster, F., Pourkashanian, P., and Williams, W., 1999. Chemical modeling and measurements of the catalytic combustion of CH₄/air mixtures on platinum and palladium catalysts. *Catalysis Today*, 47:235–244.

Montreuil, C. N., Williams, S. C., and Adamczyk, A. A., 1992. Modelling current generation catalytic converters: Laboratory experiments and kinetic parameter optimization – steady state kinetics. *Technical report, SAE Paper 920096*.

Mouaddib, N., Feumi-Jantou, C., Garbowski, E. and Primet, M., 1992. Catalytic oxidation of methane over palladium supported on alumina: Influence of the oxygen-to-methane ratio. *Applied Catalysis A: General*, 87: 129-144.

Moulder, J.F., Stickle, W.F., Sobol, P.E., and Bomben, K.D., February 1995. "Handbook of X-Ray Photoelectron Spectroscopy: A Reference Book of Standard Spectra for Identification and Interpretation of XPS Data", published by Physical Electronics,

Muller, C. A., Maciejewski, M., Koepfel, R. A., and Baiker, A., 1999. Combustion of methane over Palladium/Zirconia: effect of Pd-particle size and role of lattice oxygen. *Catalysis Today*, 47(1-4):245–252.

Narui, K., Yata, H., Furuta, K., Nishida, A., Kohtoku, Y., and Matsuzaki, T., 1999. Effects of addition of Pt to PdO/Al₂O₃ catalyst on catalytic activity for methane combustion and TEM observation of supported particles. *Applied Catalysis A: General*, 179:165 – 173.

Niemantsverdriet, J.W., 2000. *Spectroscopy in Catalysis: An Introduction*, Second Edition, WILEY-VCH.

Niwa, M., Awano, K. and Murakami, Y., 1983. Activity of supported platinum catalysts for methane oxidation. *Applied Catalysis*, 7(3): 317-325.

Oh, S.H., Mitchell, P.J. and Siewert, R.M., 1992. Methane oxidation over noble metal catalysts as related to controlling natural gas vehicle exhaust emissions. In: R.G. Silver, J.E. Sawyer and J.C. Summers (Eds.), *Catalytic Control of Air Pollution: Mobile and Stationary Sources*, 202nd National Meeting of the American Chemical Society, 25-30 August, 1991, *ACS Symposium Series*, Vol. 495, pp. 12-25.

Otto, K., 1989. Methane oxidation over Pt on α -alumina: kinetics and structure sensitivity. *Langmuir*, 5: 1364-1369.

Ozkan, U. S., Kumthekar, M. W., and Karakas, G., 1997. Self-sustained oscillatory behavior of $\text{NO}+\text{CH}_4+\text{O}_2$ reaction over titania-supported Pd catalysts. *Journal of Catalysis*, 171 (1): 67-76.

Page, J. F. Lee., 1987. Applied heterogeneous catalysis: design, manufacture, use of solid catalysts. *Editions Technip Publisher*, Chapter one.

Pfefferle, L. D., Griffin, T. A., Dyer, M. J., and Crosley, D. R., 1989. The influence of catalytic activity on the gas phase ignition of boundary layer flows Part II: Oxygen atom measurements. *Combustion and Flame*, 76(3-4):339–349.

Persson, K., Erssona, A., Jansson, K., Iverlund, N., Jaras, S., 2005. Influence of co-metals on bimetallic palladium catalysts for methane combustion. *Journal of Catalysis*, 231(1): 139–150.

Persson, K., Erssona, A., Jansson, K., Fierro, J.L.G, Jaras, S.G., 2006. Influence of molar ratio on Pd–Pt catalysts for methane combustion. *Journal of Catalysis*, 243 :14–24

Persson, K., Pfefferle, L. D, Schwartz, W., Ersson, A., and Jaras, S. D., 2007. Stability of palladium-based catalysts during catalytic combustion of methane-The influence of water. *Applied Catalysis B: Environmental*, 74:242-250.

Prasad, R., Kennedy, L.A. and Ruckenstein, E., 1984. Catalytic combustion. *Catalysis Reviews Science and Engineering.*, 26: 1-58.

Reinke, M., Mantzaras, J., Schaeren, R., Bombach, R., Inauen, A., and Schenker, S., 2004. High-pressure catalytic combustion of methane over platinum: In situ experiments and detailed numerical predictions. *Combustion and Flame*, 136(1-2):217–240.

Ribeiro, F. H., Chow, M., and Dallabetta, R. A., 1994. Kinetics of the complete oxidation of methane over supported palladium catalysts. *Journal of Catalysis*, 146(2):537–544.

Sakai, T., Chol, B. C., Osuga, R., & Ko, Y., 1991. Purification characteristics of catalytic converters for natural gas fuelled automotive engine. *SAE 912599*.

Salaun, M., Kouakou, A., Da Costa, S., and Da Costa, P., 2009. Synthetic gas bench study of natural gas vehicle commercial catalyst in monolithic form: On the effect of gas composition. *Applied catalysis B: Environmental*, 88:386:397.

Salomons, S., Hayes, R. E., Poirier, M., and Sapoundjiev, H., 2003. Flow reversal reactor for the catalytic combustion of lean methane mixtures. *Catalysis Today*, 83(1-4):59–69.

Salomons, S., Hayes, R. E., Poirier, M., and Sapoundjiev, H., 2004. Modeling a reverse flow reactor for the catalytic combustion of fugitive methane emissions. *Computers and Chemical Engineering*, 28:1599–1610.

Satterfield, C., 1980. Heterogeneous Catalysis in Practice, McGraw-Hill chemical engineering series

Seimanides, S. and Stoukides, M., 1986. Catalytic oxidation of methane on polycrystalline palladium supported on stabilized zirconia. *Journal of Catalysis*, 98(2):540–549.

Sekizawa, K., Eguchi, K., Poirier, M., Widjaja, H., Machida, M., and Arai, H., 1996. Property of Pd-supported catalysts for catalytic combustion. *Catalysis Today*, 28 (3): 245-250.

Smith, L, Karim, H., Castaldi, M., Etemad, S., Pfefferle, W.C., 2005. Rich-catalytic lean-burn combustion for low-single-digit NO_x gas turbines. *Journal of Engineering for Gas Turbines and Power*, 127:27-35.

Song, X., William, W., Schmidt, L., and Aris, R., 1991. Bifurcation behavior in homogeneous-heterogeneous combustion: II. computations for stagnation-point flow. *Combustion and Flame*, 84:292–311.

Trimm, D.L. and Lam, C.W., 1980. The combustion of methane on platinum-alumina fibre catalysts. *Chemical Engineering Science*, 35: 1405-1413.

Van de Beld, L., 1996. A kinetic study of the complete oxidation of ethane, Propane and their mixtures on a Pd/Al₂O₃ catalyst. *Fuel and Energy Abstracts*, 37(3):176–292.

Van Giezen, J. C., Van den Berg, F. R., Kleinen, J. L., Van Dillen A. J., and Geus, J. W., 1999. The effect of water on the activity of

supported palladium catalysts in the catalytic combustion of methane. *Catalysis Today*, 47 (1-4):287-293.

Vannice, M. A., 2005. Kinetics of Catalytic Reactions. *Springer; first edition*.

Vannice, M. A., 2007. An analysis of the Mars-van Krevelen rate expression. *Catalysis Today*, 123:18-22.

Voltz, S. E., Morgan, C. R., Liederman, D., and Jacob, S. M., 1973. Kinetic study of carbon monoxide and propylene oxidation on platinum catalysts. *Industrial & Engineering Chemistry Product Research and Development*, 12 (4): 294-301.

Wakao, N., Kagueie, S., 1982. Heat and mass transfer in packed beds. London: Gordon and Breach.

Williams, W. R., Stenzel, M. T., Song, X., and Schmidt, L. D., 1991. Bifurcation behavior in homogeneous-heterogeneous combustion: I. experimental results over platinum. *Combustion and Flame*, 84(3-4):277-291.

Zhu, H., 2001. Numerical modeling of methane combustion on palladium catalyst for gas turbine applications. *PhD thesis, University of Maryland*.

Appendix A: List of runs

List of Runs for methane catalytic combustion ^a						
Run #, Figure #	Catalyst g/ft ³	Procedure ^b	Reduction	CH ₄		Water
				cm ³ /min	CH ₄ , ppm	5% mol
Exploratory runs for Pt-Pd catalyst(investigating the pretreatment effect)						
Pt-Pd-01-12, Fig 4.1	95	I-E	30 min	95(2%)	5931	N
Pt-Pd-01-13, Fig 4.2	95	I-E	30 min	95(2%)	5931	N
Pt-Pd-01-14, Fig 4.3	95	I-E	N	95(2%)	5931	N
Exploratory runs for Pt catalyst(investigating the pretreatment effect)						
Pt-01-12, Fig 4.4	95	I-E	30 min	95(2%)	5931	N
Pt-01-13, Fig 4.5	95	I-E	30 min	95(2%)	5931	N
Pt-01-14, Fig 4.6	95	I-E	N	95(2%)	5931	N
Experiments to investigate the effect of methane concentration on fresh Pt-Pd catalyst						
Pt-Pd-01-15, Fig 4.7	95	I-E	30 min	9.55(10%)	4067	N
Pt-Pd-01-16, Fig 4.8	95	I-E	30 min	4.88(10%)	2122	N
Pt-Pd-01-18, Fig 4.9	95	I-E	30 min	3.48(10%)	1524	N
Pt-Pd-01-17, Fig 4.10	95	I-E	30 min	9.8(2%)	837	N
Experiments to investigate the effect of methane concentration on fresh Pt catalyst						
Pt-01-23, Fig 4.13	95	I-E	30 min	9.55(10%)	4067	N
Pt-01-24, Fig 4.14	95	I-E	30 min	4.88(10%)	2122	N
Pt-01-25, Fig 4.15	95	I-E	30 min	3.48(10%)	1524	N
Pt-01-26, Fig 4.16	95	I-E	30 min	9.8(2%)	837	N
Experiments to investigate the effect of water on the performance of the fresh Pt-Pd catalyst						
Activity test, Fig 4.19	95	N/A	N/A	9.55(10%)	4064	Y
Steam aging, Fig 4.20	95	N/A	N/A	9.55(10%)	4064	Y
Experiments to investigate the effect of water on the performance of the steam aged Pt-Pd catalyst						
Pt-Pd-01-22-26, Fig 4.21	95	I-E	N	9.55(10%)	4064	Y
Pt-Pd-01-23-28, Fig 4.22	95	I-E	N	4.88(10%)	2122	Y
Pt-Pd-01-25-29, Fig 4.23	95	I-E	N	3.48(10%)	1526	Y
Pt-Pd-01-24-27, Fig 4.24	95	I-E	N	9.84(2%)	836	Y
Pt-Pd-01-33, Fig 4.27	95	I-E	N	9.55(10%)	4067	N
Pt-Pd-01-35, Fig 4.28	95	I-E	N	4.88(10%)	2122	N
Pt-Pd-01-34, Fig 4.29	95	I-E	N	3.48(10%)	1524	N
Pt-Pd-01-36, Fig 4.30	95	I-E	N	9.8(2%)	837	N
Experiments to investigate the effect of water on the performance of the fresh Pt catalyst						
Activity test, Fig 4.33	95	N/A	N/A	9.55(10%)	4064	Y
Steam aging, Fig 4.34	95	N/A	N/A	9.55(10%)	4064	Y
Experiments to investigate the effect of water on the performance of the steam aged Pt catalyst						
Pt-01-27, Fig 4.35	95	I-E	N	9.55(10%)	4064	Y
Pt-01-28, Fig 4.36	95	I-E	N	4.88(10%)	2122	Y
Pt-01-29, Fig 4.37	95	I-E	N	3.48(10%)	1526	Y
Pt-01-30, Fig 4.38	95	I-E	N	9.84(2%)	836	Y
Pt-01-32, Fig 4.41	95	I-E	N	9.55(10%)	4067	N
Pt-01-33, Fig 4.42	95	I-E	N	4.88(10%)	2122	N
Pt-01-34, Fig 4.43	95	I-E	N	3.48(10%)	1524	N
Pt-01-31, Fig 4.44	95	I-E	N	9.8(2%)	837	N
Note:						
^a . The flow-rate of air was fixed for all runs at 225 cm ³ /min (STP) (for test in the absence of water), for the tests with water it was reduced to get the same space velocity as the dry runs. The mass of catalyst samples was 0.5 gr for all runs.						
^b . I=ignition, E=extinction, I-E=extinction after ignition						